NOTICE

The quality of this microform is heavily dependent upon the quality of the original thesis submitted for microfilming. Every effort has been made to ensure the highest quality of reproduction possible.

If pages are missing, contact the university which granted the degree.

Some pages may have indistinct print especially if the original pages were typed with a poor typewriter ribbon or if the university sent us an inferior photocopy.

Reproduction in full or in part of this microform is governed by the Canadian Copyright Act, R.S.C. 1970, c. C-30, and subsequent amendments.

AVIS

La qualité de cette microforme dépend grandement de la qualité de la thèse soumise au microfilmage. Nous avons tout fait pour assurer une qualité supérieure de reproduction.

S'il manque des pages, veuillez communiquer avec l'université qui a conféré le grade.

La qualité d'impression de certaines pages peut laisser à désirer, surtout si les pages originales ont été dactylographiées à l'aide d'un ruban usé ou si l'université nous a fait parvenir une photocopie de qualité inférieure.

La reproduction, même partielle, de cette microforme est soumise à la Loi canadienne sur le droit d'auteur, SRC 1970, c. C-30, et ses amendements subséquents.

A New Technique for Modelling Open-Ended Waveguide Structures and Its Application to Dielectric Spectroscopy

by

Christopher L. Sibbald

A thesis submitted to
the School of Graduate Studies and Research
in partial fulfillment of the
requirements for the degree of
Doctor of Philosophy

Ottawa-Carleton Institute for Electrical Engineering
Department of Electrical Engineering
Faculty of Engineering
University of Ottawa

ISBN 0-315-75030-8

UNIVERSITÉ D'OTTAWA
UNIVERSITY OF OTTAWA

I hereby declare that I am the sole author of this document. I authorize the University of Ottawa to lend this document to other institutions for the purpose of scholarly research.

Christopher L. Sibbald

I further authorize the University of Ottawa to reproduce this document by photocopying or by any other means, in total or in part, at the request of other institutions or individuals for the purpose of scholarly research.

Christopher L. Sibbald

The University of Ottawa requires the signatures of all persons using or photocopying this document.

Please sign below, and give address and date.

Abstract

A novel technique for modeling the aperture admittance of open-ended waveguide structures radiating into a homogeneous, lossy dielectric half-space is presented. This technique combines both analytical and numerical approaches to express the aperture admittance as rational function of frequency and the relative permittivity of the external medium. The coefficients of the rational approximation, which depend upon the geometry of the waveguide and aperture, are determined in a very convenient manner from a relatively small number of computed admittances. This computed data is obtained via a full-wave moment method solution and, hence, includes the effects of radiation and energy storage in the near-field and evanescent waveguide modes. The accuracy of the numerical method is demonstrated by comparison with measured values.

The new technique is successfully applied to obtain a model for the open-ended coaxial line geometry. The new model has important applications in the field of dielectric spectroscopy. In addition to yielding accurate solutions for the aperture admittance of the line as a function of the permittivity of the external medium, the model yields a unique solution to the inverse problem and permits a rigorous sensitivity and uncertainty analysis.

Acknowledgements

I would like to express my sincere gratitude to my supervisor, Dr. S. Stuchly, for his guidance and encouragement throughout this work. I would also like to thank Dr. Adiseshu Nyshadham for his help with the measurements. Finally, a heartfelt thanks is extended to my wife Ann Marie who, in addition to helping in the preparation of this document, gave me the strength to carry on when things didn't work.

Table of Contents

Chapter I Introduction 1
1.1 Motivation 2
1.2 Objective of the Thesis 5
1.3 Outline of the Thesis 5

Chapter II Past Work 8
2.1 Coaxial Lines 8
2.2 Waveguides 12
2.3 Concluding Remarks 14

Chapter III General Theory 16
3.1 Introduction 16
3.2 Analytical Treatment 18
3.3 Numerical Treatment 26

Chapter IV Coaxial Lines 44
4.1 Introduction 44
4.2 Specifics of The Method of Moments for Coaxial Lines 45
4.3 Results 47

Chapter V Rational Approximations 59
5.1 Introduction 59
5.2 The Direct Problem 61
5.3 The Inverse Problem 64
5.4 Sensitivity and Uncertainty Analysis 66

Chapter VI Polynomial Approximations 92
6.1 Introduction 92
6.2 The Direct Problem 93
6.3 The Inverse Problem 95
6.4 Sensitivity and Uncertainty 96

Chapter VII Discussion and Conclusions 111

Appendix A Calculation of the Generalized Admittance Matrices 115

Appendix B Nomenclature 119

Table of Figures

3.1: Geometry of the General Aperture Problem 42
3.2: The Equivalent Magnetic Currents 43
4.1: Geometry of an Open-Ended Coaxial Line 54
4.2: The Moment Method Discretization of an Open-Ended Coax 55
4.3: Reflection Coefficient of a 3.6mm Line in Water 56
4.4: Reflection Coefficient of a 3.6mm Line in Methanol 57
4.5: Reflection Coefficient of a 3.6mm Line in Air 58
5.1: Normalized Conductance of a Coaxial Line (MoM) 78
5.2: Normalized Susceptance of a Coaxial Line (MoM) 79
5.3: Magnitude of the Admittance of a Coaxial Line (MoM) 80
5.4: Relative Error in Rational Function Fit 81
5.5: Relative Error in Y for Lossy Dielectrics for ka=0.01 82
5.6: Relative Error in Y for Lossy Dielectrics for ka=0.05 83
5.7: Relative Error in Y for Lossy Dielectrics for ka=0.10 84
5.8: Relative Error in Y for Lossy Dielectrics for ka=0.14 85
5.9: Relative Error in Y for Lossy Dielectrics for ka=0.19 86
5.10: Inverse Sensitivity of a Coaxial Line for ka=0.01 87
5.11: Inverse Sensitivity of a Coaxial Line for ka=0.05 88
5.12: Inverse Sensitivity of a Coaxial Line for ka=0.10 89
5.13: Inverse Sensitivity of a Coaxial Line for ka=0.14 90
5.14: Inverse Sensitivity of a Coaxial Line for ka=0.19 91
6.1: Normalized Conductance of a Coaxial Line (MoM) 104
6.2: Normalized Susceptance of a Coaxial Line (MoM) 105
6.3: Magnitude of the Admittance of a Coaxial Line (MoM) 106
6.4: Relative Error in the Polynomial Fit 107
6.5: Relative Error in Y for Lossy Dielectrics for ka=0.01 108
6.6: Relative Error in Y for Lossy Dielectrics for ka=0.05 109
6.7: Relative Error in Y for Lossy Dielectrics for ka=0.10 110

Table of Tables

4.1: Convergence of the Admittance of a 3.6mm line at 1 GHz. 51
4.2: Convergence of the Admittance of 3.6mm line at 18 GHz. 52
4.3: Reflection Coefficient of 14mm line at 1 GHz. 52
4.4: Cole-Cole parameters of Water and Methanol. 53
5.1: Convergence of the Least Squares Fit 71
5.2: Best Fit Numerator Parameters of Rational Model 72
5.3: Best Fit Denominator Parameters of Rational Model 73
5.4: Solution of the Inverse Problem for ka=0.19 74
6.1: Best Fit Parameters of Polynomial Model 98
6.2: Solution of the Inverse Problem for ka=0.10 100

Chapter I

Introduction

The way in which electromagnetic fields interact with matter is determined by the electric and magnetic properties of the material. On a macroscopic scale, and under steady-state conditions, these properties are conveniently described by the material permeability and the material permittivity. This latter quantity is central to this thesis and, hence, deserves a brief discussion.

The interaction of electric fields with matter is described by the material permittivity, ε:

$$\varepsilon = \varepsilon_r \varepsilon_0 = (\varepsilon' - j\varepsilon'')\varepsilon_0 = \frac{D}{E}$$

where D is the electric flux density, E is the electric field intensity, ε_r is the relative permittivity, ε' is the relative dielectric constant, ε'' is the loss factor, ε_0 is the permittivity of free space (ε_0= 8.854 x 10^{-12} F/m) and j is the imaginary unit ($j^2 = -1$). The permittivity represents the combined macroscopic effect of various molecular phenomena causing electrical polarization. A physical interpretation of the permittivity may be given as follows: The dielectric constant, ε', is a measure of the ability of the material to store electrical energy, whereas the loss factor, ε'', is a measure of the ability of the material to dissipate electrical energy.

Similarly, the interaction of the magnetic field with matter is described on the macroscopic level by the permeability, μ. This quantity is also complex in general and has a physical interpretation which is dual to that of the permittivity. However, only non-magnetic materials, which have permeabilities equal to that of vacuum ($\mu = \mu_0 = 4\pi \times 10^{-7}$ H/m) are considered here.

Knowledge of the permeability and the permittivity of materials is paramount to the solution of any electromagnetic problem. In order to understand these problems, and to make predictions, it is necessary to know the dielectric properties of all materials involved.

1.1 Motivation

The increasing use of microwaves and millimeter waves in such diverse fields as communications, radar, space technology, medicine, biology, agriculture and industrial processes demands accurate data on the dielectric properties of materials. When an antenna, be it a communications antenna or a weather radar antenna, is immersed in a dielectric medium the driving point impedance, near-field distribution and radiation pattern are altered. Hence, knowledge of the properties of the medium are required to predict the behavior of the antenna.

In the field of medicine, microwaves have found many therapeutic and diagnostic applications. Microwave induced hyperthermia [1], when used in conjunction with conventional treatments such as chemotherapy and radiation therapy has increased the success rate of cancer treatments [2]. Microwave thermography [3] is often used in conjunction with hyperthermia in order to monitor the temperature within the tissues as well as for tumor detection. Knowledge of the dielectric properties of tissues is essential in the design of the transducers and applicators used in both these methods. Furthermore, information on the differences between the permittivity of healthy and diseased tissues is needed in non-invasive diagnostics such as cancer detection [4].

Dielectric spectroscopy has also proven useful in the study of biochemical and biophysical processes [5]. For example, the dielectric relaxation of molecules provides information on their physical structure. In biology, changes in the permeability of bilayer membranes may be detected

via permittivity measurements [6]. Microwave dosimetry requires information on the permittivity of human tissues and organs in order to assess possible health hazards associated with exposure to electromagnetic fields [7].

Microwaves are used in the field of agriculture for the drying of grain as well as for monitoring their moisture content [8]. In industrial applications, microwaves have been used for on-line monitoring of moisture content as well as for dielectric and induction heating processes.

These examples illustrate the need for an accurate means for measuring the dielectric properties of materials over a broad frequency range. Classical techniques of dielectric spectroscopy [9,10,11] generally involve measuring the complex impedance, or the complex resonant frequency, of a two terminal structure containing the material under test. At low frequencies, typically below 100 MHz, the system consists of a parallel plate capacitor loaded with the test sample [12]. Measurement of the complex capacitance of the loaded cell, either in a bridge circuit or resonated with an inductor [13], then yields the material permittivity. At higher frequencies, loaded resonators and loaded waveguides replace the lumped elements used at the lower frequencies [14,15].

These techniques generally require extensive sample preparation, cutting and polishing the material to fit in a suitable waveguide or cavity test jig. This is neither practical, nor permissible, in many applications. In particular, medical diagnostics and in-vivo measurements preclude cutting the sample from the bulk. Similar constraints are imposed in the on-line monitoring of moisture content, where the time required for sample preparation makes real-time measurements

impossible. In these, and many other applications, a non-destructive method for material characterization is required. For this reason, reflection techniques using open-ended waveguides[1] have gained popularity.

A convenient system for the non-destructive measurement of material permittivity consists of an open-ended waveguide sensor and a network analyzer. The sensor is placed in contact with the material under test and the resulting reflection coefficient is measured with the network analyzer. Knowledge of the relationship between the measured reflection coefficient (Γ) and the material permittivity (ε) then allows one to determine the latter. The difficulty, however, is that this represents an inverse problem. Although very accurate numerical methods exist for the calculation of Γ for a given ε, they are of little use in themselves for computing ε from the measured reflection coefficient. Minimization schemes, in which the numerical method is iterated until the computed and measured reflection coefficient converge are in use, however, these schemes are time consuming and yield no information regarding the sensitivity of the sensor nor the uncertainty in the "computed" permittivity. Ideally, a closed form expression for the permittivity as a function of the reflection coefficient is required. In the case of open-ended coaxial line probes some attempt has been made in this area. The results however, are based on static, or quasi-static approximations, and hence are accurate only in a restricted frequency range.

---

1. The term waveguide is used in its most general sense to include transmission lines as well as hollow pipes.

1.2 Objective of the Thesis

The objective of this thesis is to model the relationship between the normalized aperture admittance[2] of open-ended waveguide structures and the permittivity of the external medium. The model must be accurate and broadband; it must include the effects of radiation, polarization loss and energy storage in the external medium, and energy storage in the evanescent waveguide modes. The model must be invertible; it must allow direct (vs. iterative) determination of the material properties given the measured reflection coefficient. The model must be general; it must be applicable to a broad class of aperture and feed guide geometries. The model must be explicit; it must enable the determination of sensitivities and uncertainties. Finally, the model must be relatively simple.

1.3 Outline of the Thesis

The thesis is organized as follows. A review of previous work is presented in Chapter II. Existing solutions, both analytical and numerical, for the aperture admittance of open-ended coaxial line, rectangular waveguides, and circular waveguides are discussed. In each case, the simplifying assumptions and relative merits and limitations are highlighted. Finally, it is concluded that no satisfactory model is available which meets the stated objectives of this thesis.

Chapter III presents the general theory and approach used to obtain an aperture admittance model consistent with the objectives. A consideration of the physical properties of a passive one-port driving point admittance, and the resulting mathematical properties of these functions,

---

2. Knowledge of the normalized aperture admittance is equivalent to knowledge of the aperture reflection coefficient. The two are related by a simple bi-linear transform.

indicates that suitable rational function and polynomial approximations are possible. The form of these approximating functions, and their respective range of validity, is discussed. The final section of this chapter considers the general numerical aspects of determining the model parameters. These include the method of moments (MoM) solution of the electromagnetic boundary value problem and the ultimate determination of the model parameters via a Least Squares fit to this computed data.

The remainder of the thesis is an example of the general technique. An aperture admittance model for open-ended coaxial lines is developed. This example is presented in order to illustrate the application of the method via a specific example as well as to verify the approach. Chapter IV provides the details of the method of moments for this geometry and demonstrates the accuracy of this numerical method via comparison with measurements.

Chapter V considers rational function approximations to the aperture admittance. It is shown that, for any given frequency range and range of material permittivity it is possible to approximate the aperture admittance by a rational functions of the form:

$$Y(s,\varepsilon_r) = \frac{\sum_{n=1}^{N}\sum_{p=1}^{P} \alpha_{np}(\sqrt{\varepsilon_r})^p s^n}{1 + \sum_{m=1}^{M}\sum_{q=0}^{Q} \beta_{mq}(\sqrt{\varepsilon_r})^q s^m}$$

where Y is the aperture admittance of the line in contact with a homogeneous half-space of relative permittivity ε_r, s is the Laplacian variable ($s = \sigma + j\omega$), and α_{np} and β_{mq} are the model parameters which depend upon the geometry of the line. These parameters are determined for a coaxial line via a two-dimensional nonlinear least squares fit to the computed (MoM) data,

and the solution of the inverse problem is given. The accuracy of both the direct and inverse approximation is verified by comparison with the moment method results. The final section of this chapter deals with the uncertainty and sensitivity analysis for rational approximations.

Chapter VI considers polynomial approximations to the aperture admittance. It is shown that, for suitably restricted ranges of frequency and material permittivity, the aperture admittance is adequately approximated by a polynomial in two variables:

$$Y(s,\varepsilon_r) = \sum_{n=1}^{N} \sum_{p=1}^{P} c_{np} (\sqrt{\varepsilon_r})^p s^n$$

where the quantities have their usual meaning. The model parameters are determined for a coaxial line via a two dimensional least squares fit to the computed data (MoM). The inverse problem is solved and the accuracy of both the direct and inverse approximations are compared with the method of moments. Finally, the uncertainty and sensitivity analysis is performed.

The final chapter of the thesis contains a brief summary of the work done as well as some recommendations for future work. The choice of the optimum coaxial line dimensions for a given range of frequencies and permittivity is considered. A comparison of the polynomial and rational function approximations is made. Ultimately, conclusions and generalizations are made.

Chapter II

Past Work

A great deal of work has been performed over the last five decades to determine the aperture admittance of open-ended waveguide structures. The motivation for this work has come from such diverse fields as antenna design, medicine, and dielectric spectroscopy. The design of antenna feed systems and the effects of ionization on the aperture admittance of space borne antennas stimulated much work in the field of antennas. In medicine, the design of applicators for microwave hyperthermia in the treatment of cancer and the design of transducers for microwave thermography requires knowledge of the near field and aperture admittance of these structures. Recently, the use of open-ended probes for dielectric spectroscopy has added to the list of researchers devoted to the analysis of open-ended waveguides. The structures which have received most attention are open-ended coaxial lines, open-ended rectangular waveguides, and , to a lesser extent, open-ended circular waveguides.

2.1 Coaxial Lines

The earliest work concerning open-ended coaxial lines considered the homogeneous case, in which an air filled coaxial line is terminated in an infinite conducting flange and radiating into free space. Most notable is the work of Levine and Papas [16]. They derived two variational expressions for the admittance of a coaxial aperture, one based on an integral equation for the aperture electric field and one based on an integral equation for the aperture magnetic field. The resulting expressions were evaluated assuming the aperture field distribution to be that of the

dominant TEM mode. The results of this analysis may also be found in the *Waveguide Handbook* [17]. Also worth noting is the work of Harrison and Chang [18] and Tsai [19] who introduced several concepts used in this thesis. Harrison was the first to use equivalent magnetic currents and image theory to derive an integral equation for the aperture electric field and gave expressions for the near and far fields under the assumption that the aperture field is adequately described by the dominant mode distribution. Chang solved this integral equation numerically and suggested an efficient technique to extract the singularity which appears in the kernel of this integral. The effects of the higher order modes in the aperture was investigated by Chang [20] and later by Irzinski [21], with conflicting conclusions. These authors derived exact analytical solutions for the aperture admittance and subsequently invoked a small aperture assumption to simplify the resulting integrals. The contribution to the aperture admittance due to the dominant mode and the perturbation due to the higher order modes were identified and the effect of these higher order modes was assessed. Chang concluded that the higher order modes are significant, whereas Irzinski concluded the opposite.

In all of these analyses, the line was radiating into free space. When a lossy dielectric is placed in contact with the aperture the near-field distribution changes and, hence, so does the aperture admittance. No analytical treatments of this problem have been reported in the literature, however, several numerical solutions exist. Mosig et al [22] applied a point matching method to solve an integral equation for the tangential electric field in the aperture. The aperture electric field was expanded in terms of the TEM and TM_{0n} waveguide modes and the amplitudes of these modes were determined by enforcing continuity of the tangential magnetic field at discrete points on the aperture. Results obtained by considering five waveguide modes (and five match

points) were compared with the results computed according to the variational expressions of Levine and Papas. It was concluded that, for the frequency range and the dimensions of the aperture considered, the higher order modes have a significant effect.

Nevels et al [23] solved the same integral equation by the method of moments. The quantity ρE_ρ, where ρ is the radial coordinate and E_ρ is the radial components of the electric field, was expanded in terms of pulse functions whose amplitudes were determined by point matching on the aperture. Again the work of Levine and Papas was used as a benchmark and it was stated that the higher order modes can be neglected providing the aperture dimension (b-a) is smaller than 2.5 times the wavelength in the external medium. Very recently Jenkins et al [24] presented a comparison of three numerical techniques which have been applied to the open-ended coaxial line problem. The techniques compared were the point matching method of Mosig et al [22], the moment method of Nevels et al [23], and a variational method due to Hodgetts [25]. An inverse quadratic extrapolation was used in each case, in conjunction with several progressively finer discretizations, to estimate the limiting value of the reflection coefficient for a line radiating into a medium characterized by $\varepsilon_r = 100 - j100$ at 1 GHz. The results indicate that all three methods yield virtually identical values.

These numerical methods yield accurate solutions for the aperture admittance, including the effects of evanescent modes and radiation, however, prove impractical for dielectric spectroscopy. In this application one is interested in the solution of the inverse problem. That is to say, given the measured admittance of the probe in contact with the material under test, one must calculate the permittivity of the material. Although an iterative technique based on [22] can be used for dielectric spectroscopy [26], because of the complexity of this method many researchers have sacrificed accuracy for a simpler expression for the aperture admittance as a function of material properties. These approximate expression generally yield satisfactory results for a

limited range of frequencies and permittivities. The earliest reported application of open-ended coaxial lines for dielectric spectroscopy was described by Tanabe and Joines [27]. They presented a non-linear expression for the aperture admittance in terms of the dielectric constant and loss factor of the external medium. This empirical expression was determined by a static analysis. Burdette et al [28] applied an antenna modelling theorem due to Deschamps [29] in order to obtain a simple expression, explicit in the permittivity, for the impedance of a short monopole and the limiting case of an open-ended coaxial line. The parameters in this expression were determined experimentally.

The most widely reported model for the aperture admittance of the open-ended coaxial line was introduced by Stuchly and Stuchly [14]. This model consisted of two shunt capacitors, one independent of the material properties which accounted for the fringe field inside the line and one directly proportional to the permittivity which accounted for the fringe field in the material. Initially, both capacitors were assumed constant (static values). Two experimental techniques to determine the values of the two capacitors in this linear model were presented in [30]. Gajda and Stuchly [31] later presented numerical results based on Finite Element and Moment Method solutions of the static field problem. A correction for the frequency dependance of these elements was introduced by Kraszewski and Stuchly [32]. They presented empirical equations for the total fringe field capacitance of two common line sizes based on measurements performed with a rejection-type resonator. A relatively more accurate non-linear model was presented by Gajda and Stuchly [33]. In this model the external fringe field capacitance was expressed as a rational function of the dielectric constant of the medium. The parameters of this expression were determined from the results of the Moment Method analysis described in [31].

These simplified admittance models are all based on a static analysis, and hence are valid for electrically small apertures for which radiation and higher order modes may be neglected. Brady et al [34] modeled the effects of radiation by including a conductance term proportional to $\epsilon^{2.5}$ and two experimental techniques for determining the constant of proportionality were given. An analytical technique for determining this constant, based on the expression given by Marcuvitz [17], was presented by Stuchly et. al. [35] and a comparison of measurements performed with and without this term was given. Misra [36] derived a similar model consisting of two capacitors and a radiation conductance. The model parameters were obtained by making a quasi-static approximation for the integrand in a variational expression for the aperture admittance. Expressions were given for the total capacitance of two different lines which are in close agreement with those given by Kraszewski [32]. Another attempt to include radiation effects was made by Xu et. al. [37]. They applied Deschamps antenna theorem to the variational expression due to Levine. A Maclaurin series expansion of the integrand then led to a polynomial approximation, in terms of the permittivity of the external medium, for the aperture admittance. Misra et. al [38] repeated this work, giving more terms in the polynomial expansion.

2.2 Waveguides

The development of aperture admittance models for open-ended rectangular waveguides followed much the same lines. Lewin [39] derived a variational expression for the aperture admittance of a rectangular guide radiating into free space and presented results based on the dominant mode aperture field distribution. An analysis which considered higher order modes was performed by Mautz and Harrington [40]. An integral equation in terms of an equivalent

magnetic current on the aperture is formulated and solved by the method of moments. Cross polarization in rectangular apertures was considered by Jamieson and Rozzi [41] while an exact solution by the correlation matrix method was proposed by MacPhie and Zaghloul [42].

Compton [43] was the first to consider radiation into lossy dielectrics. Considering the aperture field to be composed of the TE_{10} and TE_{30} modes, he obtained input admittance values for the case of an infinite lossy medium and a finite lossy slab. The advent of space-borne antennas stimulated much more work in this area. When a space vehicle re-enters the earths atmosphere, a layer of charge particles forms over the antennas. Among those who studied this problem were: Villeneuve [44] who used a variational method to analyze the problem of radiation into homogeneous, lossless plasma; Galejs [45], who solved the more complex problem involving stratified, lossy plasma; and Croswell [46], who applied the method of Compton to the case of an inhomogeneous, lossy plasma. More recently, the model used by Galejs [45] was applied to the analysis of radiation into lossy dielectrics [47,48]. In this method, the half-space was replaced by an imaginary waveguide whose cross-sectional area was very large. For a lossy dielectric and the dimension of the second guide large enough, this waveguide discontinuity problem adequately simulates the unbounded problem.

The first application of open-ended guides for permittivity measurements was suggested by Decreton et al [49]. The input reflection coefficient of the guide as a function of the permittivity of the sample was computed using a variational approach. Computer generated charts relating the VSWR and phase shift to the complex permittivity were presented, allowing graphical inversion of the problem. In addition, a computer program which uses an optimization algorithm to invert the problem was suggested. This analysis, however, was restricted to relatively small dielectric constants. More extensive data was presented in [50]. In this case, the method of characteristic modes was used to determine the amplitudes of the waveguide modes and a polar

plot (Smith Chart) was presented relating the complex reflection coefficient to the dielectric constant and loss factor. A third order polynomial fit to the computed data was presented to simplify inversion of the problem.

Several numerical solutions for the aperture admittance of circular waveguides also appear in the literature. Gex-Fabry et. al. [51] applied the point matching method described in [22] to a circular waveguide excited by the TM_{01} mode. The results were compared with those given by Marcuvitz [17] and the effect of the flange was discussed. Fray et. al. [52] employed a Hankel Transform technique to determine the aperture admittance of a circular waveguide terminated in layered absorbing media. Finally, the method of characteristic modes described in [50] was also applied to the circular geometry.

2.3 Concluding Remarks

In conclusion, a great deal of work has been devoted to the study of open-ended waveguide structures. Although very accurate numerical methods exist for the calculation of the aperture admittance, for dielectric spectroscopy it is desirable to obtain relatively simple closed form expressions for approximating the dependance of this quantity on the properties of the external medium. In the case of coaxial lines, some attempt has been made in this area. The results however, are generally based on a static, or quasi-static analysis, and hence are useful only for restricted frequency bandwidths. In the case of waveguides, the few polynomial approximations available [50] are valid only for a limited range of material properties. Hence, a general technique for determining approximating functions relating the material properties to the admittance is needed. The technique should yield an approximating function of any desired degree of accuracy and the function itself should be explicit in the dielectric constant and loss factor. Finally, it

must be possible to determine the model parameters from a limited set of computed or measured admittance values. An excellent example of such a technique, although not applicable to aperture antennas, was presented by Smith and Nordgard [53]. They presented a rational expression, in terms of the wavenumber in the external medium, for the input impedance of a short monopole embedded in a lossy medium. The coefficients of this expression, for a third order approximation, were determined from measurements of the impedance of the antenna in a medium of known permittivity. This thesis proposes a similar technique for aperture antennas.

Chapter III

General Theory

3.1 Introduction

Open-ended waveguides have proven useful as sensors for the non-destructive measurement of material permittivity. This measurement technique is based on the sensors ability to translate changes in the permittivity into changes in the aperture admittance. Mathematically, one can state that the sensor maps (or transforms) the permittivity plane, ε, onto the admittance plane, Y, i.e.

$$Y = f(\varepsilon) \tag{3.1}$$

In practice, the aperture admittance (or equivalently the aperture reflection coefficient) is measured and the permittivity must be determined. This requires knowledge of the inverse function,

$$\varepsilon = f^{-1}(Y) \tag{3.2}$$

Determination of the inverse function directly from Maxwell's equations represents an inverse scattering problem. Analytical solutions do not exist for this type of problem. Furthermore, even numerical solutions, if unique solutions exist, are of limited use due to the uncertainties inherent in such "ill-posed" problems.

Hence, in order to characterize a given sensor one must resort to the direct problem. Again, however, direct application of Maxwell's equations is of limited value. This approach can

provide an accurate solution for an image point, Y_i, of a given permittivity, ε_i, but in itself will not provide enough information about the function to be useful in practice. If, however, one can determine an analytical expression which will approximate the function f for a given structure, a numerical solution of the inverse problem may be obtained.

The ideal form of the approximating function depends upon several important considerations.

a) The expression must be explicit in the dielectric constant and loss factor. Variations in the aperture admittance with frequency should enter the model via parameters which are independent of material properties.

b) The expression should be general enough to model a broad class of aperture and feed guide geometries.

c) It must be possible to determine the model parameters, for a given sensor geometry, from a limited set of computed or measured data points, (ε_i, Y_i)

d) The expression must be simple enough to allow determination of the permittivity from the measured aperture admittance.

e) The expression must provide information regarding the sensitivity of the sensor and the uncertainty in the measured permittivity.

The remainder of this chapter examines the basic ideas which may prove useful in obtaining approximating functions for a broad class of open-ended waveguides. Section 3.2 presents some physical, and resulting mathematical, properties of the mapping (3.1) which may be exploited in constructing closed form approximations to the function f. Section 3.3 describes the numerical methods employed in achieving this goal. Considerations of the inverse problem (3.2) are deferred until Chapters V and VI.

3.2 Analytical Treatment

Consider an open-ended waveguide in contact with a homogeneous half-space characterized by $\mu = \mu_0, \varepsilon_r = \varepsilon' - j\varepsilon''$. The guide is excited by the dominant mode and the frequency of operation is low enough to ensure single-mode propagation. In this case, one can define the normalized aperture admittance in terms of the dominant mode reflection coefficient at the aperture (Γ) by:

$$Y = \frac{1-\Gamma}{1+\Gamma} = \frac{1}{Y_0}\frac{H_{a0}}{E_{a0}} \tag{3.3}$$

Where H_{a0} represents the amplitude of the total (incident plus reflected) tangential component of the dominant mode magnetic field in the aperture, E_{a0} represents the amplitude of the total tangential component of the dominant mode electric field in the aperture, and Y_0 is the dominant mode wave admittance inside the guide.

For any given waveguide and aperture geometry, this admittance is a complex function of two complex variables,

$$Y(s, \varepsilon_r) = G(s, \varepsilon_r) + jB(s, \varepsilon_r) \tag{3.4}$$

where s is the complex frequency variable ($s = \sigma + j\omega$), G is the normalized conductance, and B is the normalized susceptance.

In general, the normalized aperture admittance may be represented by a rational function in the complex frequency plane [54]:

$$Y(s, \varepsilon_r) = A(\varepsilon_r)\frac{\prod_{n=1}^{\infty}\{s - z_n(\varepsilon_r)\}}{\prod_{m=1}^{\infty}\{s - p_n(\varepsilon_r)\}} \tag{3.5}$$

where A is a scale factor, z_n are the complex zeros of the admittance, and p_n are the complex poles of the admittance. As indicated, these quantities are all dependant upon the permittivity of the external media. By analogy with the driving point admittance of linear, passive, one-port networks one can deduce several important physical properties of the admittance function. When the half-space consists of a passive dielectric, the complex natural frequencies, z_n and p_n, must have negative real parts. This condition, known in network theory as the stability requirement, is necessary to ensure that the transient response of passive networks is damped. Furthermore, for steady state excitation, the net power delivered to the network (aperture) must be non-negative. This requires the real part of the admittance to remain non-negative for all j-axis points. In fact, due to radiation, the conductance must be strictly greater than zero for all j-axis points even for lossless dielectrics. The mathematical implications of these physical properties are summarized by stating that the aperture admittance is a positive real (p.r.) function of s for passive dielectrics [54].

A complex function of a complex variable, say $f(z)$, is called a positive real (p.r.) function if

A. the function is real for all real values of the independent variable, and,

B. the real part of the function remains positive for all values of the independent variable which have positive real parts.

In addition p.r. functions have the following useful properties (see [54] for proofs)

p1) A p.r. function can have neither zeros nor poles in the right-half plane.

p2) The poles and zeros of a p.r. function must be symmetrically distributed about the real axis.

p3) Any j-axis poles of a p.r. function must be simple and have positive, real residues.

p4) The real part of a p.r. function is non-negative for all points on the j-axis, vanishing on this axis only if the function has j-axis poles.

p5) All p.r. functions satisfy $f(z^*) = f^*(z)$, where * denotes complex conjugation.

At this point, it is convenient to write (3.5) in the following equivalent form[3]:

$$Y(s,\varepsilon_r) = \frac{\sum_{n=0}^{\infty} a_n(\varepsilon_r)s^n}{1 + \sum_{m=1}^{\infty} b_m(\varepsilon_r)s^m} \tag{3.6}$$

Where the coefficients a_n and b_n depend upon the permittivity of the external medium. In general, there will be an infinite number of such coefficients, corresponding to the infinite number of poles and zeros of the admittance of the distributed circuit. However, for a restricted frequency range only a finite number of these critical frequencies will have a significant effect on the admittance. This leads to the first approximation, truncation of the sums in (3.6).

$$Y(s,\varepsilon_r) \approx \frac{\sum_{n=0}^{N} a_n(\varepsilon_r)s^n}{1 + \sum_{m=1}^{M} b_m(\varepsilon_r)s^m} \tag{3.7}$$

The final step in obtaining the approximating function is to model the dependance of the coefficients a_n and b_n of (3.7) on the permittivity. Consider the aperture admittance for $s = 0$,

$$Y(0,\varepsilon_r) = a_0(\varepsilon_r) \tag{3.8}$$

---

3. Although the two forms are mathematically equivalent, the latter form is more suitable for solution of the inverse problem.

Since the admittance must be a p.r. function for all passive dielectrics requires a_0 to be a positive real quantity (condition A). Furthermore, since the admittance must be an analytic function of ε_r for all j-axis frequencies, the Cauchy-Riemann equations require:

$$\frac{\partial \Re\{a_0\}}{\partial \varepsilon'} = \frac{\partial \Im\{a_0\}}{\partial \varepsilon''} \tag{3.9a}$$

$$\frac{\partial \Re\{a_0\}}{\partial \varepsilon''} = -\frac{\partial \Im\{a_0\}}{\partial \varepsilon'} \tag{3.9b}$$

where $\Re$ and $\Im$ denote the real and imaginary part of a complex quantity, respectively.

Since the right hand side of (3.9) is identically zero, one concludes that a_0 must be a positive real constant, independent of the material permittivity. In fact, this coefficient represents the d.c. conductance of the probe and is a measure of the d.c. conductivity of the material. In the following a_0 is assumed to vanish, the validity of this assumption is easily established in practice.

The remainder of the coefficients certainly depend upon the permittivity. The p.r. character of the admittance requires the following three relation to hold:

$$\Im\{Y(s)\}|_{\omega=0} = 0 \tag{3.10}$$

$$\Re\{Y(s)\}|_{\sigma\geq 0} \geq 0 \tag{3.11}$$

$$Y(s^*) = Y^*(s) \tag{3.12}$$

The Kronig-Kramers relations for passive dielectrics state, in a slightly different form, that the permittivity of passive dielectrics is also a p.r. function of frequency. This requires,

$$\Im\{\varepsilon_r(s)\}|_{\omega=0} = 0 \tag{3.13}$$

$$\Re\{\varepsilon_r(s)\}|_{\sigma\geq 0} \geq 0 \tag{3.14}$$

$$\varepsilon_r(s^*) = \varepsilon_r^*(s) \tag{3.15}$$

Expanding (3.10), (3.11) and (3.12), and introducing (3.13), (3.14) and (3.15) respectively, one obtains:

$$\Im\left\{\frac{\sum_{n=1}^{N} a_n(\varepsilon_r)\sigma^n}{1+\sum_{m=1}^{M} b_m(\varepsilon_r)\sigma^m}\right\}\Bigg|_{\varepsilon''=0} = 0 \tag{3.16}$$

$$\Re\left\{\frac{\sum_{n=1}^{N} a_n(\varepsilon_r)\sigma^n}{1+\sum_{m=1}^{M} b_m(\varepsilon_r)\sigma^m}\right\}\Bigg|_{\sigma\geq 0,\varepsilon'\geq 0} \geq 0 \tag{3.17}$$

$$\frac{\sum_{n=1}^{N} a_n(\varepsilon_r^*)(s^*)^n}{1+\sum_{m=1}^{M} b_m(\varepsilon_r^*)(s^*)^m} = \left(\frac{\sum_{n=1}^{N} a_n(\varepsilon_r)s^n}{1+\sum_{m=1}^{M} b_m(\varepsilon_r)s^m}\right)^* = \frac{\sum_{n=1}^{N} a_n^*(\varepsilon_r)s^n}{1+\sum_{m=1}^{M} b_m^*(\varepsilon_r)s^m} \tag{3.18}$$

These last three equations impose the following constraints on the coefficients:

$$\Im\{a_n(\varepsilon_r)\}|_{\varepsilon''=0} = 0 \tag{3.19}$$

$$\Re\{a_n(\varepsilon_r)\}|_{\varepsilon'\geq 0} \geq 0 \tag{3.20}$$

$$a_n(\varepsilon_r^*) = a_n^*(\varepsilon_r) \tag{3.21}$$

$$\Im\{b_m(\varepsilon_r)\}|_{\varepsilon''=0} = 0 \tag{3.22}$$

$$\Re\{b_m(\varepsilon_r)\}|_{\varepsilon'\geq 0} \geq 0 \tag{3.23}$$

$$b_m(\varepsilon_r^*) = b_m^*(\varepsilon_r) \tag{3.24}$$

These are precisely the conditions which characterize p.r. functions. One thus concludes that the coefficients a_n and b_m are p.r. functions of ε_r. This has one very important implication with regard to approximating these functions for passive dielectrics, namely, they must be analytic in the right half of the ε-plane. Therefore, Taylor's theorem is applicable and one may write:

$$a_n = \sum_{p=0}^{\infty} \alpha_{np}(\varepsilon_r - c)^p \qquad n = 1,2,\ldots,N \tag{3.25}$$

$$b_m = \sum_{q=0}^{\infty} \beta_{mq}(\varepsilon_r - c)^q \qquad m = 1,2,\ldots,M \tag{3.26}$$

where c is any point in the right half plane. These series converge uniformly for all points which lie in the largest open disk with center c which lies in the right-half plane.

This guarantees that a power series expansion, in terms of ε_r, for the coefficients will converge for all points in the right-half plane. Experience shows, however, that the aperture admittance is strongly dependant on the wavenumber in the external medium. Since this quantity is proportional to the square root of the material permittivity, a more suitable (i.e. faster converging) expansion is[4]:

---

4. An argument similar to the one presented demonstrates that $a_n(\sqrt{\varepsilon_r})$ and $b_m(\sqrt{\varepsilon_r})$ are also analytic in the right-half of the $\sqrt{\varepsilon_r}$-plane, hence Taylor's theorem is applicable.

$$a_n = \sum_{p=0}^{\infty} \alpha_{np} (\sqrt{\varepsilon_r} - c)^p \qquad n = 1, 2, \ldots, N \tag{3.27}$$

$$b_m = \sum_{q=0}^{\infty} \beta_{mq} (\sqrt{\varepsilon_r} - c)^q \qquad m = 1, 2, \ldots, M \tag{3.28}$$

In (3.27) and (3.28) the coefficients α_{np} and β_{mq} must be real and the principal value of $\sqrt{\varepsilon}$ must be used. On physical grounds one concludes that, if the wavenumber in the external medium vanishes (i.e. $\varepsilon_r = 0$) the admittance become identically zero. This requires α_{n0} to be identically zero, for all n. No such restriction is imposed on β_{m0}.

Substitution of (3.27) and (3.28) into (3.7), truncating the sums, and absorbing the various powers of c into the coefficients yields the final form of the rational function approximation to the normalized aperture admittance:

$$Y(s, \varepsilon_r) \approx \frac{\sum_{n=1}^{N} \sum_{p=1}^{P} \alpha_{np} (\sqrt{\varepsilon_r})^p s^n}{1 + \sum_{m=1}^{M} \sum_{q=0}^{Q} \beta_{mq} (\sqrt{\varepsilon_r})^q s^m} \tag{3.29}$$

A physical description of the approximation (3.29) is possible. For each given permittivity the admittance is specified by a set of dominant poles and zeros. For passive dielectrics, these poles and zeros remain in the left half of the s-plane. As the permittivity is varied these poles and zeros trace out loci in the s-plane which are determined by (3.27) and (3.28). In view of this discussion, an appropriate name for this approximation technique might well be "pole-zero tracking" in the s-plane. Inspection of (3.29) reveals, that for a given range of permittivities and frequencies, it is possible to obtain an equivalent circuit consisting of elements (RLC) which depend upon the permittivity of the external medium. However, for our purposes this equivalent circuit representation is neither convenient nor necessary.

A further simplification is possible. For a given range of frequencies and permittivities there exists a Taylor series approximation (polynomial approximation) for the aperture admittance.

$$Y(s,\varepsilon_r) \approx \sum_{n=1}^{N} \sum_{p=1}^{P} c_{np} (\sqrt{\varepsilon_r})^p s^n \tag{3.30}$$

This approximation will converge for frequencies within the circle of convergence centered on the origin of the s-plane with radius equal to the distance from the origin to the nearest pole of the admittance. Note that the radius of this circle of convergence depends upon the permittivity of the medium.

With suitable models available, the approximation problem becomes one of parametric modelling, i.e. the determination of the coefficients of the approximating functions. A logical technique for this purpose is the Least Squares method. Although (3.29) and (3.30) are functions of four variables, the properties of these functions reduce this task to a two-dimensional least squares problem. A convenient data set for this purpose is the computed admittance for j-axis points in the s-plane ("real" frequencies) and lossless dielectrics. A general technique for obtaining this admittance data and the details of the Least Squares method are the topic of the following section.

One final generalization is possible. Although the coefficients of the aperture admittance models presented will depend upon the physical dimensions of the waveguide and aperture, the theory of electromagnetic scale models [55] states that the admittance remains invariant under the following transformations:

$$l_2 = \frac{l_1}{x}$$

$$\sigma_2 = \sigma_1 x$$

$$\varepsilon_2 = \varepsilon_1$$

$$\mu_2 = \mu_1$$

$$s_2 = s_1 x$$

Where $l_1, \sigma_1, \varepsilon_1, \mu_1, s_1$ represent the units of length, d.c. conductivity, permittivity, permeability, and frequency of the original electromagnetic system; $l_2, \sigma_2, \varepsilon_2, \mu_2, s_2$ represent the corresponding quantities of the scaled system; and x represents the scale factor. If the conductivity of all materials in the system are assumed either infinite (perfect conductors) or zero, this states that the same admittance will be obtained for any given permittivity if one simultaneously scales the dimensions of the waveguide and aperture by a factor $1/x$ and the frequency by a factor x.. This enables the same set of coefficients to be used for a given **class** of structures providing the dimensions and frequency are suitably scaled.

3.3 Numerical Treatment

In the previous section it was demonstrated that rational function and polynomial expansions could be used to approximate the aperture admittance function. Furthermore, it was observed that the coefficients (or model parameters) of these models could be determined from the calculated admittance for "real" frequencies ω and lossless dielectrics. This computed data is obtained via a full-wave moment method solution of Maxwell's equations applied to the two-region aperture problem. The technique is efficient and accurate, taking into account the effects of radiation and energy storage in the evanescent waveguide modes and near-field.

The Method of Moments for Waveguide-Fed Aperture Problems [56]

Consider a uniform waveguide terminated in the plane z=0 by a perfectly conducting screen containing the aperture (Fig. 3.1[5]). The guide is excited by the dominant mode and the frequency of operation is low enough to ensure mono-mode operation. The half space z>0 is filled with a homogeneous, linear, isotropic, non-magnetic dielectric having relative permittivity $\varepsilon_r = \varepsilon' - j\varepsilon''$.

The equivalence principle [57] is used to divide the problem into two equivalent problems as shown in Fig. 3.2. In the waveguide region, denoted R_I, the aperture is modeled by a short circuit on which flows the equivalent magnetic current defined by,

$$\overrightarrow{M}_1 = \vec{n}_1 \times \overrightarrow{E}_t^I \tag{3.31}$$

where $\vec{n}_1$ is an outward directed normal to R_I and $\overrightarrow{E}_t^I$ is the actual electric field in the aperture at $z = 0^-$.

Similarly, in the half-space region (R_{II}) the aperture is replaced by a perfect electric conductor supporting an equivalent magnetic current defined by,

$$\overrightarrow{M}_2 = \vec{n}_2 \times \overrightarrow{E}_t^{II} \tag{3.32}$$

where $\vec{n}_2$ is an outward directed normal to R_{II} and $\overrightarrow{E}_t^{II}$ is the actual electric field in the aperture at $z = 0^+$.

The continuity of the tangential component of the electric field across the aperture requires

---

5. All figures may be found at the end of the chapter.

$$\vec{M} = \vec{M}_1 = -\vec{M}_2 \tag{3.33}$$

The remaining boundary condition to be applied is the continuity of the tangential component of the magnetic field across the aperture. The tangential magnetic field at $z = 0^-$ may be expressed in terms of $\vec{M}_1$ as,

$$\vec{H}_t^I = \vec{H}_t^{inc} + \vec{H}_t^I(\vec{M}_1) \tag{3.34}$$

where $\vec{H}_t^{inc}$ is the tangential magnetic field due to the incident waveguide mode and $\vec{H}_t^I(\vec{M}_1)$ is the tangential magnetic field due to the magnetic current $\vec{M}_1$. Both of these fields are computed with aperture covered by the perfect electric conductor.

In the half-space region, the magnetic field is produced by the magnetic current $\vec{M}_2$. In operator notation,

$$\vec{H}_t^{II} = \vec{H}_t^{II}(\vec{M}_2) \tag{3.35}$$

This field is also computed in the presence of the perfect electric conductor and, hence, image theory may be applied.

Imposing the continuity condition yields,

$$-\vec{H}_t^I(\vec{M}) - \vec{H}_t^{II}(\vec{M}) = \vec{H}_t^{inc} \tag{3.36}$$

In writing (3.36) use has been made of (3.33) and the linearity of the $\vec{H}_t$ operator.

Following the general method of moments [58], the unknown magnetic current is expressed in terms of a set of expansion functions, $\vec{M}_j$, as

$$\vec{M} = \sum_{j=1}^{N} V_j \vec{M}_j \tag{3.37}$$

where V_j are unknown amplitude coefficients and N is the total number of expansion functions used to approximate the magnetic current.

Substituting (3.37) into (3.36) and exploiting the linearity of the $\vec{H}_t$ operators leads to,

$$-\sum_{j=1}^{N} V_j \vec{H}_t^{I}(\vec{M}_j) - \sum_{j=1}^{N} V_j \vec{H}_t^{II}(\vec{M}_j) = \vec{H}_t^{inc} \tag{3.38}$$

Next, define the symmetric product

$$\langle \vec{A}, \vec{B} \rangle = \int_{Aperture} \vec{A} \cdot \vec{B}\, dS \tag{3.39}$$

and choose as weighting functions the set of expansion functions (Galerkin's method). Taking the symmetric product of (3.38) with each of the weighting functions, one obtains the following set of equations:

$$-\sum_{j=1}^{N} V_j \langle \vec{M}_i, \vec{H}_t^{I}(\vec{M}_j) \rangle - \sum_{j=1}^{N} V_j \langle \vec{M}_i, \vec{H}_t^{II}(\vec{M}_j) \rangle = \langle \vec{M}_i, \vec{H}_t^{inc} \rangle \qquad i = 1,2,\ldots,N \tag{3.40}$$

Equation (3.40) may be cast in matrix notation as,

$$[Y^I + Y^{II}] \cdot [V] = [I] \tag{3.41}$$

Comparing (3.41) and (3.40), one identifies the following terms:

The generalized aperture admittance matrix seen from the waveguide region,

$$Y_{ij}^{I} = -\langle \vec{M}_i, \vec{H}_t^{I}(\vec{M}_j) \rangle \qquad \begin{cases} i = 1,2,\ldots,N \\ j = 1,2,\ldots,N \end{cases} \tag{3.42}$$

the generalized aperture admittance matrix seen from the half-space region,

$$Y_{ij}^{II} = -\langle \vec{M}_i, \vec{H}_t^{II}(\vec{M}_j) \rangle \qquad \begin{cases} i = 1,2,\ldots,N \\ j = 1,2,\ldots,N \end{cases} \tag{3.43}$$

the source vector,

$$I_i = \langle \vec{M}_i, \vec{H}_t^{inc} \rangle \qquad i = 1,2,\ldots,N \tag{3.44}$$

and the coefficient vector,

$$V_i \qquad i = 1,2,\ldots,N$$

The solution of (3.41) for the coefficient vector yields the magnetic current, and hence the aperture electric field, according to (3.37) and (3.31).

Evaluation of the admittance matrix for the waveguide region proceeds as follows. The transverse electric and magnetic field inside the guide may be expanded in terms of the transverse mode function as:

$$\vec{E}_t = \vec{e}_0 e^{-\gamma_0 z} + \Gamma_0 \vec{e}_0 e^{\gamma_0 z} + \sum_{k=1}^{\infty} \Gamma_k \vec{e}_k e^{\gamma_k z} \tag{3.45}$$

$$\vec{H}_t = Y_0 \vec{z} \times \vec{e}_0 e^{-\gamma_0 z} - Y_0 \Gamma_0 \vec{z} \times \vec{e}_0 e^{\gamma_0 z} - \sum_{k=1}^{\infty} Y_k \Gamma_k \vec{z} \times \vec{e}_k e^{\gamma_k z} \tag{3.46}$$

Here γ_k represents the modal propagation constant defined by

$$\gamma_k = \sqrt{k_k^2 - k_o^2}$$

where k_k is the cutoff wavenumber for the k-th mode and k_o is the free space wavenumber. The other symbols denote the modal amplitudes (Γ_k), the z-directed wave admittance (Y_k), and the

transverse mode functions ($\vec{e}_k$). In particular, the index 0 refers to the incident mode. For a waveguide with perfectly conducting boundaries, the transverse mode functions are orthogonal and may be normalized such that:

$$\int\int_{guide} \vec{e}_m \cdot \vec{e}_n dS = \begin{cases} 1 & n = m \\ 0 & n \neq m \end{cases} \tag{3.47}$$

The transverse fields due to the magnetic current $\overrightarrow{M}_j$ are similar to (3.45) and (3.46), except the incident mode is not present. Hence these fields are given by,

$$\overrightarrow{E}_t(\overrightarrow{M}_j) = \sum_{k=0}^{\infty} A_{jk}\vec{e}_k e^{\gamma_k z} \tag{3.48}$$

$$\overrightarrow{H}_t(\overrightarrow{M}_j) = -\sum_{k=0}^{\infty} A_{jk} Y_k \vec{z} \times \vec{e}_k e^{\gamma_k z} \tag{3.49}$$

At z=0, equation (3.31) must hold. Therefore,

$$\overrightarrow{M}_j = \sum_{k=0}^{\infty} A_{jk}(\vec{z} \times \vec{e}_k) \tag{3.50}$$

Taking the symmetric product of this equation with $\vec{z} \times \vec{e}_l$ and exploiting the orthogonality condition (3.47), one obtains the following expression for the modal amplitudes.

$$A_{jk} = \int\int_{Aperture} \overrightarrow{M}_j \cdot (\vec{z} \times \vec{e}_k) dS \tag{3.51}$$

Note that the integration is performed over the aperture since the magnetic current vanishes elsewhere.

Finally, substituting (3.51) into (3.49) and the resulting expression for the tangential magnetic field into (3.42) one obtains the formula for the elements of the waveguide admittance matrix,

$$Y_{ij}^{I} = \sum_{k=0}^{K} \left(\int\int_{Aperture} \overrightarrow{M}_j \cdot (\vec{z} \times \vec{e}_k) dS \right) Y_k \left(\int\int_{Aperture} \overrightarrow{M}_i \cdot (\vec{z} \times \vec{e}_k) dS \right) \tag{3.52}$$

Where the infinite sum has been truncated to K modes for computational purposes.

Next the source vector, $[I]$ is evaluated. The incident magnetic field is given by the first term of (3.46). When the aperture is covered by the electric conductor the guide is short circuited. According to image theory, the tangential magnetic field at z=0 is twice the incident field, i.e.

$$\overrightarrow{H}_t^{inc} = 2Y_0 \vec{z} \times \vec{e}_0 \tag{3.53}$$

Substitution into (3.44) provides the formula for the elements of the source vector,

$$I_i = 2Y_0 \int\int_{Aperture} \overrightarrow{M}_i \cdot (\vec{z} \times \vec{e}_0) dS \tag{3.54}$$

Calculation of the half-space admittance matrix requires knowledge of the magnetic field at $z=0^+$ due to the magnetic current $\overrightarrow{M}_j$ flowing in front of the conductor. Applying image theory,

$$\overrightarrow{H}_t^{II}(\overrightarrow{M}_j) = -2j\omega \overrightarrow{F}_j - 2\nabla\psi_j \tag{3.55}$$

where $\overrightarrow{F}_j$ is the electric vector potential due to the magnetic current $\overrightarrow{M}_j$ flowing in unbounded space and ψ_j is the corresponding magnetic scalar potential. These quantities may be computed from the following potential integrals:

$$\overrightarrow{F}_j = \frac{\varepsilon}{4\pi} \int\int_{Aperture} \overrightarrow{M}_j \frac{e^{-jk|\vec{r}-\vec{r}'|}}{|\vec{r}-\vec{r}'|} dS' \tag{3.56}$$

$$\psi_j = \frac{1}{4\pi\mu_o} \iint_{Aperture} m_j \frac{e^{-jk|\vec{r}-\vec{r}'|}}{|\vec{r}-\vec{r}'|} dS' \tag{3.57}$$

where $\varepsilon = \varepsilon_o \varepsilon_r$ is the permittivity of the material filling the half-space, k is the complex wave-number in this material, $|\vec{r}-\vec{r}'|$ is the distance between the source point (primed coordinates) and the field point (unprimed coordinates) and m_j is the equivalent magnetic charge density. This latter quantity is related to the magnetic current density through the equation of continuity,

$$m_j = -\frac{\nabla \cdot \vec{M}_j}{j\omega} \tag{3.58}$$

Finally, substitution of (3.55) into (3.43) yields the formula for the elements of the free-space admittance matrix,

$$Y_{ij}^{II} = 2 \iint_{Aperture} \vec{M}_i \cdot (j\omega \vec{F}_j + \nabla \psi_j) dS \tag{3.59}$$

The total aperture admittance matrix may now be assembled according to (3.41) and solved for the unknown coefficients,

$$[V] = [Y^I + Y^{II}]^{-1} \cdot [I] \tag{3.60}$$

Once these coefficients are found, $\vec{M}$ is obtained from (3.37).

The quantity of prime importance in this study is the aperture admittance seen by the dominant mode. This is easily obtained from the knowledge of the aperture field distribution. Combining (3.31) and (3.45) allows one to write,

$$\vec{M} = \vec{z} \times \vec{E}_t|_{z=0} = (1+\Gamma_0)\vec{z} \times \vec{e}_0 + \sum_{k=1}^{K} \Gamma_k (\vec{z} \times \vec{e}_k) \tag{3.61}$$

Taking the symmetric product of (3.61) and $(\vec{z} \times \vec{e}_l)$ and exploiting the orthogonality condition (3.47) one obtains:

$$\int\int_{Aperture} \overrightarrow{M} \cdot (\vec{z} \times \vec{e}_k) dS = \begin{cases} 1+\Gamma_0 & k=0 \\ \Gamma_k & k \neq 0 \end{cases} \tag{3.62}$$

Replacing $\overrightarrow{M}$ by the expansion (3.37) yields the formula for computing the dominant mode reflection coefficient, Γ_0 and the modal amplitudes Γ_k,

$$\sum_{j=1}^{N} V_j \int\int_{Aperture} \overrightarrow{M}_j \cdot (\vec{z} \times \vec{e}_k) dS = \begin{cases} 1+\Gamma_0 & k=0 \\ \Gamma_k & k \neq 0 \end{cases} \tag{3.63}$$

Once the dominant mode reflection coefficient is computed, the usual bilinear transform is used to compute the aperture admittance.

Linear Least Squares

With an accurate technique for determining the aperture admittance at our disposal, we turn our attention to the problem of determining the model parameters. As demonstrated in section 3.1, this represents a non-linear least squares problem in the case of (3.29), whereas (3.30) reduces to the simpler linear least squares problem. We begin our discussion with the latter. A suitable technique for this purpose is Chi-squared minimization, which is based on the statistical method known as maximum likelihood estimation [59]. The basics of this technique follow.

Given a set of data points $Y_i(\omega_i, \zeta_i)$, $i = 1, .., i$, where Y_i is the admittance computed via the method of moments for the frequency ω_i and the dielectric constant $\zeta_i = \sqrt{\varepsilon'_i}$, construct the merit function

$$\chi^2 = \sum_{i=1}^{I} \left| \frac{Y_i - \sum_{k=1}^{K} a_k X_k(\omega_i, \zeta_i)}{\sigma_i} \right|^2 \tag{3.64}$$

In (3.64) a_k represents the unknown model parameters (real numbers), $X_k(\omega_i, \zeta_i)$ are the basis functions (c.f. (3.30)) defined by:

$$X_k(\omega_i, \zeta_i) = \zeta_i^p (j\omega_i)^n \tag{3.65}$$

with

$$p = 1, 2, \ldots, P$$

$$n = 1, 2, \ldots, N$$

$$k = N \times (p-1) + n$$

and σ_i is the standard deviation in Y_i. In this work, the standard deviation is assumed to be 1%, i.e.

$$\sigma_i = 0.01 \times Y_i \tag{3.66}$$

With these definitions (3.64) represents the sum, over all data points, of the square of the magnitude of the relative error vector:

$$\Delta Y_i = \frac{Y_i - Ymodel(\omega_i, \zeta_i)}{0.01 \times Y_i} \tag{3.67}$$

Minimization of (3.64) will yield the maximum likelihood parameters of the model. The relative error, as opposed to the absolute error, was chosen in the definition of the χ^2 so that small and large values of the computed admittance would contribute equally to this minimization. Since most available least squares algorithms are written for real data, it is convenient to expand (3.64) as follows:

$$\chi^2 = \sum_{i=1}^{I} \left(\frac{G_i - \sum_{k=1}^{K} a_j \Re\{X_k(\omega_i, \zeta_i)\}}{|\sigma_i|} \right)^2 + \left(\frac{B_i - \sum_{k=1}^{K} a_j \Im\{X_k(\omega_i, \zeta_i)\}}{|\sigma_i|} \right)^2 \tag{3.68}$$

where G_i and B_i are the real and imaginary part, respectively, of the normalized admittance. Finally, by defining

$$y_i = \frac{G_i}{|\sigma_i|} \qquad i = 1, 2, \ldots, I$$

$$y_{I+i} = \frac{B_i}{|\sigma_i|} \qquad i = 1, 2, \ldots, I$$

$$A_{i,k} = \frac{\Re\{X_k(\omega_i, \zeta_i)\}}{|\sigma_i|} \qquad i = 1, 2, \ldots, I$$

$$A_{I+i,k} = \frac{\Im\{X_k(\omega_i, \zeta_i)\}}{|\sigma_i|} \qquad i = 1, 2, \ldots, I$$

one obtains,

$$\chi^2 = \sum_{i=1}^{2 \times I} \left(y_i - \sum_{k=1}^{K} a_k A_{i,k} \right)^2 \tag{3.69}$$

The matrix $A_{i,k}$ appearing in (3.69) is known as the "design matrix" of the fitting problem. The minimum of (3.69) occurs where the derivative of χ^2 with respect to all K parameters a_k vanishes. This condition yields the K equations:

$$2\sum_{i=1}^{2\times I}\left(y_i - \sum_{k=1}^{K} a_k A_{ik}\right)A_{il} = 0 \qquad l = 1,2,\ldots,K \tag{3.70}$$

Interchanging the order of summations, one can write (3.70) as the matrix equation,

$$\sum_{k=1}^{K} \alpha_{lk} a_k = \beta_k \qquad l = 1,2,\ldots K \tag{3.71}$$

where

$$\alpha_{lk} = \sum_{i=1}^{2\times I} A_{ik}A_{il} \qquad \begin{cases} k = 1,2,\ldots K \\ l = 1,2,\ldots K \end{cases} \tag{3.72}$$

$$\beta_k = \sum_{i=1}^{2\times I} y_i A_{ik} \qquad k = 1,2,\ldots,K \tag{3.73}$$

In least-squares parlance, (3.71) is known as the normal equations of the least squares problem. In terms of the design matrix $[A]$ and the vector $[y]$ these equations may be written:

$$[A]^T \cdot [A] \cdot [a] = [A]^T \cdot [y] \tag{3.74}$$

where ^{T} denotes matrix transposition and $[a]$ is a column vector whose elements are the unknown parameters. Direct solution of the normal equations, however, is not the preferred method of solving the least squares problem. In many cases these equations are ill-conditioned, i.e. very close to singular. A more stable technique utilizes Singular Value Decomposition [59] to determine the best-fit parameters by direct minimization of

$$\chi^2 = |[A] \cdot [a] - [y]|^2 \tag{3.75}$$

This technique uses Householder reduction and QR decomposition [60] to decompose the $2I \times K$ design matrix $[A]$ into the product of a $2I \times K$ column-orthogonal matrix $[U]$, a $K \times K$ diagonal matrix $[W]$ with positive or zero elements, and the transpose of a $K \times K$ orthogonal matrix $[V]$.

$$[A] = [U] \cdot [W] \cdot [V]^T \tag{3.76}$$

In terms of these new matrices, the solution vector $[a]$ which minimizes (3.75) is given by:

$$[a] = [V] \cdot \left[\frac{1}{W}\right] \cdot ([U]^T \cdot [y]) \tag{3.77}$$

More details of this technique, and the FORTRAN code used, may be found in [59].

Non-Linear Least Squares

We now consider fitting model (3.29), which depends non-linearly on the parameters. As in the linear case this is accomplished by defining a merit function χ^2 and determining the parameters by its minimization. In the non-linear case, however, this minimization must proceed iteratively. The Levenberg-Marquardt method has become the standard method for non-linear least-squares fitting. This technique combines the inverse-Hessian method and the steepest descent method to simultaneously minimize a set of non-linear equations. A brief description of this algorithm follows [59].

Consider the generic merit function:

$$\chi^2(a) = \sum_{i=1}^{I} \left(\frac{y_i - y(x_i;a)}{\sigma_i} \right)^2 \tag{3.78}$$

where x_i represents the column vector of independent variables for data point i, y_i is the given ordinate for data point i, a is the vector of model parameters, and $y(x_i;a)$ is the chosen model

evaluated at x_i with parameters a.

Now consider a particular point, a in parameter space. In the vicinity of this point, the merit function (3.78) can be approximated by its Taylor series:

$$\chi^2(a+\delta a) = \chi^2(a) + \sum_{k=1}^{K} \frac{\partial \chi^2}{\partial a_k}\bigg|_a \delta a + \frac{1}{2}\sum_{k=1}^{K}\sum_{i=1}^{K} \frac{\partial^2 \chi^2}{\partial a_k \partial a_i}\bigg|_a \delta a + \ldots.$$

$$\approx c - [b]^T \cdot [\delta a] + \frac{1}{2}[\delta a]^T \cdot [A] \cdot [\delta a] \tag{3.79}$$

where

$$c \equiv \chi^2(a) \tag{3.80}$$

$$b_k \equiv -\frac{\partial \chi^2}{\partial a_k}\bigg|_a \tag{3.81}$$

$$A_{ik} = \frac{\partial^2 \chi^2}{\partial a_k \partial a_i}\bigg|_a \tag{3.82}$$

The matrix $[A]$ defined by (3.82) is called the Hessian of χ^2 at a. The gradient of (3.79) is readily obtained as:

$$\nabla \chi^2 = [A] \cdot [\delta a] - [b] \tag{3.83}$$

Hence, (3.79) will have a minimum at $a + \delta a$ when (3.83) vanishes. This implies,

$$[A] \cdot [\delta a] = [b] \tag{3.84}$$

and, the minimum will occur at:

$$a_{\min} = a + \delta a = a + [A]^{-1} \cdot [b] \tag{3.85}$$

This equation will yield the desired parameters in one iteration, providing the initial a was sufficiently close to the minimum of (3.78) for the quadratic form (3.79) to be an accurate approximation to the local behavior of χ^2. This technique is called the inverse-Hessian method for obvious reasons. When this condition is not met, one may obtain the next approximation, $a + \delta a$, to the solution by performing a line minimization along the line passing through the point a, in the direction of the local downhill gradient b. This approach is known as the steepest-descent method, mathematically it states:

$$a_{new} = a_{old} + \delta a = a_{old} + \lambda' \cdot b \tag{3.86}$$

where λ' is a positive real constant chosen small enough not to overshoot the minimum.

The Levenberg-Marquardt combines (3.85) and (3.86), the steepest-descent method being used far from the minimum, switching continuously to the inverse Hessian method as the minimum is approached. This blend of techniques is accomplished by defining the matrix $[\alpha]$ according to,

$$\alpha_{jj} = A_{jj}(1 + \lambda) \tag{3.87}$$

$$\alpha_{jk} = A_{jk} \qquad j \neq k \tag{3.88}$$

and replacing (3.84) by:

$$[\alpha] \cdot [\delta a] = [b] \tag{3.89}$$

The parameter λ is called the Marquardt parameter. When this parameter is very large, (3.89) becomes diagonal dominant approximating (3.86). For very small values of this parameter, (3.89) approximates (3.85).

The actual program used to fit (3.30) is the MINPACK [61] routine LMDER1. This routine is a modified Levenberg-Marquardt algorithm uses implicitly scaled variables to achieve scale invariance and limit the size of the correction in any direction where the function is changing rapidly. At each iteration, the algorithm determines the optimum choice for the Marquardt parameter and solves the resulting system of equations via QR decomposition. This guarantees global convergence from starting points far from the solution and a fast rate of convergence for small residuals.

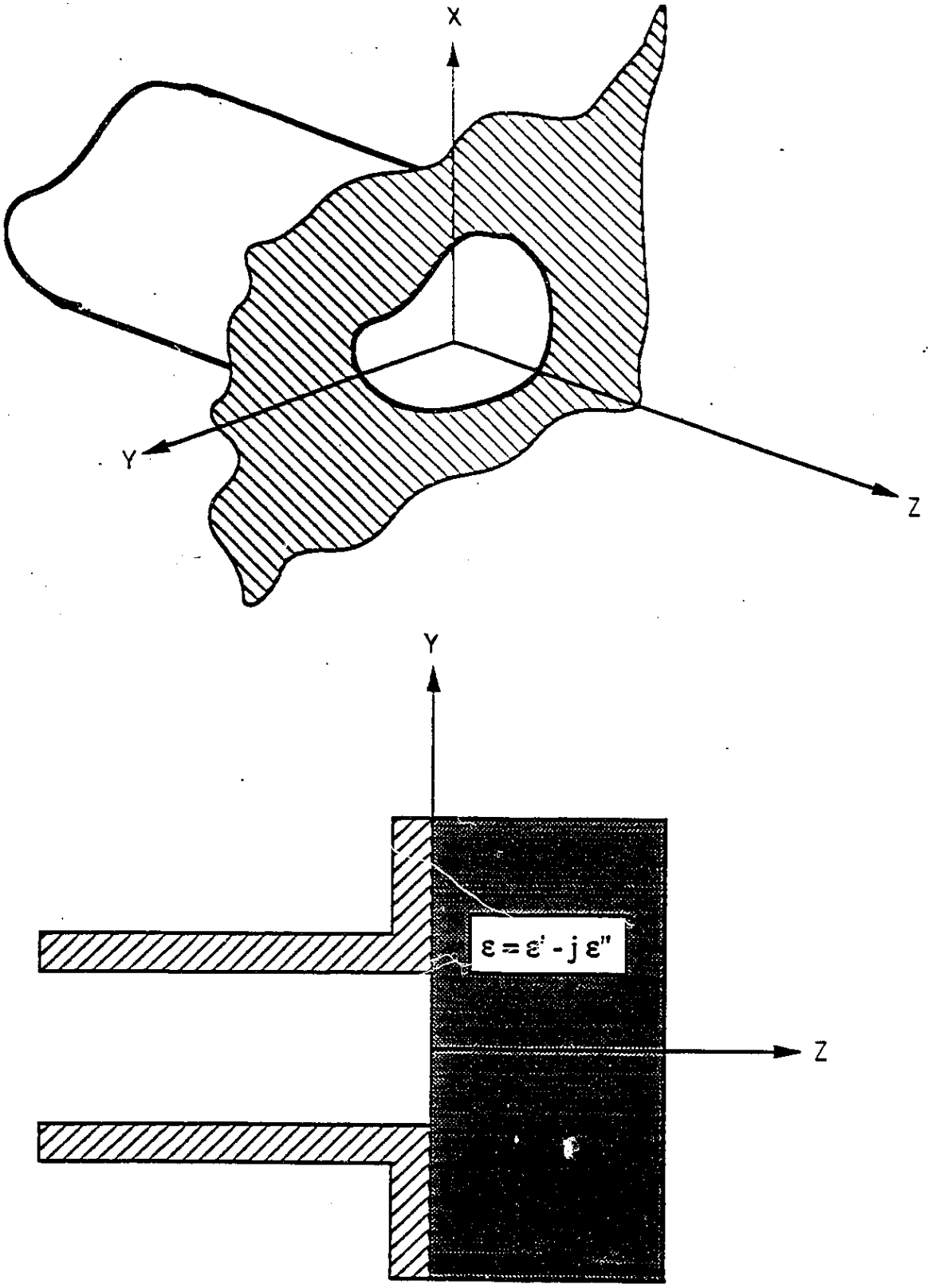

Fig. 3.1: Geometry of the General Problem

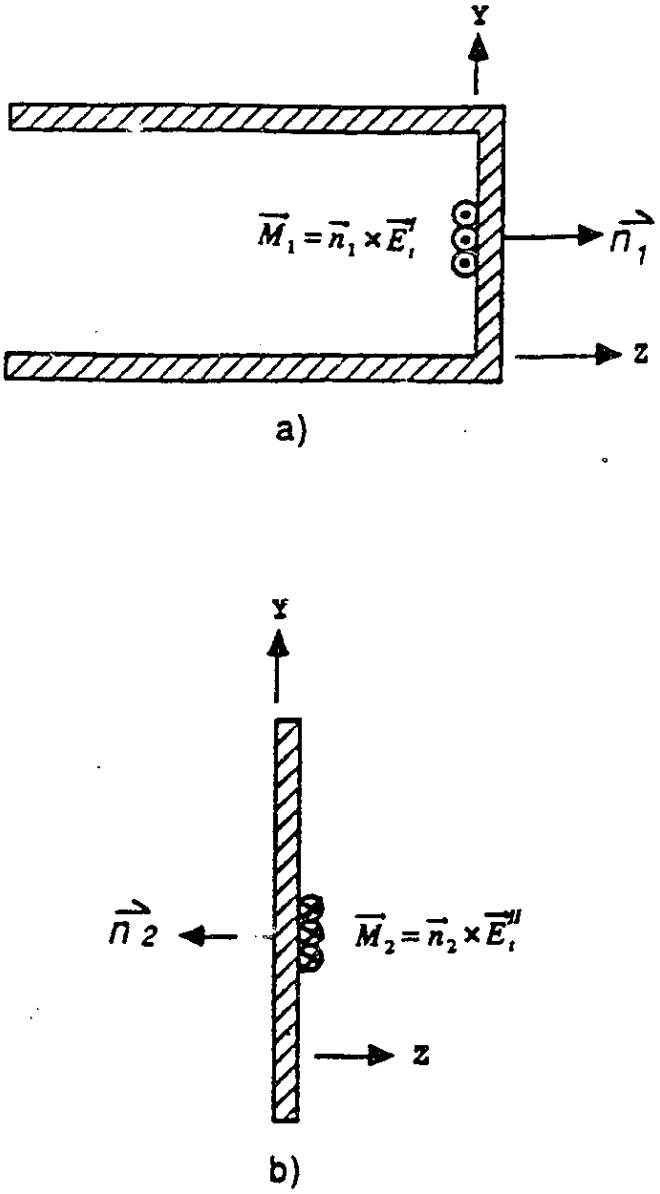

Fig. 3.2: Equivalent Magnetic Currents used in Mathematical Derivation

Chapter IV

Coaxial Lines

4.1 Introduction

The theory presented in the previous chapter made no assumptions about the specific geometry of the waveguide or aperture, and hence may be applied to open-ended hollow waveguides (rectangular, circular, elliptical etc.) or open-ended coaxial lines. In the following three chapters the general theory is specialized to the case of open-ended coaxial line. This specialization has three main purposes:

a) To verify the validity of the general theory.

b) To illustrate the general theory by a concrete example.

c) To obtain an improved model for the aperture admittance of coaxial lines.

This chapter presents the details of the method of moments as applied to the coaxial geometry. The appropriate modal expansion in the waveguide region and a suitable discretization of the aperture are given. The techniques used for the analytical and numerical evaluation of the resulting integrals are outlined. A convergence study is performed to determine the optimum, with respect to accuracy and execution time, number of modes and basis functions to retain. Finally, the computed results are validated by comparison with experiment and other numerical results.

4.2 Specifics of The Method of Moments for Coaxial Lines

The geometry of the open-ended coaxial waveguide is shown in Fig. 4.1 [6]. Cylindrical coordinates are used. The inner and outer conductors have radius a and b, respectively, and the guide is filled with a homogeneous dielectric (assumed lossless) of dielectric constant ε_c. The guide is excited by the dominant TEM mode and the discontinuity caused by the aperture and the change in permittivity excites higher order modes. Due to the ϕ-symmetry of the structure and of the incident mode, only the TM_{0n} modes, which have no ϕ variation, are excited. The transverse mode functions (transverse electric field) for this mode set may be written as:

$$\vec{e}_0 = \vec{\rho}\frac{1}{\rho\sqrt{2\pi \ln\frac{b}{a}}} \tag{4.1}$$

for the dominant mode, and

$$\vec{e}_n = \vec{\rho}\frac{\sqrt{\pi}Y_0(k_n b)k_n}{2\sqrt{Y_0^2(k_n a) - Y_0^2(k_n b)}}\{J_0'(k_n\rho)Y_0(k_n a) - J_0(k_n a)Y_0'(k_n\rho)\} \tag{4.2}$$

for the TM_{0n} modes. In these expressions $J_0(x)$ and $Y_0(x)$ correspond to the 0th order Bessel functions of the first and second kind, respectively, and the prime is used to denote differentiation with respect to the argument. The parameter k_n is the cutoff wavenumber of the nth TM mode. These parameters are obtained from the solutions of the eigenvalue equation,

$$J_0(k_n b)Y_0(k_n a) - J_0(k_n a)Y_0(k_n b) = 0 \tag{4.3}$$

The transverse mode functions have been normalized according to (3.47), as follows:

---

6. All figures and tables may be found at the end of the chapter.

$$\int_0^{2\pi}\int_a^b \vec{e}_n \cdot \vec{e}_m \rho d\rho d\phi = \begin{cases} 0 & m \neq n \\ 1 & m = n \end{cases} \tag{4.4}$$

As a consequence of the ϕ symmetry, the magnetic current vector has a single component and possesses axial symmetry. According to (3.31),

$$\vec{M} = \vec{\phi} M(\rho) \tag{4.5}$$

Hence, it is necessary to define suitable expansion functions for the scalar $M(\rho)$. For this study the method of subsectional bases is used. The aperture is divided into coaxial rings of width $\Delta\rho_j$ and the magnetic current is approximated by triangle functions as follows:

$$M_j(\rho) = \begin{cases} \dfrac{\rho - \rho_{j-2}}{\Delta\rho_{j-1}} & \rho_{j-2} \le \rho \le \rho_{j-1} \\ \dfrac{\rho_j - \rho}{\Delta\rho_j} & \rho_{j-1} \le \rho \le \rho_j \\ 0 & \text{elsewhere} \end{cases} \tag{4.6}$$

where $\Delta\rho_k = \rho_k - \rho_{k-1}$ and $j = 2, 3, \ldots, J-1$. J is the total number of expansion functions. In addition, two special expansion functions are required to include the edge effect at the inner and outer conductors.

$$M_1(\rho) = \begin{cases} \dfrac{\rho_1 - \rho}{\Delta\rho_1} & a \le \rho \le \rho_1 \\ 0 & \text{elsewhere} \end{cases} \tag{4.7}$$

$$M_J(\rho) = \begin{cases} \dfrac{\rho - \rho_{J-1}}{\Delta\rho_{J-1}} & \rho_{J-2} \le \rho \le b \\ 0 & \text{elsewhere} \end{cases} \tag{4.8}$$

This discretization is shown in Fig. 4.2, and leads to a piecewise linear approximation for the magnetic current.

Finally, substitution of these expansion functions and eigenmodes into (3.52) and (3.59) yields the expressions for the elements of the generalized admittance matrices. The details for the evaluation of these expressions is given in Appendix A.

A computer program has been developed to implement the method of moments for open-ended coaxial lines[7]. The program is written in FORTRAN and a listing may be obtained from the author upon request. A high order Romberg integration technique [62] is used for the numerical integrations and the roots of equation (4.3) are determined by a Van Wijngaarden-Dekker-Brent Method [63] which employes root bracketing, bisection and inverse quadratic interpolation to converge from the neighborhood of a root.

Input to the program are the inner and outer radii of the coaxial line, the dielectric constant of the material filling the line, the frequency of operation, the permittivity of the half-space region, the number of expansion functions, and the number of waveguide modes. Outputs of the program are the amplitudes of the magnetic current expansion functions, the modal amplitudes, the aperture admittance seen by the dominant mode, and the complex power at the aperture plane.

4.3 Results

Several convergence studies were performed to validate the program. In these studies there were two parameters which could be varied: the number of waveguide modes considered, and the number of unknowns (number of subsections). Table 4.1 shows the calculated admittance

7.The author has also developed a similar program for open-ended rectangular waveguides.

of a 3.6 mm line at 1 GHz as a function of these two parameters for the homogeneous case. It was observed that, if the number of expansion functions is greater than the number of waveguide modes, unacceptable results were obtained. This phenomenon is similar to the relative convergence problem encountered in the mode matching method [48]. For this reason, only cases for which the number of modes was at least equal to the number of expansion functions were considered.

Examination of Table 4.1 reveals that very little is gained by increasing the number of waveguide modes beyond the number of subsections. This behavior was evident in for all cases examined.

To investigate the effect of frequency on the convergence of the method several other frequencies were considered. Table 4.2 shows the results for the homogeneous case at 18 GHz. Again convergence is evident. Several other convergence studies were performed at various frequencies and for various values for the half-space permittivity. In all cases the behavior was similar. Based on these results it is concluded that a reasonable trade-off between execution time and accuracy for a 3.6 mm line operating at frequencies up to 20 GHz occurs when 11 waveguide modes and 11 subsections are retained. For these values, the execution time per analysis on a VAX 3200 computer varies from 2 minutes to 4.5 minutes. This variability in execution time is due to number of samples required for convergence during the numerical integrations. More samples, and coreespondingly longer execution times are required at higher frequencies.

Convergence, however, does not guarantee accuracy. Therefore, a comparison of computed results with published data and measurements was made. Table 4.3 compares the extrapolated value of the reflection coefficient obtained by the present method with that obtained by Jenkins et. al. [24] for the case of a 14 mm line radiating into a lossy dielectric ($\varepsilon_r = 100.0 - j100.0$) at

1 GHz. These extrapolated values were obtained from the formula:

$$\Gamma_n = \Gamma_\infty + \frac{\alpha}{n} + \frac{\beta}{n^2} \tag{4.9}$$

where α and β are constants and Γ_n is the reflection obtained by considering n modes. The solution of the problem for three progressively finer discretizations allows one to compute an estimate for the limiting value of the reflection coefficient. The result presented by Jenkins was obtained by three different numerical methods, all yielding virtually identical results ($\Delta \mid \Gamma \mid \leq 0.0001, \Delta\phi \leq 0.014°$).

Measurements were performed using a 3.6 mm semi-rigid coaxial line approximately 10 cm in length. The line was fitted with an SMA connector and the end of the line was polished flat using fine sand paper. No ground plane was used in the measurements. Measurements were performed with an HP8510 network analyzer with time domain capabilities. The frequency range 50 MHz - 20.050 GHz was selected, and a sweep time of 50 seconds in step mode was used. Following calibration with factory standards, the probe was connected to the test port of an HP8510 automatic network analyzer. The probe was short circuited using a piece of metal foil, and the time domain options of the 8510 were used to establish the reference plane at the end of the sensor and the gating feature was used to remove the reflection due to the connector. A magnitude slope of 0.038 dB/GHz was added to account for the loss in the line. The probe was immersed in water at 25° C and the aperture reflection coefficient was measured. Figure 4.3 compares the results obtained via the moment method to those obtained by this measurement procedure. For the numerical analysis, the permittivity of water at 25° C was calculated according to the Cole-Cole equation:

$$\varepsilon_r = \varepsilon' - j\varepsilon'' = \varepsilon_\infty + \frac{\varepsilon_s - \varepsilon_\infty}{1 + (j\omega\tau)^{1-\alpha}} \tag{4.10}$$

Where ε_∞ is the optical permittivity, ε_s is the static permittivity, τ is the characteristic relaxation time, and α is the distribution parameter. The values of these parameters for water at 25° C are given in Table 4.4.

The measurements were repeated using methanol and air as the test material. The Cole-Cole parameters for material are also given in Table 4.4. Figures 4.4 and 4.5 compare the measured and calculated results for these cases.

The results presented in this chapter demonstrate the accuracy of the method of moments. Although no analytical attempt has been made to quantify the errors in this method it is evident that these errors are "insignificant in comparison with the predicted measurement uncertainties" [24]. Hence, for the remainder of this work, the results computed by the method of moments will be considered to be the stnadard values in assessing the performance of the approximate models. This indirect validation of the new models is not only convenient but also necessary, since only a limited number of standard materials are available for measurements.

Table 4.1

Admittance of a 3.6 mm Coaxial Line at 1 GHz

$a = 0.456mm, \quad b = 1.49mm, \quad \varepsilon_c = \varepsilon_r = 2.1 - j0.0$

Number of modes	Number of unknowns	G [$x10^{-9}$ mS]	ΔG [$x10^{-9}$ mS]	B [$x10^{-4}$ mS]	ΔB [$x10^{-4}$ mS]
9	9	1.9837	-	2.8264	-
11	9	1.9839	0.0002	2.8266	0.0002
13	9	1.9839	0.0000	2.8266	0.0000
15	9	1.9839	0.0000	2.8266	0.0000
17	9	1.9839	0.0000	2.8266	0.0000
11	11	1.9769	**-0.0070**	2.8122	**-0.0144**
13	11	1.9770	0.0001	2.8124	0.0002
15	11	1.9771	0.0001	2.8125	0.0001
17	11	1.9771	0.0000	2.8125	0.0000
13	13	1.9728	**-0.0043**	2.8035	**-0.0090**
15	13	1.9729	0.0001	2.8036	0.0001
17	13	1.9729	0.0000	2.8037	0.0001
15	15	1.9701	**-0.0028**	2.7976	**-0.0061**
17	15	1.9701	0.0000	2.7977	0.0001
17	17	1.9682	**-0.0019**	2.7934	**-0.0043**

Table 4.2

Admittance of a 3.6 mm Coaxial Line at 18 GHz

$a = 0.456mm, \quad b = 1.49mm, \quad \varepsilon_c = \varepsilon_r = 2.1 - j0.0$

Number of modes	Number of unknowns	G [x10^{-4} mS]	ΔG [x10^{-4} mS]	B [x10^{-3} mS]	ΔB [x10^{-3} mS]
9	9	1.8623	-	5.4802	-
11	11	1.8548	-0.0075	5.4529	-0.0273
13	13	1.8503	-0.0045	5.4360	-0.0169
15	15	1.8473	-0.0030	5.4246	-0.0114
17	17	1.8452	-0.0021	5.4165	-0.0081

Table 4.3

Reflection Coefficient of a 14 mm Coaxial Line at 1 GHz

$a = 2.333mm, \quad b = 7.549mm, \quad \varepsilon_c = 2.15, \quad \varepsilon_r = 100.0 - j100.0$

Magnitude of reflection coefficient			Phase of reflection coefficient		
$\lvert\Gamma_\infty\rvert$ This Work	$\lvert\Gamma_\infty\rvert$ Jenkins [24]	$\Delta\lvert\Gamma_\infty\rvert$	$\phi°$ This Work	$\phi°$ Jenkins [24]	$\Delta\phi°$
0.6709	0.6715	0.0006	-165.52	-165.55	-0.03

Table 4.4

Cole-Cole Parameters of Water and Methanol at 25° C

Parameter	Water	Methanol
ε_s	78.3	33.7
ε_∞	4.5	4.35
τ [ps]	8.12	49.64
α	0.02	0.043

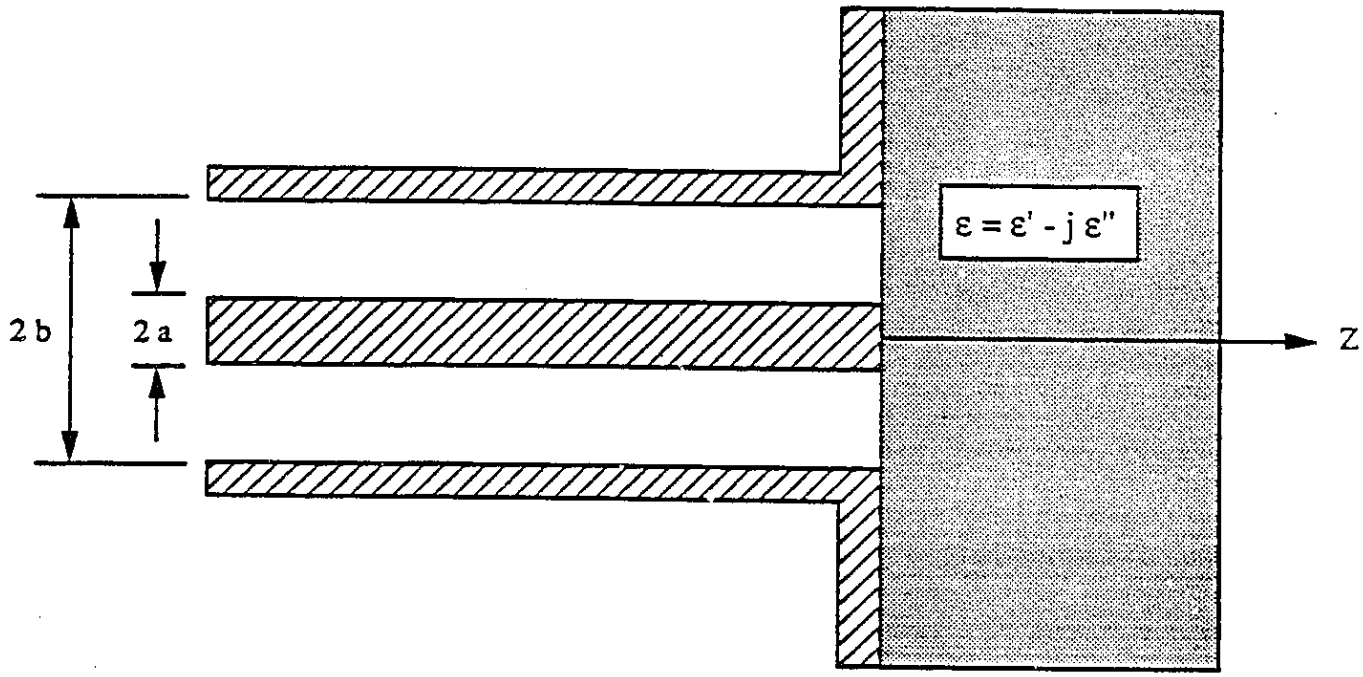

Fig. 4.1: Geometry of Open-Ended Coaxial Line

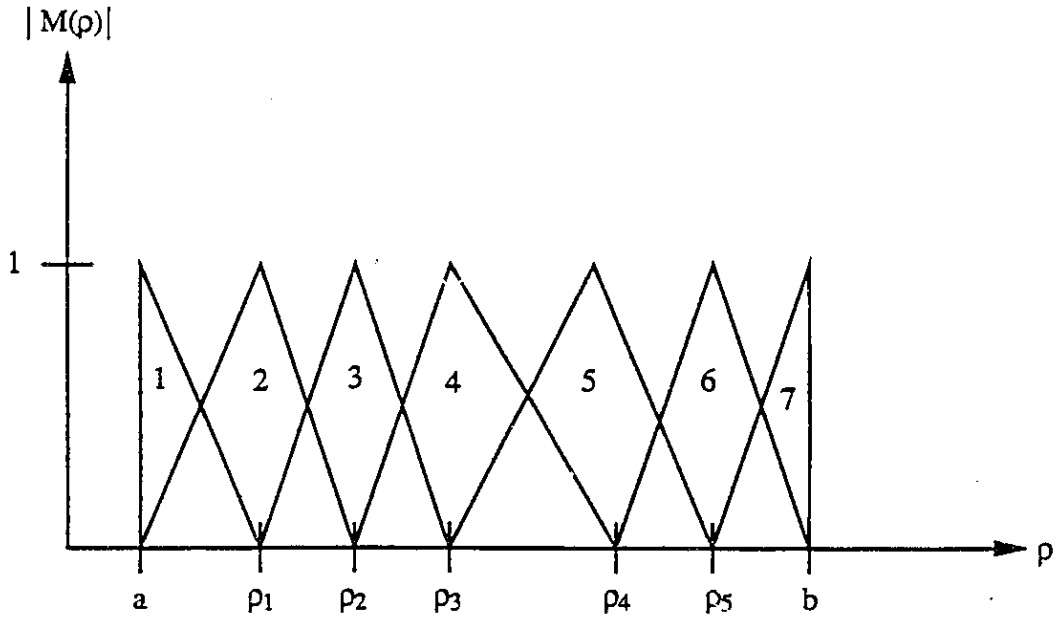

Fig. 4.2: Moment Method Discretization of Coaxial Aperture

FIG. 4.3:

APERTURE REFLECTION COEFFICIENT OF 3.6 mm COAXIAL LINE RADIATING INTO WATER AT 25° C

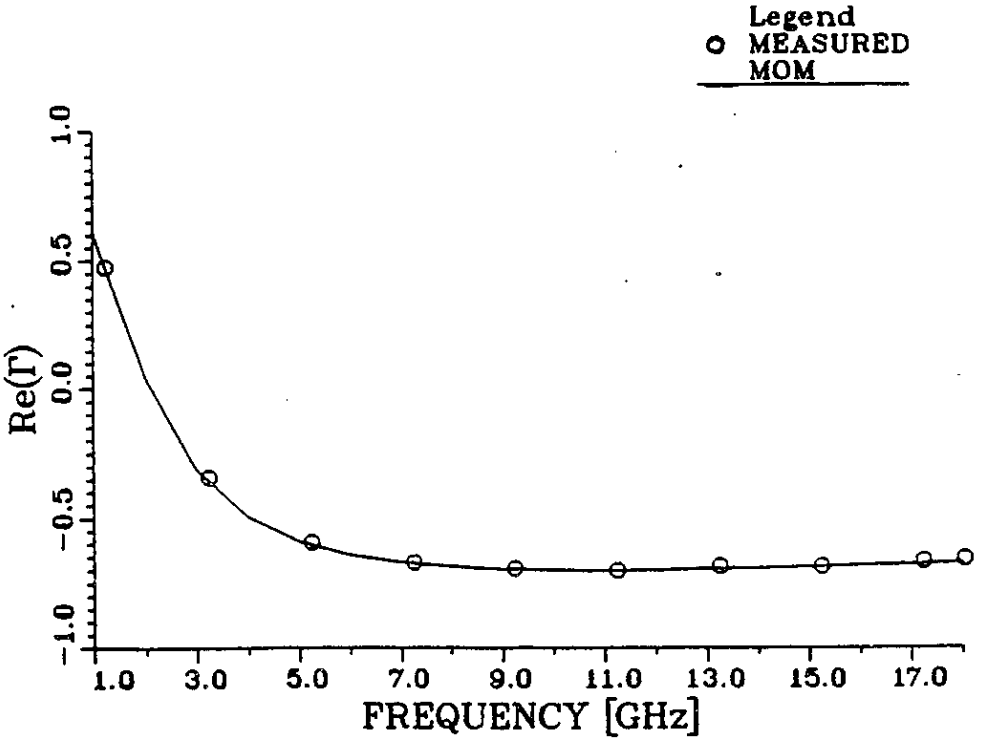

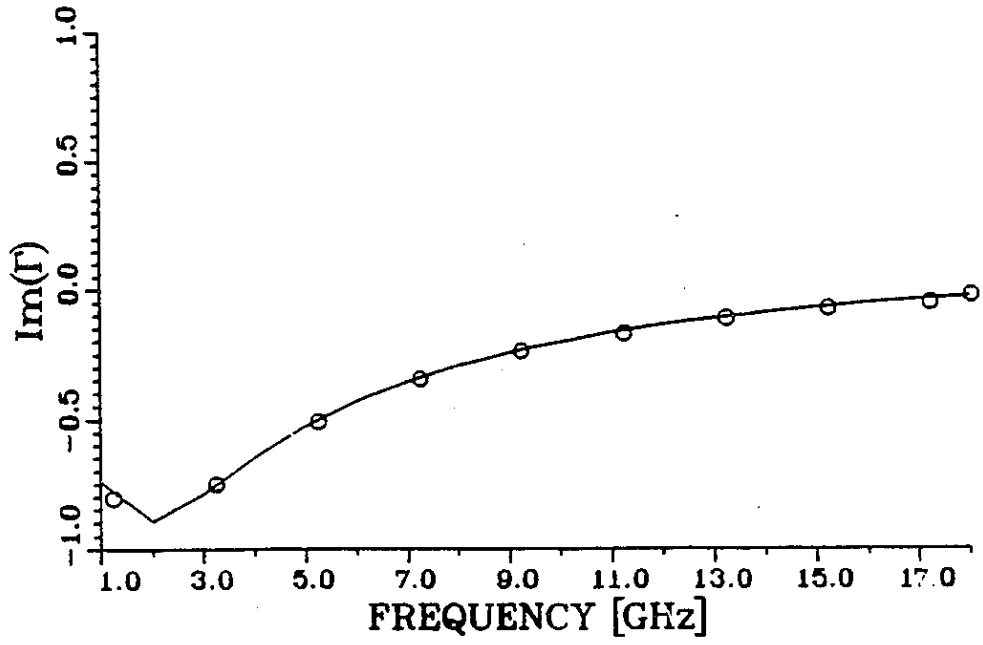

FIG. 4.4:

APERTURE REFLECTION COEFFICIENT OF 3.6 mm COAXIAL LINE RADIATING INTO METHANOL AT 25° C

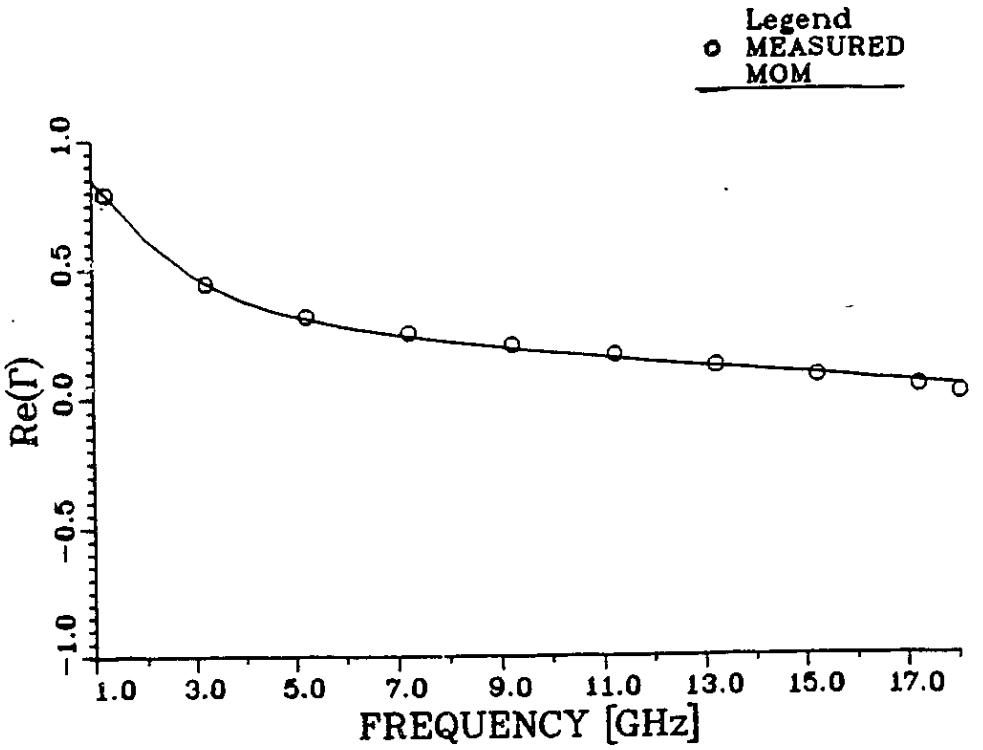

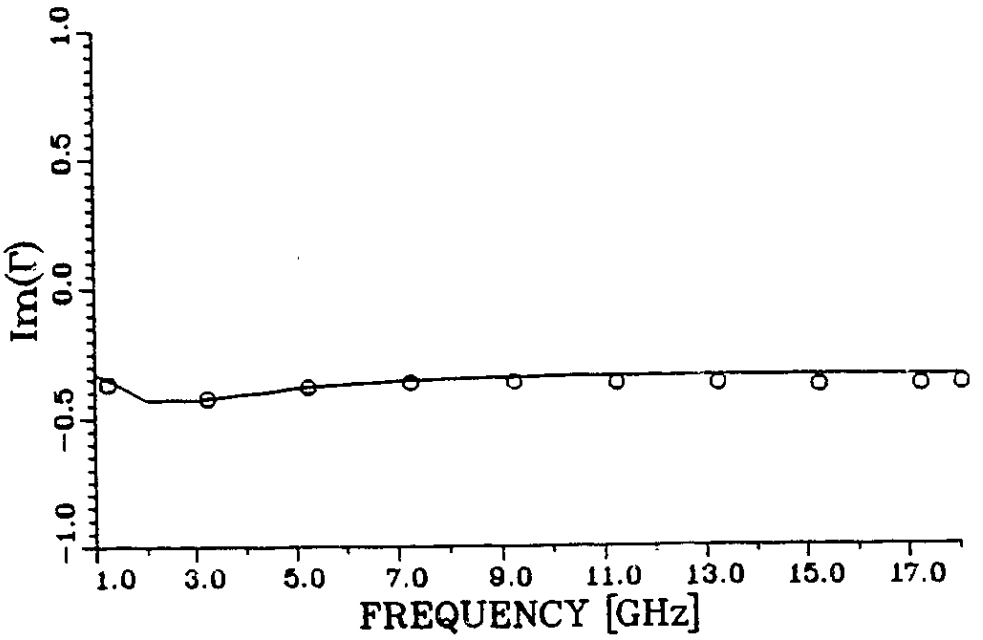

FIG. 4.5:

APERTURE REFLECTION COEFFICIENT OF 3.6 mm COAXIAL LINE RADIATING INTO AIR

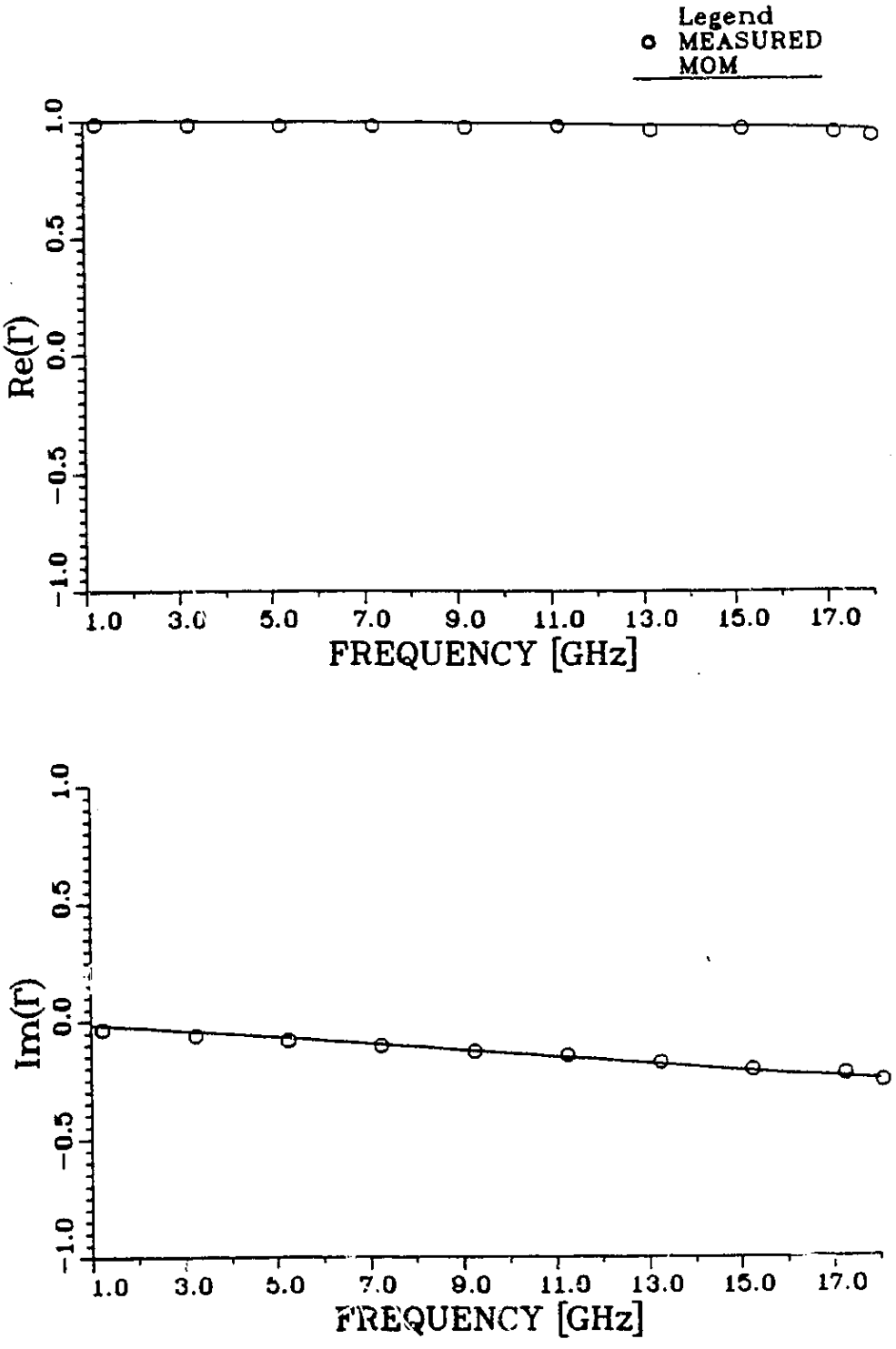

Chapter V

Rational Approximations

5.1 Introduction

Having gained some confidence in the method of moments, we may proceed with the curve fitting. In this chapter we consider the rational function approximation discussed in Section 3.2 (c.f. (3.29)). The moment method program is used to compute the aperture admittance of an open-ended coaxial line in contact with several lossless dielectrics. Since this numerical treatment requires specific numbers, the case of a 3.6 mm, 50 Ω semi-rigid coaxial line is considered. This line has an inner conductor of radius $a = 0.456 \quad mm$ and an outer conductor of inner radius $b = 1.49 \quad mm$. The space between the conductors is filled with Teflon which has a dielectric constant of $\varepsilon_c = 2.1$. The analysis is performed over the frequency range 1 GHz - 20 GHz. The upper frequency limit was chosen for ease of measurement, whereas the lower frequency limit was chosen since the linear models discussed in Section 2 are adequate up to this frequency.

As discussed at the end of Section 3.2, however, the theory of electromagnetic scale models may be used to generalize these results to any 50 Ω, Teflon filled line by a suitable frequency normalization. The most common frequency normalization is expressed in terms of the free-space wavenumber, k_0 and the inner conductor radius a. All results in this chapter are given in terms of the normalized frequency $k_0 a$.

Section 5.2 considers the direct problem. The results of the moment method analysis are presented and the model parameters are determined based on this data. The resulting rational function model is given and the accuracy of this model in predicting the aperture admittance for lossless and lossy dielectrics is demonstrated.

The formulation of the inverse problem, based on the rational function model, is presented in Section 5.3. This problem reduces to one of determining the roots of a polynomial. A numerical technique which uses deflation and root polishing to find all the roots of this polynomial is proposed. Several examples illustrate that the selection of the appropriate root, which is based on physical requirements, is straight forward and leads to a unique solution.

Finally, a sensitivity and uncertainty analysis is performed in Section 5.4. This is perhaps one of the most important consequences of obtaining an accurate closed form expression for the aperture admittance. Explicit expressions for the sensitivity and resulting measurement uncertainties of the probe enables one to choose the optimum probe for a given application and to recognize the inherent limitations on the attainable accuracy. Furthermore, valuable insight is gained which may prove useful in the design of probes with better sensitivity.

5.2 The Direct Problem

The moment method program described in Chapter IV was used to compute the aperture admittance of a 3.6 mm, 50 Ω coaxial line in contact with lossless dielectrics. This line has an inner conductor of radius $a = 0.456 \quad mm$ and an outer conductor of inner radius $b = 1.49 \quad mm$. The line is loaded with Teflon. The analysis was performed every 1 GHz for frequencies in the range 1 - 20 GHz. This frequency range corresponds to a normalized frequency ($k_0 a$) range of 0.01 - 0.19. At each frequency 56 dielectric constants ($\varepsilon'' = 0$) in the range 1 - 80 were considered[8] yielding a total of 1120 data points. The aperture field was modelled by 11 expansion functions (triangle basis functions) and 10 TM_{0n} modes were retained in the coaxial line. Execution time per analysis varied from 2 - 4.5 minutes on a VAX 3200 computer. The results of this analysis are given in Figures 5.1 - 5.3[9], which show the real part, the imaginary part and the magnitude of the normalized admittance, respectively. The grid lines defining these surfaces are drawn every second data point for clarity.

With a suitable data set available, we turn out attention to the determination of the model parameters. The rational function approximation is given by (3.29), and is repeated here for convenience.

$$Ymodel = \frac{\sum_{n=1}^{N} \sum_{p=1}^{P} \alpha_{np} (\sqrt{\varepsilon_r})^p s^n}{1 + \sum_{m=1}^{M} \sum_{q=0}^{Q} \beta_{mq} (\sqrt{\varepsilon_r})^q s^m} \tag{5.1}$$

8. Most biological materials have dielectric constants which lie in this range.
9. All figures and tables may be found at the end of the chapter.

The non-linear least squares routine LMDER1 [61] was used to perform the curve fit. In order to determine the number of model parameters required the following observation was made. As the dielectric constant increases, the s-plane poles and zeros of the admittance function moved closer to the origin. Hence, the most rapid variation of the aperture admittance vs. frequency will occur for the largest dielectric constant. A one dimensional fit versus frequency for a dielectric constant of 80 indicated that four s-plane poles and four s-plane zeros were sufficient to model the frequency variation. In order to deduce a suitable number of terms in the sums over $\sqrt{\epsilon_r}$, a simple convergence study was performed. Beginning with P=Q=4, the number of terms was increased until an appropriate χ^2 was obtained. Table 5.1 shows the convergence of this quantity, where

$$\chi^2 = \sum_{i=1}^{1120} \left| \frac{Ymom_i - Ymodel_i}{0.01 \times Ymom_i} \right|^2 \tag{5.2}$$

Based on these results, eight terms (P=Q=8) were retained, yielding a total of 68 model parameters. The normalized best fit parameters are given in Tables 5.2 and 5.3., where the following normalizations were used:

$$\hat{\alpha}_{np} = \frac{\alpha_{np}}{a^n} \qquad \left[\frac{\sec^n}{\text{Gigarad}^n \cdot \text{meters}^n} \right] \tag{5.3}$$

$$\hat{\beta}_{mq} = \frac{\beta_{mq}}{a^m} \qquad \left[\frac{\sec^m}{\text{Gigarad}^m \cdot \text{meters}^m} \right] \tag{5.4}$$

where $a = 0.456 \times 10^{-3}$ m is the radius of the inner conductor of the line analyzed.

Ten significant figures are given in Tables 5.2 and 5.3. In all computation, however, 16 significant figures (double precision data type) were used.

With these normalized parameters the universal model for the normalized aperture admittance of 50 Ω, Teflon lines is:

$$Ymodel = \frac{\sum_{n=1}^{4}\sum_{p=1}^{8} \hat{\alpha}_{np}(\sqrt{\varepsilon_r})^p (sa)^n}{1+\sum_{m=1}^{4}\sum_{q=0}^{8} \hat{\beta}_{mq}(\sqrt{\varepsilon_r})^q (sa)^m} \tag{5.5}$$

Where s is specified in Giga-radians per second, and a is specified in meters.

Figure 5.4 shows the magnitude of the resulting relative error in the admittance over the range of data considered. The relative error is defined in parts-per-thousand as follows,

$$\Delta Y = \frac{Ymodel - Ymom}{|Ymom|} \times 1000 \qquad ppt \tag{5.6}$$

In order to verify the accuracy of the model for lossy dielectrics a comparison with the moment method results was performed at several frequencies. Figure 5.5 is a plot of the magnitude of the relative error (5.6) for a normalized frequency $k_0 a = 0.01$ and permittivities in the range

$$1 \le \varepsilon' \le 75$$
$$0 \le \varepsilon'' \le -35 \tag{5.7}$$

Grid lines are drawn for

$$\varepsilon' = 1, 5, 10, \ldots, 75$$
$$\varepsilon'' = 0, -5, -10, \ldots -35$$

Figure 5.6 - 5.9 are similar plots for normalized frequencies of 0.05, 0.10, 0.14 and 0.19, respectively. Note that the scale for the relative error is in parts-per-thousand [ppt]. Examination

of these plots reveals that the relative error is very small, and relatively constant, for relative permittivities which lie inside the circle of radius $R = 40$ center at $C = 40 - j0$. This is in agreement with the theory presented in Chapter 3 concerning the radius of convergence of the Taylor series. Furthermore, the error is largest for materials having very large loss tangents. This is not a concern in practice, since very few materials have loss tangents larger than one.

From the results presented, one concludes that the error in using the approximating function (5.5) is negligible in comparison with typical measurement uncertainties and may be used with confidence for $0.01 \le k_0 a \le 0.19$ and $|\varepsilon_r - 40| \le 40$.

5.3 The Inverse Problem

We turn our attention now to the solution of the inverse problem. Given a measured admittance, what is the permittivity of the external medium? Define the following functions:

$$b_p = \sum_{m=1}^{4} \hat{\alpha}_{mp} (sa)^m \qquad p = 1, 2, \ldots, 8 \tag{5.8}$$

$$b_0 = 0 \tag{5.9}$$

$$c_q = \sum_{m=1}^{4} \beta_{mq} (sa)^m \qquad q = 1, 2, \ldots, 8 \tag{5.10}$$

$$c_0 = 1 + \sum_{m=1}^{4} \beta_{m0} (sa)^m \tag{5.11}$$

$$\zeta = \sqrt{\varepsilon_r} \tag{5.12}$$

Where, as usual, the principal value of the square root is implied in (5.12). In terms of these new quantities, (5.5) may be written as

$$Y = \frac{\sum_{p=0}^{8} b_p \zeta^p}{\sum_{q=0}^{8} c_q \zeta^q} \tag{5.13}$$

Considering Y to be the measured quantity, the desired permittivity is related (via (5.12)) to the solutions of:

$$\sum_{i=0}^{8} (b_i - Y c_i)\zeta^i = 0 \tag{5.14}$$

Mathematically, (5.14) is multi-valued, yielding eight solutions. These solutions are easily determined numerically. The technique used in this work is Laguerre's method [63] which uses deflation and root polishing to determine all of the roots of (5.13) to machine accuracy. For double precision data types this corresponds to a relative error of approximately 2.7×10^{-17}, which may be considered negligible. The error in the solution of the inverse problem is thus dominated by the error in the coefficients b_i, c_i and the measured admittance, the latter being the dominant factor. A detailed discussion of this measurement uncertainty is presented in the following section.

Selection of the appropriate root is based on physical considerations. Experience shows that the mapping (5.5) is one-to-one for permittivities in the range:

$$|\varepsilon_r| \leq 80$$

$$0° \leq \tan\left(\frac{-\varepsilon''}{\varepsilon'}\right) < -90°$$

for which the model is valid [10]. Hence, only one root is admissible. In order to verify this statement, the inverse problem is solved for several frequencies. The method of moments is used to compute the admittance of the probe for permittivities in the range specified by (5.7) and for the normalized frequencies k_0a=0.01, 0.05, 0.10, 0.14, and 0.19. Using these computed admittances, the roots of (5.14) are found by Laguerre's method. In all cases only one admissible root is obtained. For brevity, only the results for k_0a=0.19 are given in Table 5.4. These results are typical of those obtained at all frequencies. The actual criteria used for the selection of the appropriate root was:

$$|\varepsilon_r| \leq 80$$

$$0.2° \leq \tan\left(\frac{-\varepsilon''}{\varepsilon'}\right) < -90°$$

This range was arbitrarily chosen since, for lossless dielectrics, a very small relative error in the loss factor lead to solutions with $\varepsilon'' < 0$.

5.4 Sensitivity and Uncertainty Analysis

Perhaps the most important implication of obtaining a closed form expression for the admittance of the probe is that it permits an analytical investigation of the sensitivity of the probe for permittivity measurements, and of the related measurement uncertainty. This information is vital for the correct choice of probe for a given application. We begin our discussion by defining

---

10. An analytical verification of this statement is possible but has not been attempted.

sensitivity and showing its relationship to measurement uncertainty. In doing so, it is assumed that the model parameters are exact. This ignores the error involved in approximating the admittance by the rational function.

The sensitivity of a function f to variations in parameter A is defined as:

$$S_A^f = \frac{|A|}{|f|}\frac{\partial f}{\partial A} \tag{5.15}$$

In terms of this sensitivity, the relative change in the function for perturbations in the independent variables may be written as:

$$\frac{\Delta f}{|f|} = S_A^f \frac{\Delta A}{|A|} + S_B^f \frac{\Delta B}{|B|} + S_C^f \frac{\Delta C}{|C|} + \ldots \tag{5.16}$$

Where $A, B, \ldots$ represent the independent variables and $\Delta A, \Delta B, \ldots$. are the corresponding perturbations.

In the present case, the quantities of interest are the aperture reflection coefficient[11] (Γ), the measurement frequency (s), and the relative permittivity of the external medium (ε_r). The relevant expression is thus;

$$\frac{\Delta\Gamma}{|\Gamma|} = S_\varepsilon^\Gamma \frac{\Delta\varepsilon_r}{|\varepsilon_r|} + S_s^\Gamma \frac{\Delta s}{|s|} \tag{5.17}$$

---

11. The aperture reflection coefficient is the measured quantity and is related to the aperture admittance by the bi-linear transformation

$$\Gamma = \frac{1-Y}{1+Y}$$

With modern automatic network analyzers, the uncertainty in the measurement frequency is very small. Hence, the second term of (5.17) may be neglected. Solving the resulting expression for the relative change in the permittivity for a given change in the reflection coefficient, one obtains:

$$\frac{\Delta\varepsilon_r}{|\varepsilon_r|} = \frac{1}{S_\varepsilon^\Gamma} \frac{\Delta\Gamma}{|\Gamma|} \tag{5.18}$$

This last equation represents the relative uncertainty in the permittivity due to the measurement uncertainty of the network analyzer. It is apparent, therefore, that the sensitivity is a critical parameter in probe selection. A large sensitivity will ensure good measurement resolution and small measurement uncertainties. An explicit expression for the sensitivity of open-ended coaxial lines may be obtained as follows.

Applying definition (5.15) and the chain rule for differentiation, one obtains:

$$S_\varepsilon^\Gamma = \frac{|\varepsilon_r|}{|\Gamma|} \frac{\partial Y}{\partial \zeta} \frac{\partial \zeta}{\partial \varepsilon_r} \frac{\partial \Gamma}{\partial Y} \tag{5.19}$$

Expressing Γ in terms of the admittance (see footnote 11, p.67), and carrying out the differentiation yields:

$$S_\varepsilon^\Gamma = -\frac{|\varepsilon_r|\,|1+Y|}{|1-Y|\,\zeta(1+Y)^2} \frac{\partial Y}{\partial \zeta} \tag{5.20}$$

Where the final derivative is obtained by straightforward differentiation of (5.5). It must be remembered that the sensitivity is a **complex** function of frequency and permittivity. Any rigorous uncertainty analysis must consider the complex nature of this function. For illustrative

purposes, however, the magnitude of (5.20) is evaluated for several normalized frequencies and material permittivities. The results are presented in Fig. 5.10-5.14 for normalized frequencies $k_0a = 0.01, 0.05, 0.10, 0.14$, and 0.15. The quantity plotted is the inverse of the sensitivity:

$$\log_{10}\left(\frac{1}{|S_\varepsilon^\Gamma|}\right) \tag{5.21}$$

Where the logarithm is taken for obvious reasons. With reference to (5.18), the interpretation of these plots are straightforward, large positive values of (5.21) correspond to large measurement uncertainty, whereas large negative values correspond to small measurement uncertainty. Inspection of these plots reveals that electrically small apertures yield lower uncertainties for materials with large permittivity (ex. high water content material) whereas electrically large apertures yield smaller uncertainties for materials with small permittivities.

It is interesting to note that a significant dip occurs in the inverse sensitivity along the line $\varepsilon' \approx 1$. This may be attributed to the fact that a matched condition ($\Gamma \rightarrow 0$) occurs in this region and that the inverse sensitivity is proportional to the reflection coefficient. Nevertheless, this dip does indeed correspond to a region of low uncertainty for permittivity measurements since network analyzers offer almost constant relative uncertainty for the measurement of the reflection coefficient.

Hence, we see that the benefits of having a closed form expression for the sensitivity go beyond being able to quatify the measurement uncertainty. By differentiating (5.20) the optimum k_0a, that is the normalized frequency which minimizes $\frac{\Delta\varepsilon_r}{|\varepsilon_r|}$, can be found. This enables one to choose the optimum aperture size for any dielectric at any desired frequency.

Furthermore, similar models for other waveguide and aperture geometries are easily obtained. A comparison of the sensitivity of various geometries will reveal the optimum geometry for a given application.

Table 5.1: Convergence of the Least Squares Fit	
P=Q	χ^2
4	15.29
5	4.036
6	0.9789
7	0.5303
8	0.4808

Table 5.2: Best Fit Numerator Parameters of Rational Model $\hat{\alpha}_{np}$				
p \ n	1	2	3	4
1	-8.722935960E-2	-2.736691458E-1	-1.331006537E+0	-1.786212838E+2
2	2.771453557E+0	2.677771388E+0	-1.362520251E+2	-1.238502220E+2
3	-4.554783138E-1	2.528569538E+1	2.897578856E+2	4.687150602E+2
4	1.478100521E-1	-3.162043715E+0	-1.283998714E+2	-1.498663651E+2
5	-2.795124463E-2	1.111641620E+0	4.915768480E+1	1.025494262E+1
6	3.109709465E-3	-1.785393900E-1	-6.173278690E+0	2.981787613E+1
7	-1.884650574E-4	1.271588489E-2	3.385300196E-1	-3.894272872E+0
8	4.792334923E-6	-2.961361621E-4	-5.138860166E-3	1.704865497E-1

Table 5.3: Best Fit Denominator Parameters of Rational Model β_{mq}				
q \ m	1	2	3	4
0	1.179822339E+0	-6.215241209E+1	-2.421351711E+2	-1.301296937E+3
1	9.232343254E+0	1.290383908E+2	3.614243321E+2	2.951231536E+3
2	5.702906421E-1	-4.071091715E+1	-9.551098369E+1	-3.052392656E+3
3	-2.125883946E-1	2.110289940E+1	6.893079687E+1	2.104569939E+3
4	7.771185355E-2	-2.738208768E+0	8.102513739E+0	-8.078160667E+2
5	-1.662311920E-2	2.100809324E-1	1.530034858E+0	2.096199949E+2
6	1.819660462E-3	-1.603532831E-2	-5.611239306E-1	-2.517959967E+1
7	-9.594515436E-5	1.219194488E-3	4.993129279E-2	1.485669226E+0
8	2.029455124E-6	-3.811355733E-5	-1.251988868E-3	-3.307737882E-2

Table 5.4: Solution of the Inverse Problem for k_0a=0.19

ε_r		ε_r solution		$\Delta\varepsilon_r$ [%]	
ε'	ε''	ε'	ε''	Re	Im
1.000E+00	-3.500E+01	8.873E-01	-3.506E+01	-0.32	-0.18
5.000E+00	-3.500E+01	4.947E+00	-3.507E+01	-0.15	-0.20
1.000E+01	-3.500E+01	9.999E+00	-3.506E+01	0.00	-0.17
1.500E+01	-3.500E+01	1.503E+01	-3.504E+01	0.07	-0.10
2.000E+01	-3.500E+01	2.004E+01	-3.501E+01	0.09	-0.02
2.500E+01	-3.500E+01	2.503E+01	-3.498E+01	0.07	0.04
3.000E+01	-3.500E+01	3.002E+01	-3.497E+01	0.04	0.07
3.500E+01	-3.500E+01	3.499E+01	-3.496E+01	-0.01	0.08
4.000E+01	-3.500E+01	3.997E+01	-3.497E+01	-0.05	0.06
4.500E+01	-3.500E+01	4.495E+01	-3.498E+01	-0.08	0.03
5.000E+01	-3.500E+01	4.994E+01	-3.501E+01	-0.10	-0.01
5.500E+01	-3.500E+01	5.494E+01	-3.503E+01	-0.10	-0.05
6.000E+01	-3.500E+01	5.995E+01	-3.506E+01	-0.08	-0.09
6.500E+01	-3.500E+01	6.496E+01	-3.508E+01	-0.05	-0.11
7.000E+01	-3.500E+01	6.998E+01	-3.508E+01	-0.02	-0.11
7.500E+01	-3.500E+01	7.500E+01	-3.507E+01	0.00	-0.08
1.000E+00	-3.000E+01	9.236E-01	-3.000E+01	-0.25	0.01
5.000E+00	-3.000E+01	4.957E+00	-3.002E+01	-0.14	-0.07
1.000E+01	-3.000E+01	9.989E+00	-3.003E+01	-0.04	-0.09
1.500E+01	-3.000E+01	1.501E+01	-3.002E+01	0.03	-0.06
2.000E+01	-3.000E+01	2.002E+01	-3.001E+01	0.05	-0.02
2.500E+01	-3.000E+01	2.502E+01	-2.999E+01	0.04	0.02
3.000E+01	-3.000E+01	3.001E+01	-2.998E+01	0.02	0.04
3.500E+01	-3.000E+01	3.499E+01	-2.998E+01	-0.01	0.04
4.000E+01	-3.000E+01	3.998E+01	-2.998E+01	-0.04	0.03
4.500E+01	-3.000E+01	4.497E+01	-2.999E+01	-0.06	0.01
5.000E+01	-3.000E+01	4.996E+01	-3.001E+01	-0.06	-0.02
5.500E+01	-3.000E+01	5.496E+01	-3.003E+01	-0.06	-0.05
6.000E+01	-3.000E+01	5.997E+01	-3.005E+01	-0.05	-0.07
6.500E+01	-3.000E+01	6.497E+01	-3.007E+01	-0.04	-0.09
7.000E+01	-3.000E+01	6.998E+01	-3.007E+01	-0.03	-0.09
7.500E+01	-3.000E+01	7.498E+01	-3.006E+01	-0.03	-0.08

Table 5.4: Solution of the Inverse Problem
for k_0a=0.19
(Continued)

ε_r		ε_r solution		$\Delta\varepsilon_r$ [%]	
ε'	ε''	ε'	ε''	Re	Im
1.000E+00	-2.500E+01	9.684E-01	-2.497E+01	-0.13	0.11
5.000E+00	-2.500E+01	4.977E+00	-2.500E+01	-0.09	0.01
1.000E+01	-2.500E+01	9.991E+00	-2.501E+01	-0.03	-0.03
1.500E+01	-2.500E+01	1.500E+01	-2.501E+01	0.00	-0.03
2.000E+01	-2.500E+01	2.001E+01	-2.500E+01	0.02	-0.01
2.500E+01	-2.500E+01	2.501E+01	-2.500E+01	0.02	0.01
3.000E+01	-2.500E+01	3.000E+01	-2.499E+01	0.01	0.02
3.500E+01	-2.500E+01	3.500E+01	-2.499E+01	-0.01	0.02
4.000E+01	-2.500E+01	3.999E+01	-2.499E+01	-0.03	0.01
4.500E+01	-2.500E+01	4.498E+01	-2.500E+01	-0.03	0.00
5.000E+01	-2.500E+01	4.998E+01	-2.501E+01	-0.04	-0.02
5.500E+01	-2.500E+01	5.498E+01	-2.503E+01	-0.03	-0.05
6.000E+01	-2.500E+01	5.998E+01	-2.504E+01	-0.03	-0.07
6.500E+01	-2.500E+01	6.499E+01	-2.506E+01	-0.02	-0.09
7.000E+01	-2.500E+01	6.998E+01	-2.507E+01	-0.02	-0.10
7.500E+01	-2.500E+01	7.497E+01	-2.508E+01	-0.04	-0.10
1.000E+00	-2.000E+01	1.002E+00	-1.998E+01	0.01	0.11
5.000E+00	-2.000E+01	4.995E+00	-1.999E+01	-0.02	0.04
1.000E+01	-2.000E+01	9.996E+00	-2.000E+01	-0.02	0.00
1.500E+01	-2.000E+01	1.500E+01	-2.000E+01	0.00	-0.01
2.000E+01	-2.000E+01	2.000E+01	-2.000E+01	0.01	0.00
2.500E+01	-2.000E+01	2.500E+01	-2.000E+01	0.01	0.01
3.000E+01	-2.000E+01	3.000E+01	-2.000E+01	0.00	0.01
3.500E+01	-2.000E+01	3.500E+01	-2.000E+01	-0.01	0.01
4.000E+01	-2.000E+01	3.999E+01	-2.000E+01	-0.02	0.00
4.500E+01	-2.000E+01	4.499E+01	-2.000E+01	-0.02	-0.01
5.000E+01	-2.000E+01	4.999E+01	-2.001E+01	-0.02	-0.03
5.500E+01	-2.000E+01	5.499E+01	-2.003E+01	-0.01	-0.04
6.000E+01	-2.000E+01	6.000E+01	-2.004E+01	0.00	-0.06
6.500E+01	-2.000E+01	6.500E+01	-2.006E+01	0.00	-0.09
7.000E+01	-2.000E+01	7.000E+01	-2.008E+01	0.00	-0.11
7.500E+01	-2.000E+01	7.499E+01	-2.010E+01	-0.02	-0.13

Table 5.4: Solution of the Inverse Problem
for k_0a=0.19
(Continued)

ε_r		ε_r solution		$\Delta\varepsilon_r$ [%]	
ε'	ε''	ε'	ε''	Re	Im
1.000E+00	-1.500E+01	1.011E+00	-1.500E+01	0.08	0.01
5.000E+00	-1.500E+01	5.002E+00	-1.500E+01	0.01	0.01
1.000E+01	-1.500E+01	9.999E+00	-1.500E+01	0.00	0.00
1.500E+01	-1.500E+01	1.500E+01	-1.500E+01	0.00	0.00
2.000E+01	-1.500E+01	2.000E+01	-1.500E+01	0.00	0.00
2.500E+01	-1.500E+01	2.500E+01	-1.500E+01	0.00	0.00
3.000E+01	-1.500E+01	3.000E+01	-1.500E+01	0.00	0.00
3.500E+01	-1.500E+01	3.500E+01	-1.500E+01	0.01	0.00
4.000E+01	-1.500E+01	4.000E+01	-1.500E+01	0.01	0.00
4.500E+01	-1.500E+01	4.500E+01	-1.500E+01	0.01	0.01
5.000E+01	-1.500E+01	5.000E+01	-1.501E+01	0.00	0.02
5.500E+01	-1.500E+01	5.501E+01	-1.502E+01	0.01	0.03
6.000E+01	-1.500E+01	6.002E+01	-1.503E+01	0.03	0.05
6.500E+01	-1.500E+01	6.503E+01	-1.505E+01	0.04	0.08
7.000E+01	-1.500E+01	7.003E+01	-1.508E+01	0.04	0.12
7.500E+01	-1.500E+01	7.502E+01	-1.513E+01	0.03	0.16
1.000E+00	-1.000E+01	9.983E-01	-1.001E+01	0.02	0.07
5.000E+00	-1.000E+01	5.000E+00	-1.000E+01	0.00	0.01
1.000E+01	-1.000E+01	1.000E+01	-1.000E+01	0.00	0.00
1.500E+01	-1.000E+01	1.500E+01	-1.000E+01	0.00	0.00
2.000E+01	-1.000E+01	2.000E+01	-1.000E+01	0.00	0.00
2.500E+01	-1.000E+01	2.500E+01	-1.000E+01	0.00	0.00
3.000E+01	-1.000E+01	3.000E+01	-1.000E+01	0.00	0.00
3.500E+01	-1.000E+01	3.500E+01	-1.000E+01	0.00	0.00
4.000E+01	-1.000E+01	4.000E+01	-1.000E+01	0.00	0.00
4.500E+01	-1.000E+01	4.500E+01	-1.000E+01	0.00	0.00
5.000E+01	-1.000E+01	5.000E+01	-1.000E+01	0.01	0.01
5.500E+01	-1.000E+01	5.502E+01	-1.001E+01	0.03	0.02
6.000E+01	-1.000E+01	6.003E+01	-1.002E+01	0.05	0.03
6.500E+01	-1.000E+01	6.505E+01	-1.004E+01	0.08	0.06
7.000E+01	-1.000E+01	7.007E+01	-1.008E+01	0.10	0.11
7.500E+01	-1.000E+01	7.508E+01	-1.014E+01	0.11	0.18

Table 5.4: Solution of the Inverse Problem
for k_0a=0.19
(Continued)

ε_r		ε_r solution		$\Delta\varepsilon_r$ [%]	
ε'	ε''	ε'	ε''	Re	Im
1.000E+00	-5.000E+00	9.994E-01	-4.996E+00	-0.01	0.07
5.000E+00	-5.000E+00	5.000E+00	-5.000E+00	-0.01	0.00
1.000E+01	-5.000E+00	1.000E+01	-5.000E+00	0.00	0.00
1.500E+01	-5.000E+00	1.500E+01	-5.000E+00	0.00	0.00
2.000E+01	-5.000E+00	2.000E+01	-5.000E+00	0.00	0.00
2.500E+01	-5.000E+00	2.500E+01	-5.000E+00	0.00	0.00
3.000E+01	-5.000E+00	3.000E+01	-5.000E+00	0.00	0.00
3.500E+01	-5.000E+00	3.500E+01	-5.000E+00	0.00	0.00
4.000E+01	-5.000E+00	4.000E+01	-5.000E+00	0.00	0.00
4.500E+01	-5.000E+00	4.500E+01	-4.999E+00	0.00	0.00
5.000E+01	-5.000E+00	5.001E+01	-4.996E+00	0.01	0.01
5.500E+01	-5.000E+00	5.502E+01	-4.993E+00	0.03	0.01
6.000E+01	-5.000E+00	6.004E+01	-4.994E+00	0.07	0.01
6.500E+01	-5.000E+00	6.508E+01	-5.006E+00	0.12	0.01
7.000E+01	-5.000E+00	7.012E+01	-5.044E+00	0.18	0.06
7.500E+01	-5.000E+00	7.517E+01	-5.121E+00	0.22	0.16
1.000E+00	0.000E+00	1.000E+00	-6.701E-07	0.00	0.00
5.000E+00	0.000E+00	5.000E+00	3.159E-05	0.00	0.00
1.000E+01	0.000E+00	1.000E+01	-2.901E-05	0.00	0.00
1.500E+01	0.000E+00	1.500E+01	-4.193E-05	0.00	0.00
2.000E+01	0.000E+00	2.000E+01	-1.943E-04	0.00	0.00
2.500E+01	0.000E+00	2.500E+01	-4.502E-04	0.00	0.00
3.000E+01	0.000E+00	3.000E+01	-7.967E-04	0.00	0.00
3.500E+01	0.000E+00	3.500E+01	-1.069E-03	0.00	0.00
4.000E+01	0.000E+00	4.000E+01	-5.035E-04	-0.01	0.00
4.500E+01	0.000E+00	4.500E+01	2.655E-03	-0.01	0.01
5.000E+01	0.000E+00	5.000E+01	1.030E-02	0.00	0.02
5.500E+01	0.000E+00	5.501E+01	2.416E-02	0.02	0.04
6.000E+01	0.000E+00	6.004E+01	4.186E-02	0.06	0.07
6.500E+01	0.000E+00	6.509E+01	5.071E-02	0.14	0.08
7.000E+01	0.000E+00	7.018E+01	2.718E-02	0.26	0.04
7.500E+01	0.000E+00	7.528E+01	-6.314E-02	0.37	0.08

Fig. 5.1: Normalized Aperture Conductance
of a Coaxial Line in Contact with Lossless Dielectrics
Computed via the Method of Moments

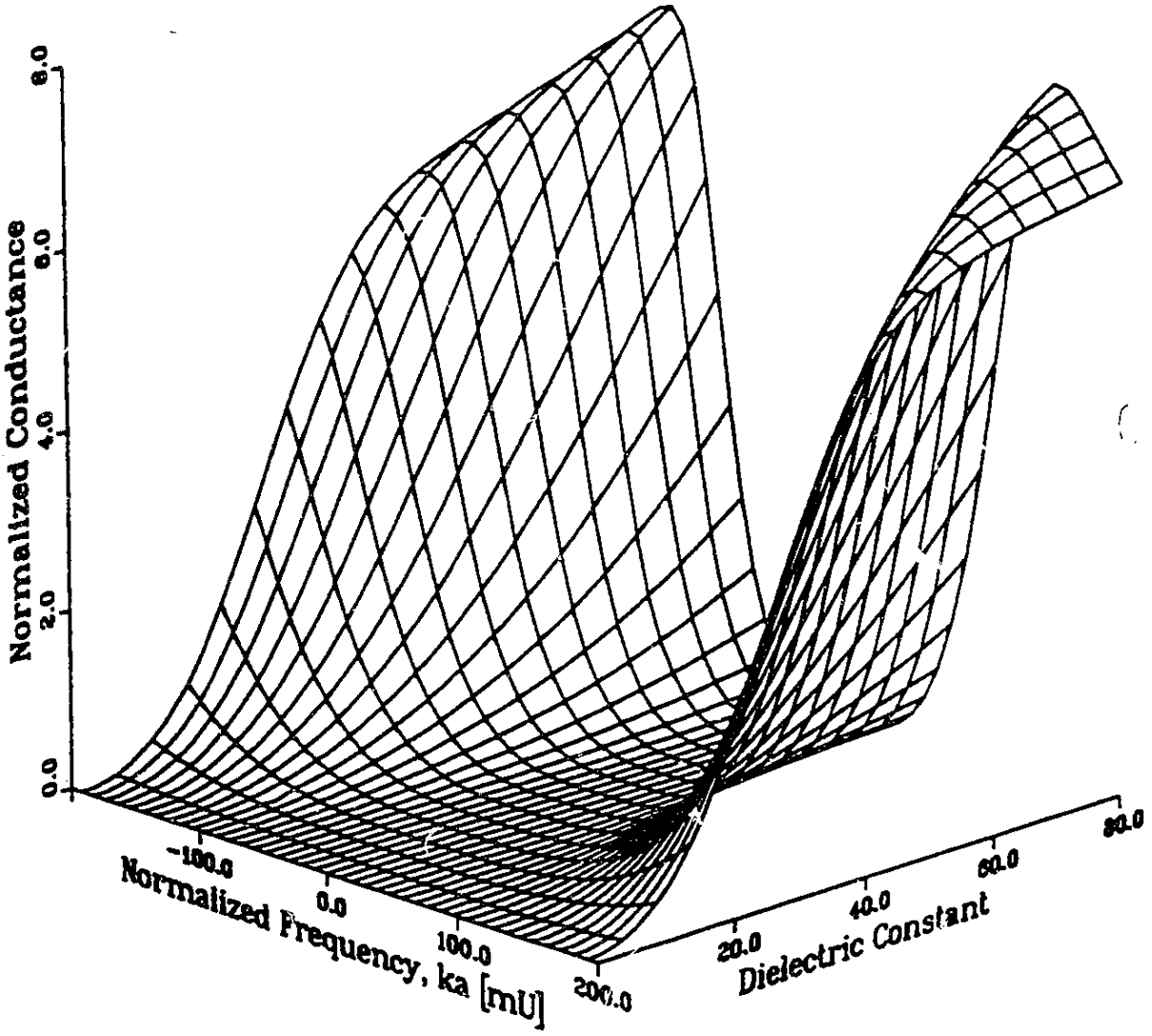

Fig. 5.2: Normalized Aperture Susceptance
of a Coaxial Line in Contact with Lossless Dielectrics
Computed via the Method of Moments

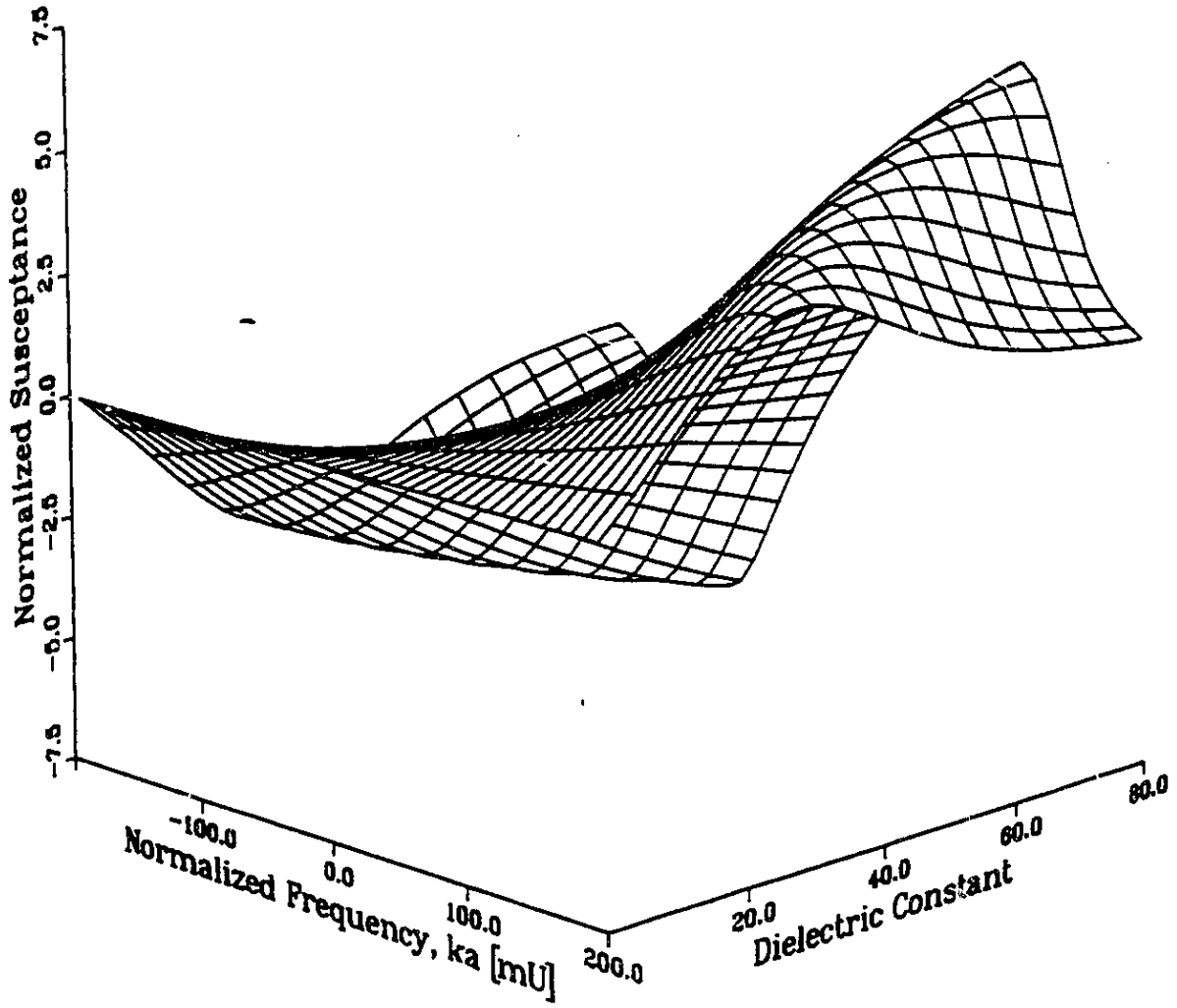

Fig. 5.3: Magnitude of the Normalized Aperture Admittance of a Coaxial Line in Contact with Lossless Dielectrics Computed via the Method of Moments

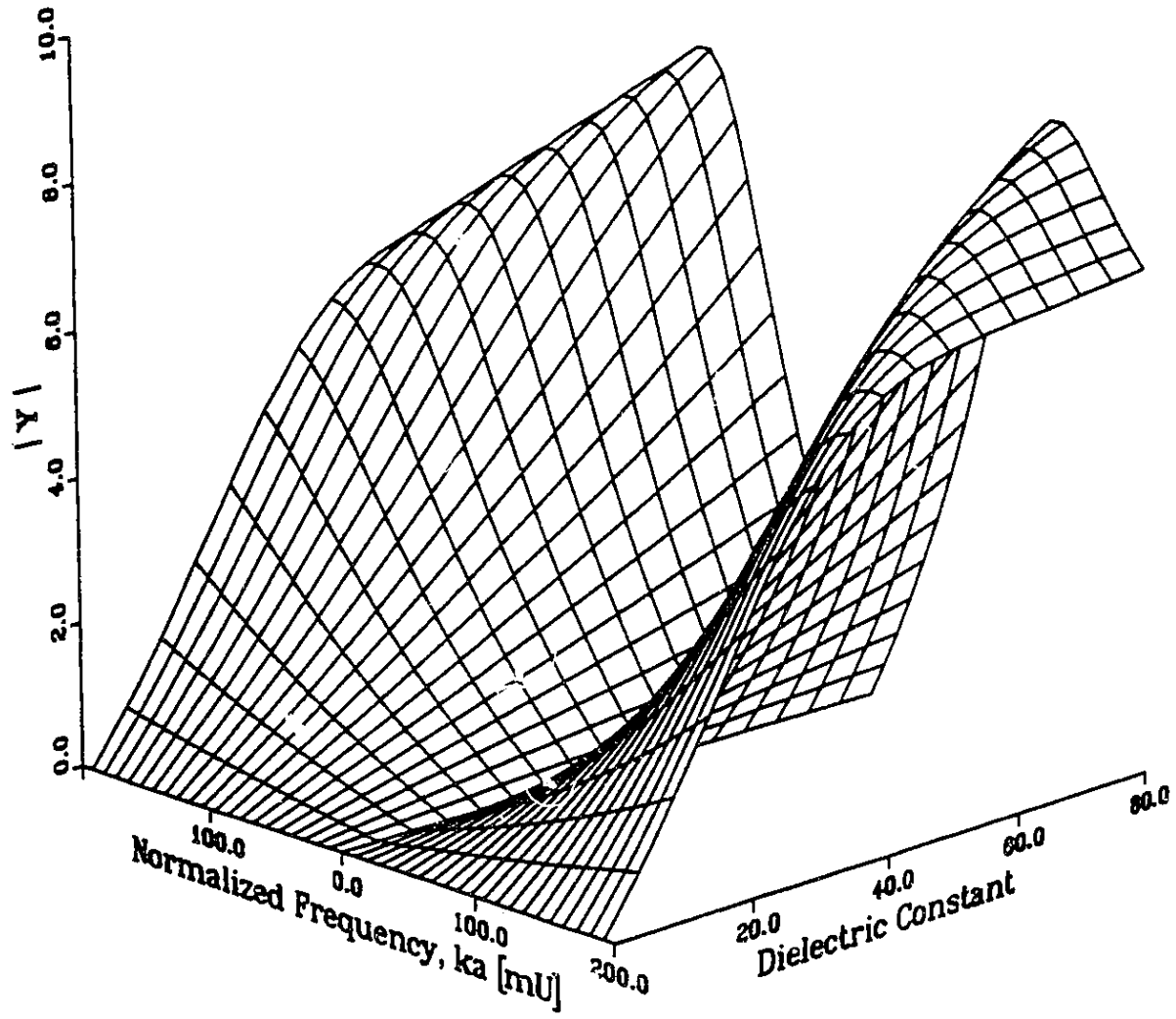

Fig. 5.4: Relative Error in the Magnitude of the Aperture Admittance as Computed by the Rational Function Approximation

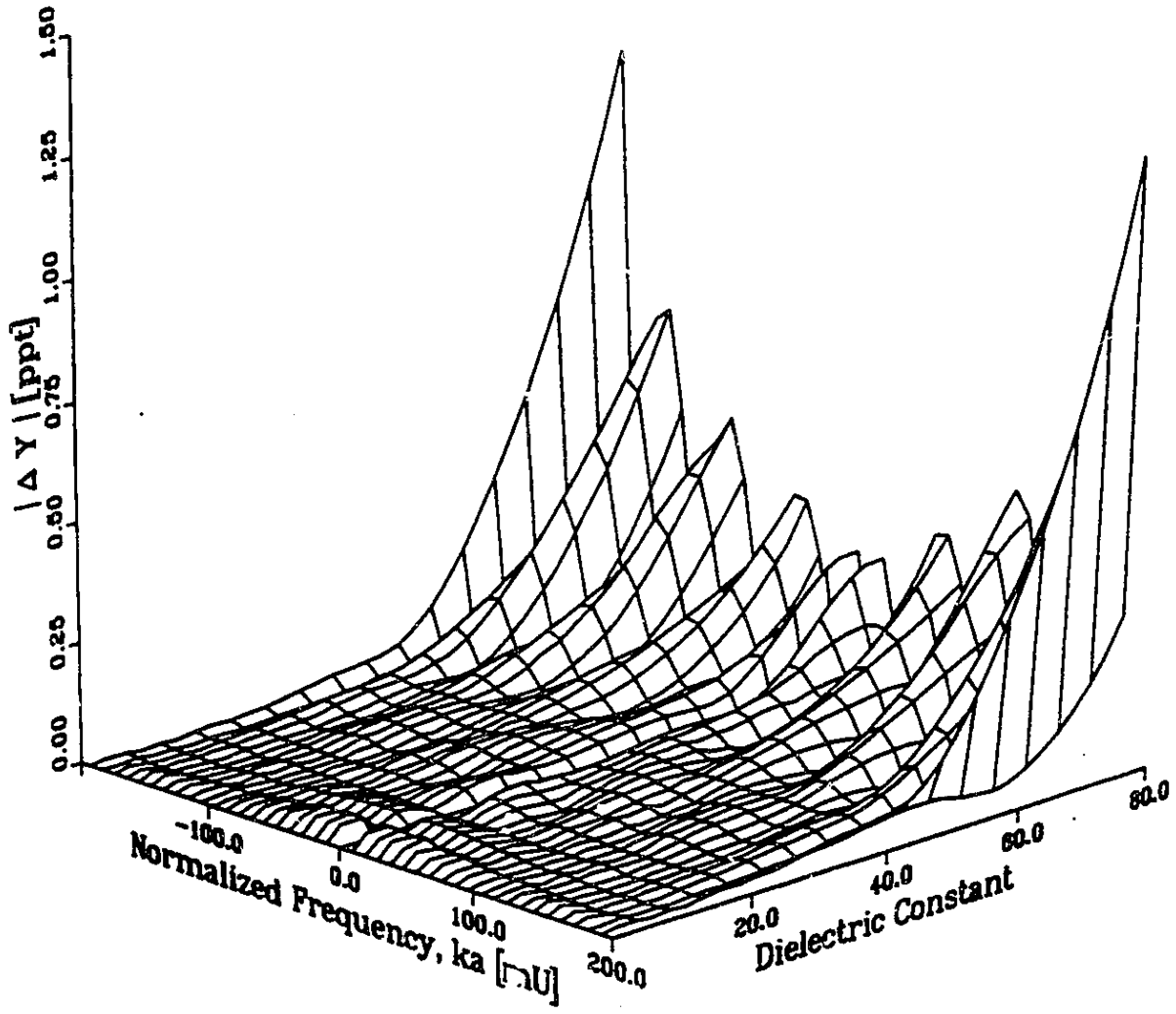

Fig. 5.5: Relative Error in the Computed Aperture Admittance of a Coaxial Line in Contact with Lossy Dielectrics for a Normalized Frequency, Ka=0.01

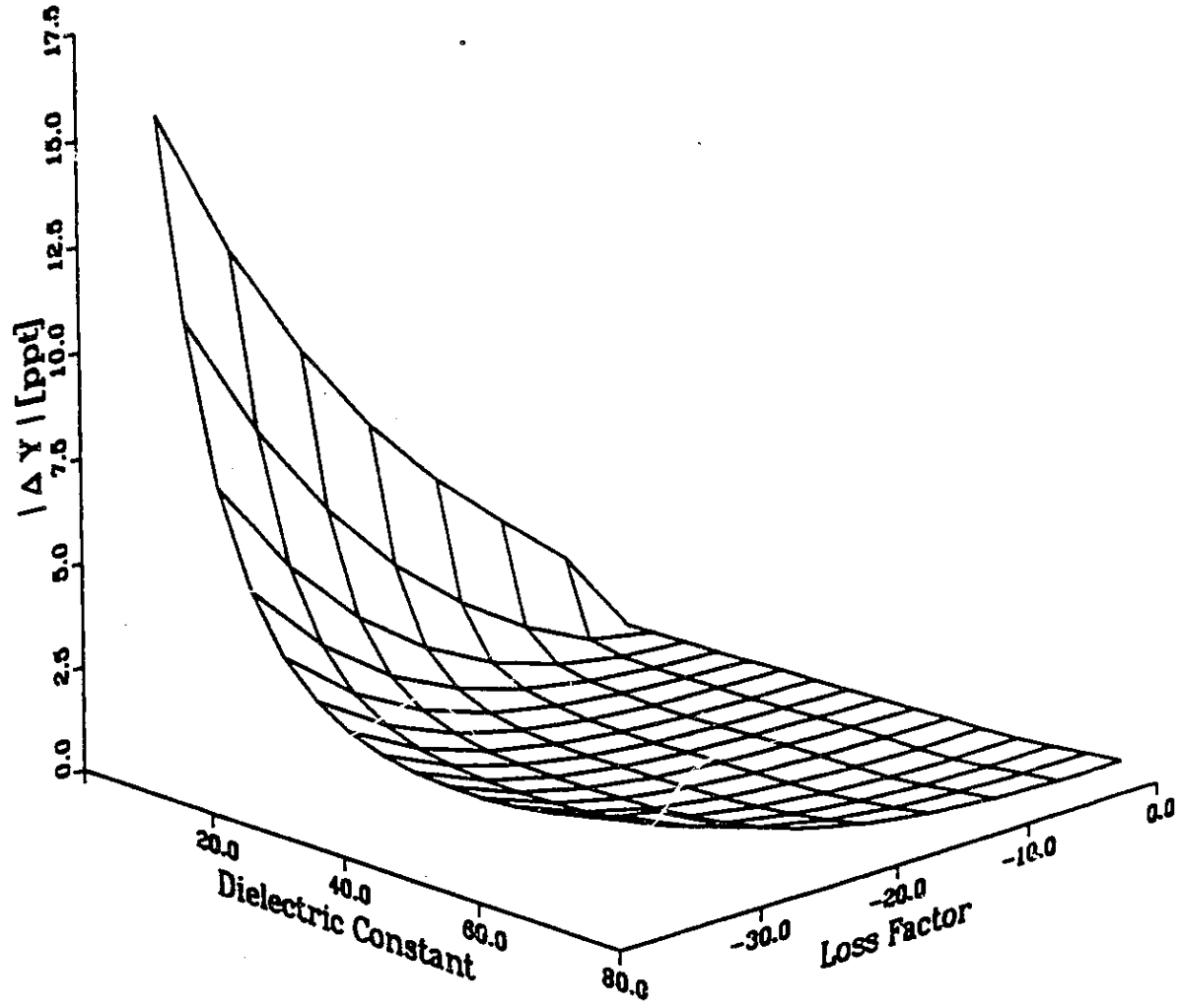

Fig. 5.6: Relative Error in the Computed Aperture Admittance of a Coaxial Line in Contact with Lossy Dielectrics for a Normalized Frequency, Ka=0.05

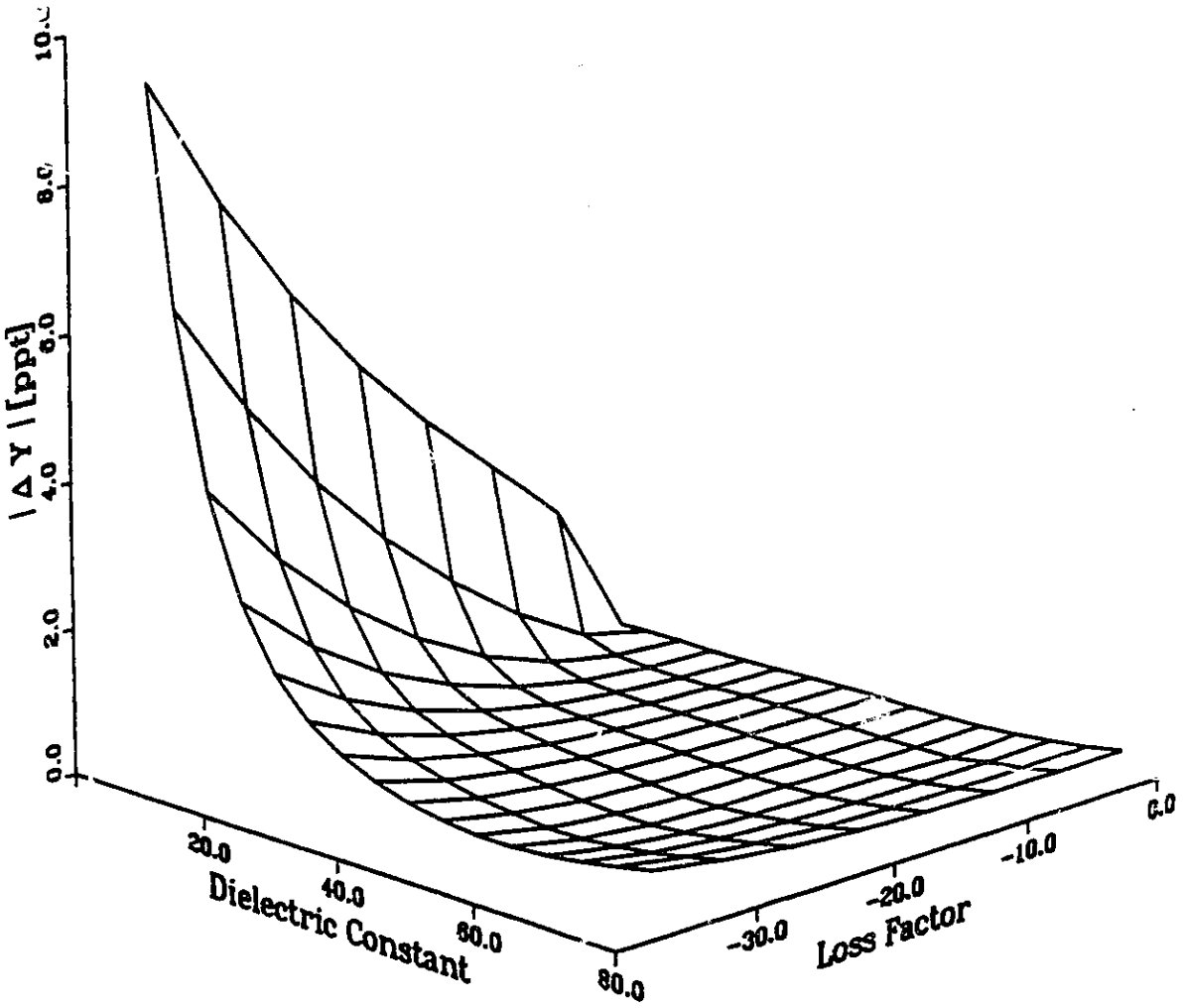

Fig. 5.7: Relative Error in the Computed Aperture Admittance of a Coaxial Line in Contact with Lossy Dielectrics for a Normalized Frequency, Ka=0.10

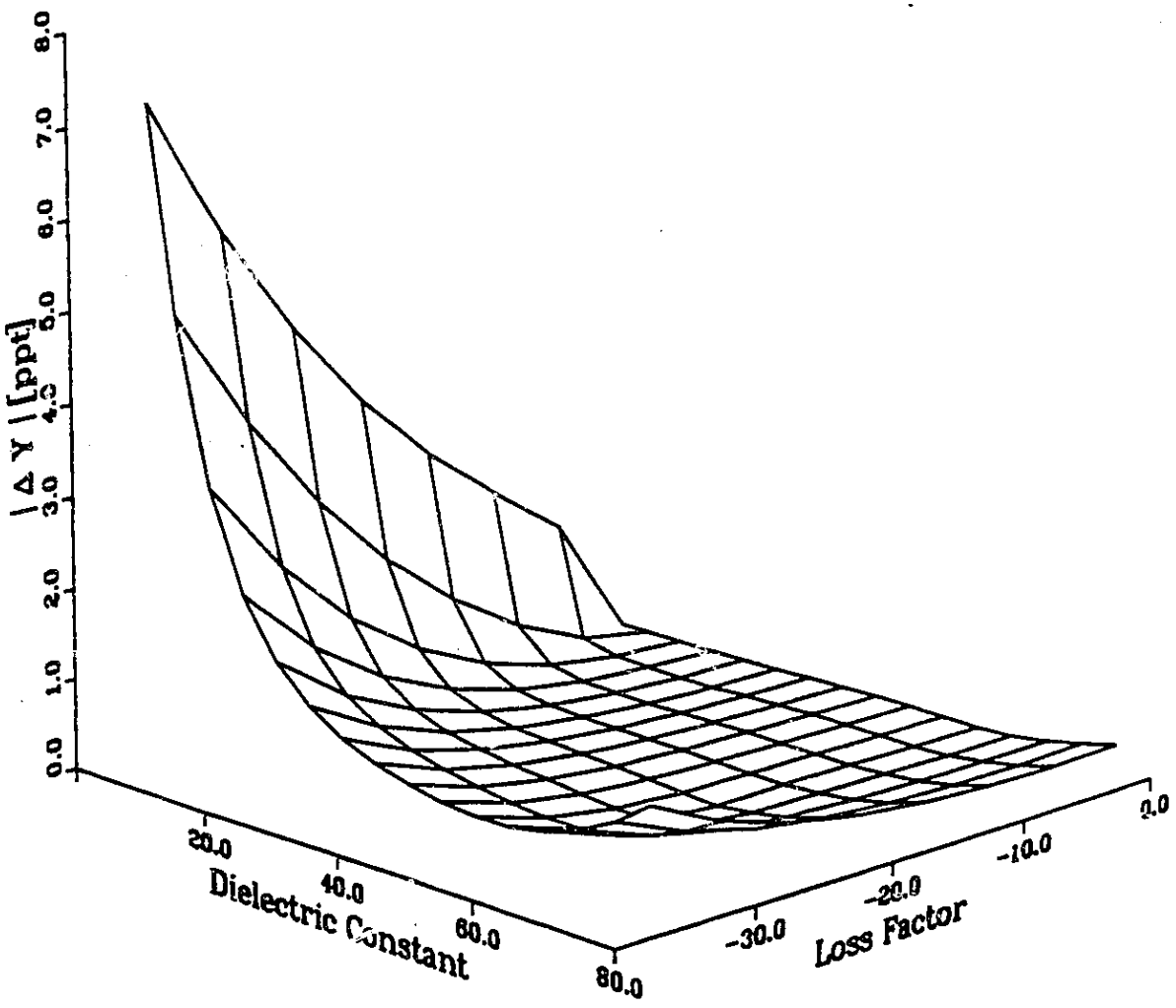

Fig. 5.8: Relative Error in the Computed Aperture Admittance of a Coaxial Line in Contact with Lossy Dielectrics for a Normalized Frequency, Ka=0.14

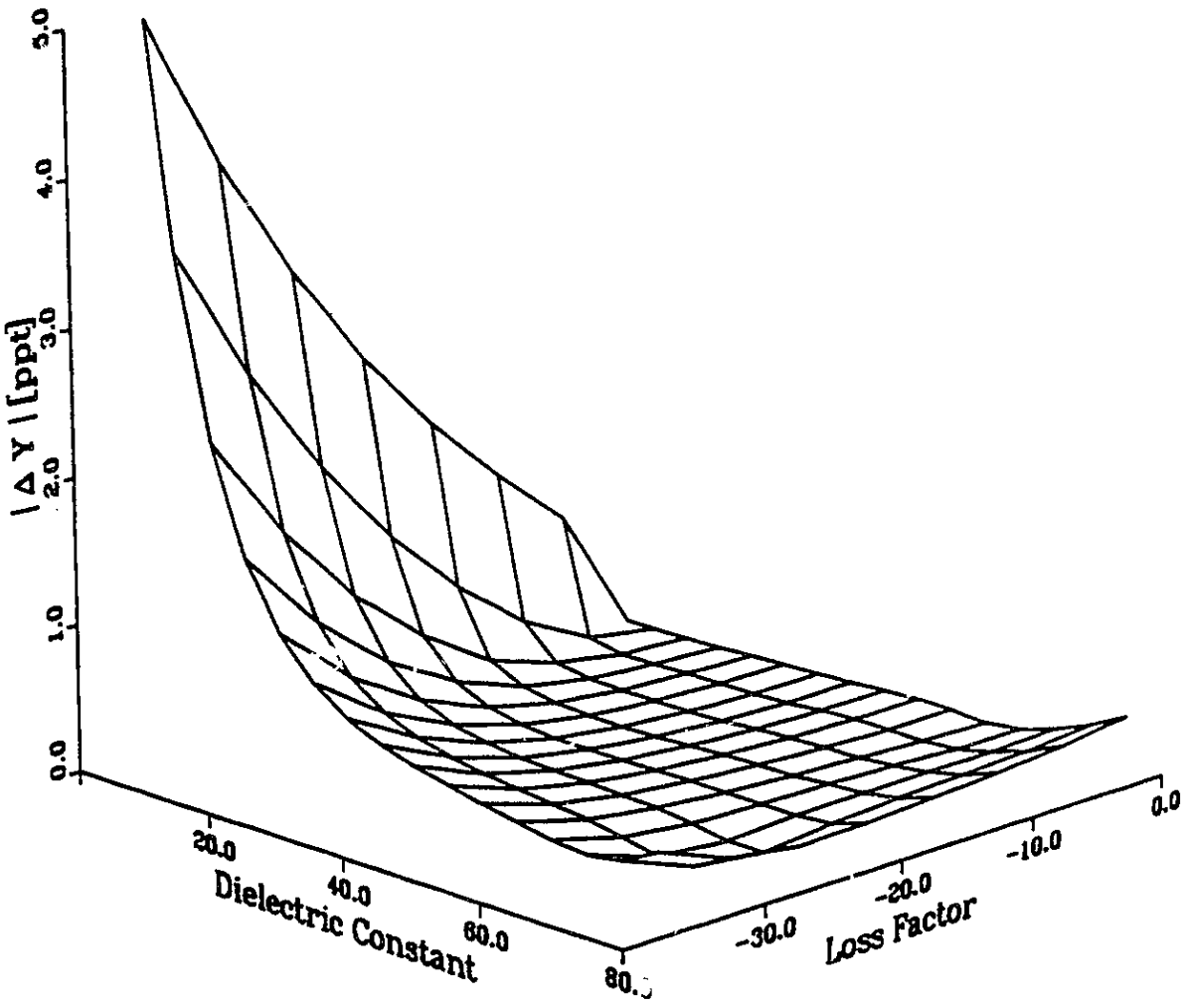

Fig. 5.9: Relative Error in the Computed Aperture Admittance of a Coaxial Line in Contact with Lossy Dielectrics for a Normalized Frequency, Ka=0.19

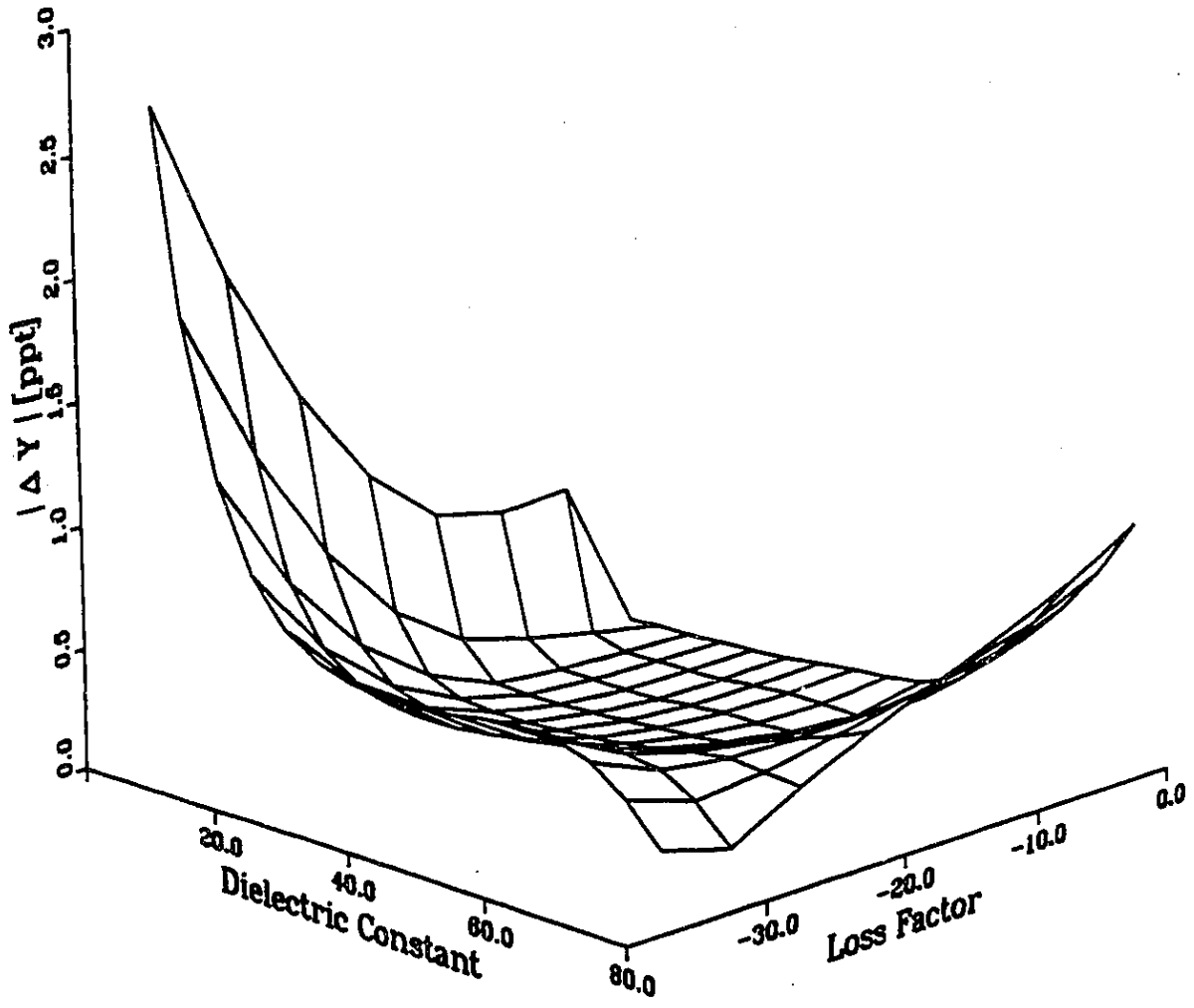

Fig. 5.10: Inverse of the Sensitivity
of an Open–Ended Coaxial Line
in Contact with Lossy Dielectrics
for a Normalized Frequency, ka=0.01

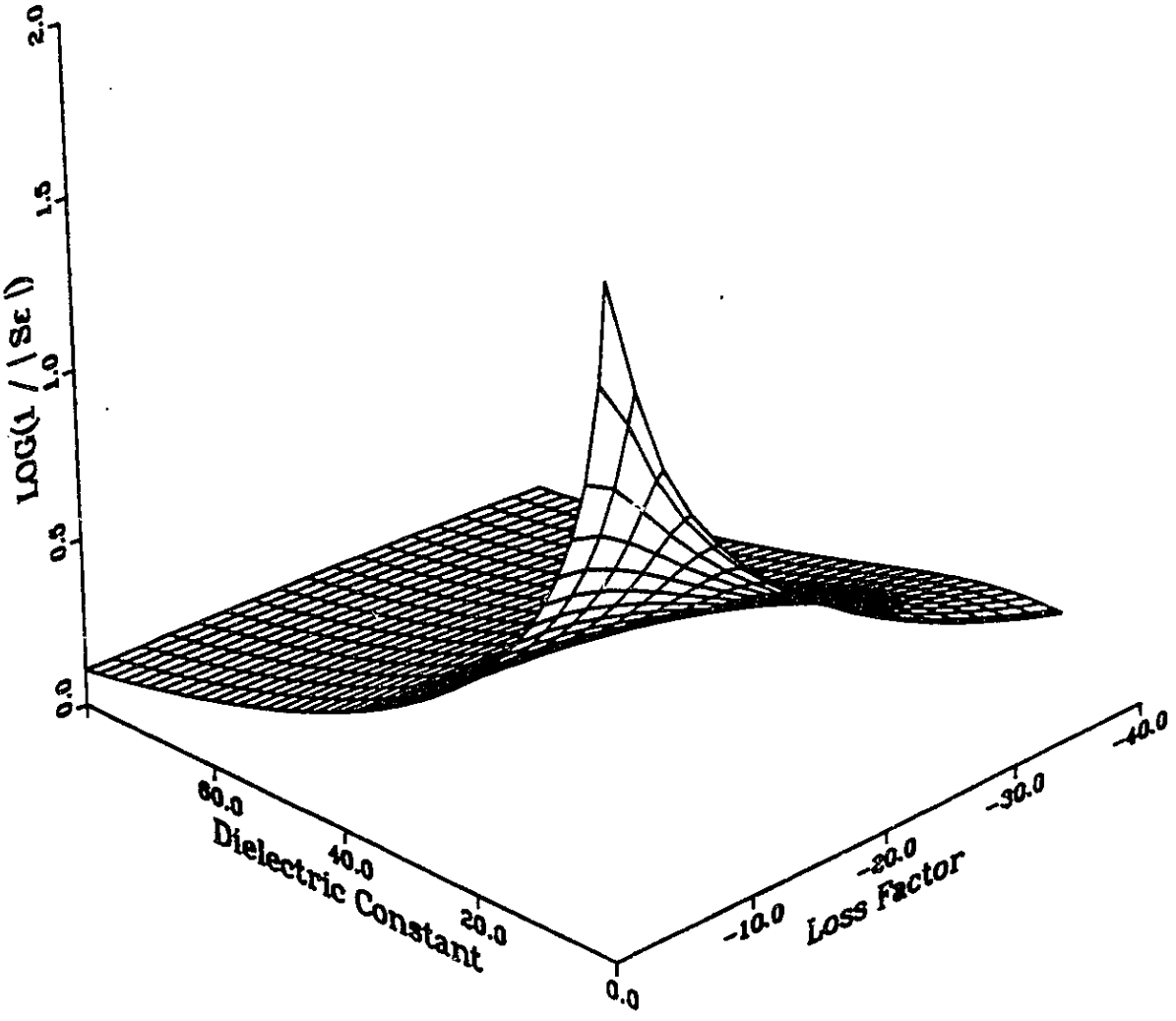

Fig. 5.11: Inverse of the Sensitivity
of an Open–Ended Coaxial Line
in Contact with Lossy Dielectrics
for a Normalized Frequency, ka=0.05

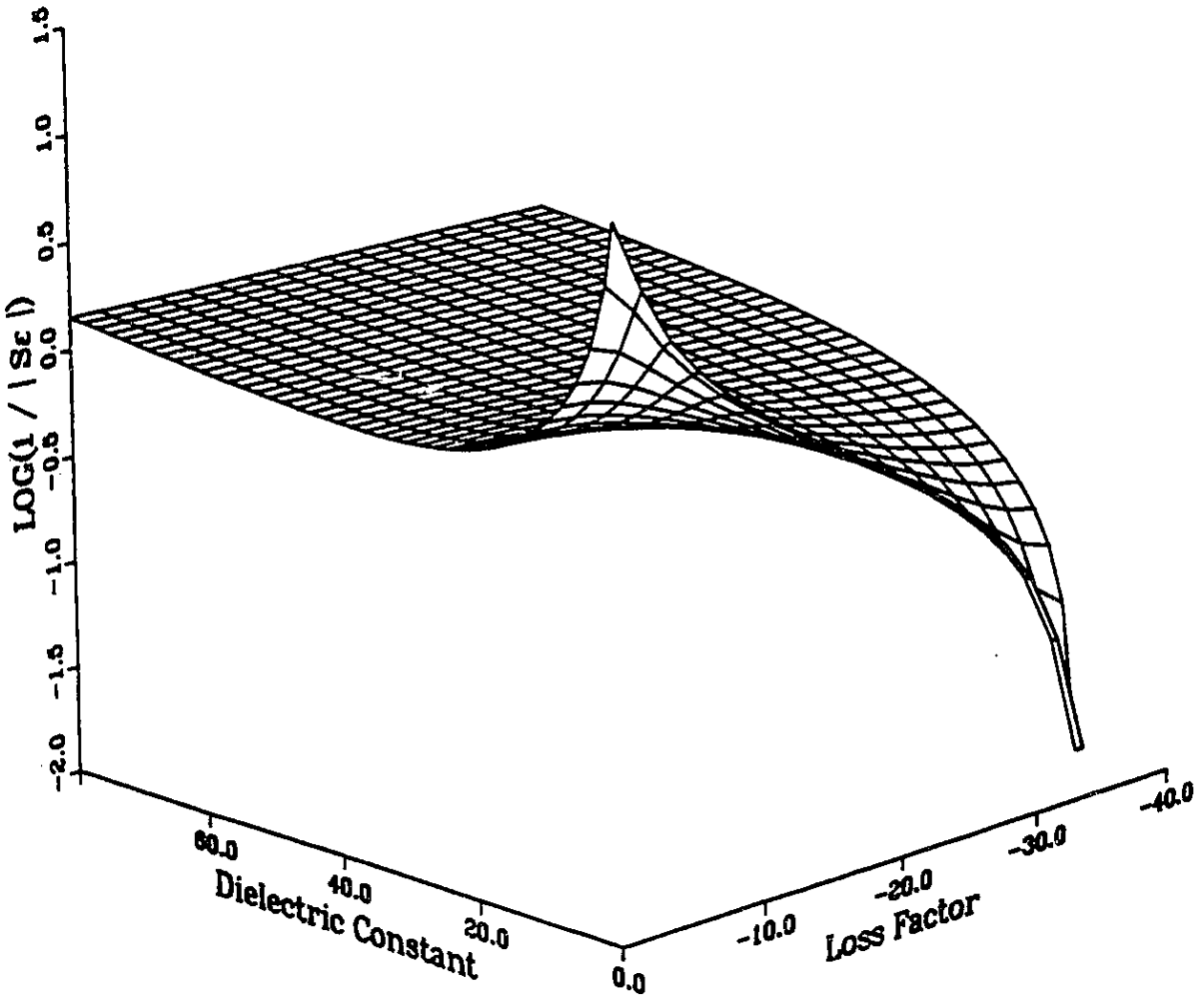

Fig. 5.12: Inverse of the Sensitivity
of an Open–Ended Coaxial Line
in Contact with Lossy Dielectrics
for a Normalized Frequency, ka=0.10

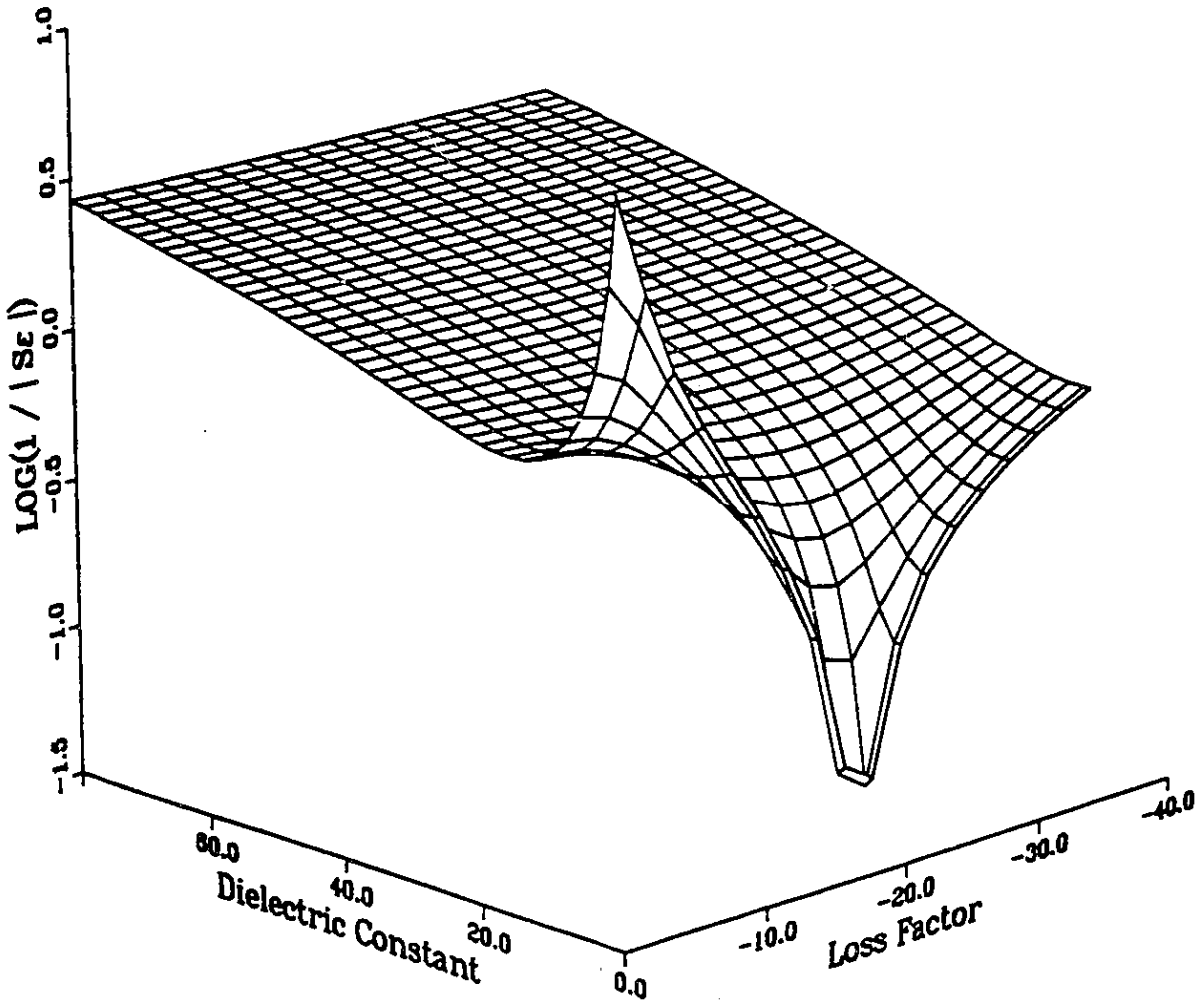

Fig. 5.13: Inverse of the Sensitivity
of an Open–Ended Coaxial Line
in Contact with Lossy Dielectrics
for a Normalized Frequency, ka=0.14

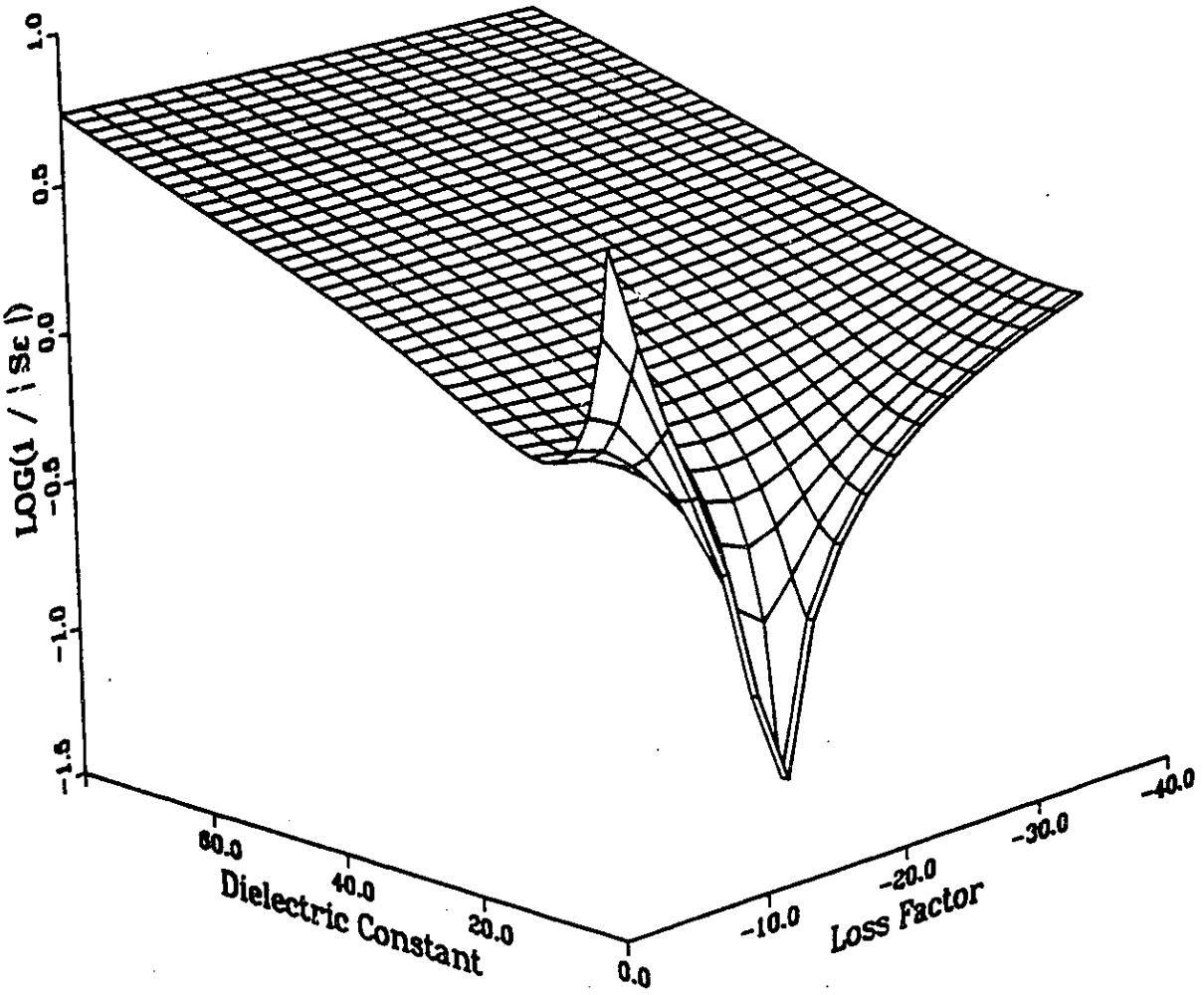

Fig. 5.14: Inverse of the Sensitivity
of an Open–Ended Coaxial Line
in Contact with Lossy Dielectrics
for a Normalized Frequency, ka=0.19

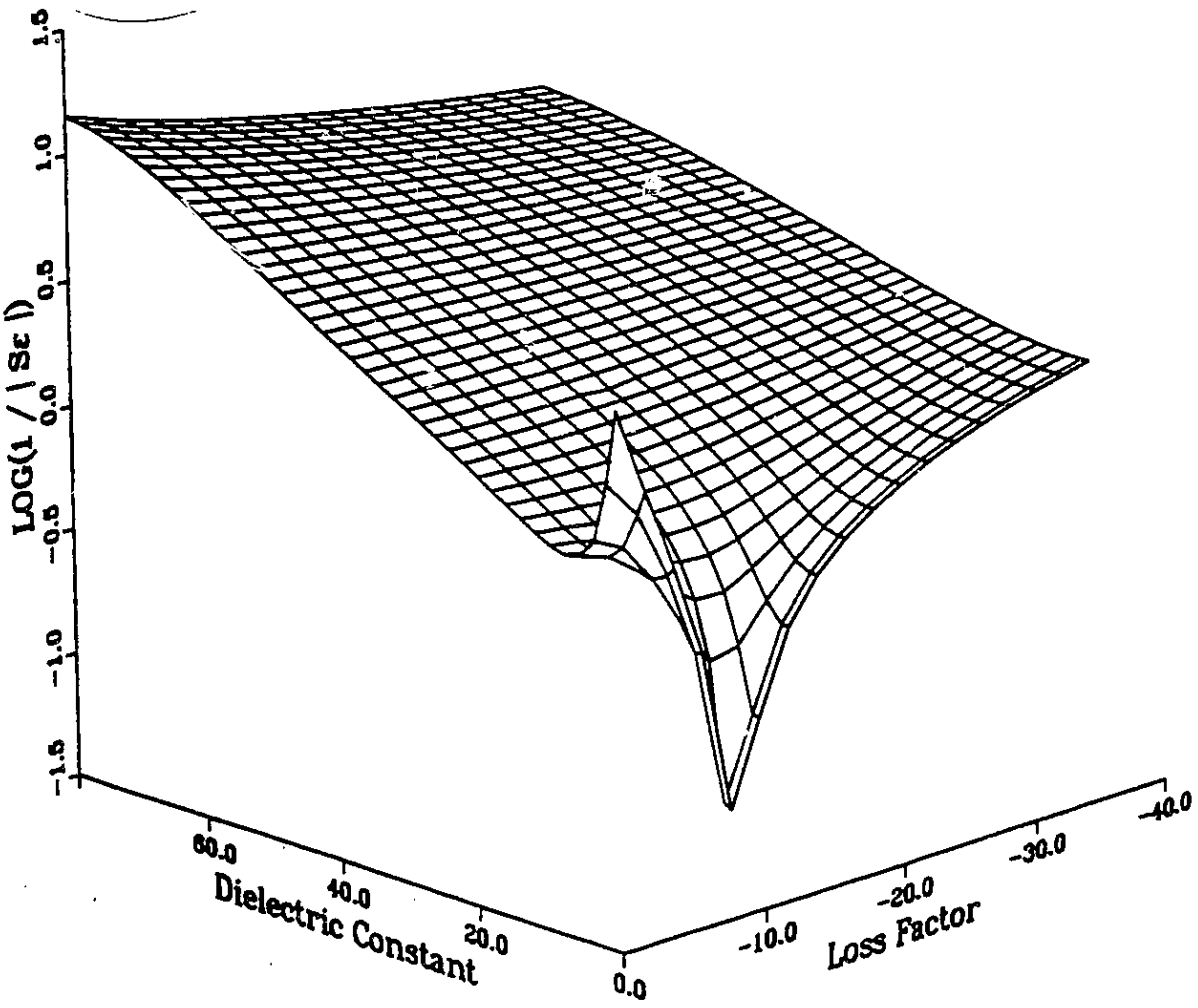

Chapter VI

Polynomial Approximations

6.1 Introduction

This chapter considers polynomial approximations to the aperture admittance of open-ended coaxial lines. As stated in Section 3.2, if the frequency range and range of material permittivities are suitably restricted, a polynomial approximation to the aperture admittance will converge. The range of independent variables for which this is true depends upon the distance from the origin of the s-plane to the nearest pole.

The specific structure examined is a 3.6 mm semi-rigid coaxial line, however, frequency scaling is used to generalize the results for any 50 Ω, Teflon line. For this specific probe, and permittivities in the range $|\varepsilon_r| \leq 80$, the upper frequency limit for polynomial approximations is approximately 10 GHz. This limit was determined by trial and error, and corresponds to a normalized frequency of $k_0 a$=0.096.

The organization of this chapter mirrors that of the previous chapter. The results of the moment method analysis are presented and the model parameters are determined based on this data. The formulation of the inverse problem is given, and the accuracy of the resulting solution is demonstrated by an example. Finally, a brief sensitivity and uncertainty analysis is performed. It is shown that, except for the quasi-static case, the polynomial approximation offers no advantage over a rational function approximation. This model is included, however, for continuity with previous models (c.f. Chapter II) which are exclusively polynomial approximations.

6.2 The Direct Problem

The moment method program was used to compute the aperture admittance of a 3.6 mm coaxial line. The analysis was performed every 0.5 GHz for frequencies in the range 0.5 - 10.0 GHz, which corresponds to a normalized frequency range of 0.005 - 0.096. At each frequency 56 dielectric constants in the range 1 -80 were considered yielding a total of 1120 data points. The aperture field was modelled by 11 expansion functions and 11 modes were retained in the coaxial line. The results of this analysis are presented in Figures 6.1 - 6.3 [12], which show the real part, the imaginary part, and the magnitude of the normalized admittance, respectively.

The model to be fitted is given by (3.30), and is repeated here for convenience.

$$Ymodel = \sum_{n=1}^{N} \sum_{p=1}^{P} c_{np} (\sqrt{\varepsilon_r})^p s^n \tag{6.1}$$

Although this represents a linear least squares problem which may be solved directly (c.f. Section 3.3), the iterative algorithm LMDER1 [61] was used for convenience. This is not as inefficient as it seems. Since the model is linear in the parameters, the second derivative of the merit function with respect to all parameters vanishes. This implies that the quadratic approximation (3.79) is very good, and the minimum is found in one or two iterations. The merit function used is:

$$\chi^2 = \sum_{i=1}^{1120} \left| \frac{Ymom_i - Ymodel_i}{0.01 \times Ymom_i} \right|^2 \tag{6.2}$$

---

12. All figures and tables may be found at the end of the chapter.

The number of parameters required was determined by monitoring the convergence of the merit function. Based on this study, 88 parameters were chosen (N=11, P=8). The normalized best fit parameters are given in Table 6.2, where the following normalization was used:

$$\hat{c}_{np} = \frac{c_{np}}{a^n} \qquad \left[\frac{\text{sec}^n}{\text{Gigarad}^n \cdot \text{meters}^n}\right] \tag{6.3}$$

where $a = 0.456 \times 10^{-3}$ m is the radius of the inner conductor of the line analyzed. Ten significant figures are given in Table 6.2, however, all computations retained 16 significant figures. In terms of these normalized parameters, the universal polynomial model for the normalized aperture admittance of 50 Ω, Teflon lines is:

$$Ymodel = \sum_{n=1}^{11} \sum_{p=1}^{8} \hat{c}_{np} (\sqrt{\varepsilon_r})^p (sa)^n \tag{6.4}$$

where s is the complex frequency in Giga-radians per second, and a is the radius of the inner conductor of the probe specified in meters. This model is valid for $0.005 \le k_0 a \le 0.096$ and $|\varepsilon_r - 40| \le 40$.

Figure 6.4 shows the magnitude of the relative error:

$$\Delta Y = \frac{Ymodel - Ymom}{|Ymom|} \times 1000 \qquad ppt \tag{6.5}$$

Comparing Fig. 6.4 with Fig. 5.4 several observations may be made. Although the maximum relative error in the case of the polynomial approximation is acceptable, the polynomial is far more oscillatory than the rational function approximation. Also for low dielectric constants, the relative error of the rational function remains flat for a much larger interval. These obser-

vations illustrate the general rule that polynomial expansions tend to be "wiggly" and the error increases rapidly towards the end of the interval. In general, rational functions yield better approximations.

The accuracy of the model for lossy dielectrics is demonstrated in Fig. 6.5 - 6.7. Figure 6.5 is a plot of the magnitude of the relative error defined by (6.5) for a normalized frequency $ka = 0.01$ and permittivities in the range

$$1 \le \varepsilon' \le 75$$

$$0 \le \varepsilon'' \le -35 \tag{6.6}$$

Figures 6.6 and 6.7 are similar plots for normalized frequencies of 0.05 and 0.10.

6.3 The Inverse Problem

Solution of the inverse problem for the polynomial model is similar to the solution of the inverse problem for the rational function model. Define the following functions:

$$b_p = \sum_{n=1}^{11} \hat{c}_{np} (sa)^n \qquad p = 1, 2, \ldots, 8 \tag{6.7}$$

$$\zeta = \sqrt{\varepsilon_r} \tag{6.8}$$

In the last equation the principal value of the square root is implied. In terms of these new quantities the polynomial model may be written as:

$$Y = \sum_{p=1}^{8} b_p \zeta^p \tag{6.9}$$

Considering Y to be the given quantity, the desired permittivity is related , via (6.9), to the physically meaningful solution of:

$$\sum_{p=1}^{8} b_p \zeta^p - Y = 0 \tag{6.10}$$

The details of the solution of (6.10) may be found in Chapter V.

In order to verify the accuracy and uniqueness of the inversion, several tests were performed. The moment method program was used to compute the admittance for normalized frequencies 0.01, 0.05 and 0.10 and permittivities in the range given by (6.6). Using these computed admittances, all the mathematical solutions of (6.10) were found by Laguerre's method. In all cases only one physically meaningful root was obtained. For brevity, only the results for k_0a=0.10 are given in Table 6.3. The results for the other frequencies investigated were at least as accurate.

6.4 Sensitivity and Uncertainty

Following the definitions given in Section 5.4, the sensitivity of the aperture reflection coefficient for changes in the permittivity is given by:

$$S_\varepsilon^\Gamma = \frac{|\varepsilon_r|}{|\Gamma|} \frac{\partial Y}{\partial \zeta} \frac{\partial \zeta}{\partial \varepsilon_r} \frac{\partial \Gamma}{\partial Y} \tag{6.11}$$

Performing the indicated differentiations one obtains:

$$S_\varepsilon^\Gamma = -\frac{|\varepsilon_r|\,|1+Y|}{|1-Y|\,(1+Y)^2} \sum_{n=1}^{11} \sum_{p=1}^{8} p \hat{c}_{np} \zeta^{p-2} (sa)^n \tag{6.12}$$

All of the statements made in Section 5.4, with regard to measurements uncertainty and sensitivity are applicable in the case of polynomial approximations if one simply substitutes (6.12) for (5.20). These two expression must yield virtually identical results. Therefore, for brevity, we end our discussion here.

Table 6.1: Best Fit Parameters of Polynomial Model $\hat{C}_{np}$				
n \ p	1	2	3	4
1	-8.563719815E-02	2.767505947E+00	-4.517186427E-01	1.459920826E-01
2	4.234622256E-02	-1.078753768E-01	1.035847858E-01	-4.811639529E-02
3	1.748923445E+00	8.764312375E+00	-2.853206543E+01	-2.249288756E+01
4	9.391736375E+02	-2.304870477E+03	1.980692597E+03	-6.213425750E+02
5	1.097086475E+05	-3.078703706E+05	3.394463560E+05	-1.913418488E+05
6	1.622987576E+06	-3.074551867E+06	1.337290451E+06	6.199157705E+05
7	6.128601205E+08	-1.697456834E+09	1.836289949E+09	-1.008678720E+09
8	-7.204254496E+08	4.223273672E+09	-7.539009813E+09	5.996858407E+09
9	1.193294771E+12	-3.255485800E+12	3.450756037E+12	-1.846332189E+12
10	-3.986655001E+12	1.201202421E+13	-1.425965101E+13	8.611688564E+12
11	7.799683606E+14	-2.108127883E+15	2.208944382E+15	-1.166975564E+15

Table 6.1: Best Fit Parameters of Polynomial Model

$\hat{C}_{np}$

(Continued)

n \ p	5	6	7	8
1	-2.746154978E-02	3.035669364E-03	-1.826851362E-04	4.616058147E-06
2	1.134711409E-02	-1.248613107E-03	4.434580665E-05	-2.569890767E-07
3	8.511295322E-01	-3.623430299E-01	4.432889132E-02	-1.691136442E-03
4	2.572823685E+02	-1.155617943E+00	-1.384069549E+00	6.218789236E-02
5	5.973925973E+04	-1.137215947E+04	9.451963961E+02	-2.985333894E+01
6	-6.789820704E+05	2.069898844E+05	-1.826465785E+04	5.471168083E+02
7	3.047424426E+08	-5.003220063E+07	3.894702070E+06	-1.209035597E+05
8	-2.377095138E+09	4.616293132E+08	-3.677046684E+07	1.199736829E+06
9	5.400927718E+11	-8.598056747E+10	6.806907958E+09	-2.223077546E+08
10	-2.838299782E+12	5.027949942E+11	-4.343418192E+10	1.594548529E+09
11	3.373660502E+14	-5.345459768E+13	4.300176306E+12	-1.423677224E+11

Table 6.2: Solution of the Inverse Problem for k_0a=0.10					
ε_r		ε_r solution		$\Delta\varepsilon_r$ [%]	
ε'	ε''	ε'	ε''	Re	Im
1.000E+00	-3.500E+01	1.226E+00	-3.514E+01	0.65	-0.41
5.000E+00	-3.500E+01	5.212E+00	-3.502E+01	0.60	-0.05
1.000E+01	-3.500E+01	1.014E+01	-3.492E+01	0.40	0.23
1.500E+01	-3.500E+01	1.506E+01	-3.488E+01	0.15	0.33
2.000E+01	-3.500E+01	1.998E+01	-3.489E+01	0.06	0.28
2.500E+01	-3.500E+01	2.492E+01	-3.493E+01	0.18	0.16
3.000E+01	-3.500E+01	2.990E+01	-3.499E+01	0.21	0.02
3.500E+01	-3.500E+01	3.492E+01	-3.505E+01	0.16	-0.10
4.000E+01	-3.500E+01	3.997E+01	-3.509E+01	0.06	-0.16
4.500E+01	-3.500E+01	4.503E+01	-3.509E+01	0.05	-0.16
5.000E+01	-3.500E+01	5.009E+01	-3.506E+01	0.14	-0.10
5.500E+01	-3.500E+01	5.512E+01	-3.499E+01	0.18	0.01
6.000E+01	-3.500E+01	6.011E+01	-3.491E+01	0.16	0.13
6.500E+01	-3.500E+01	6.505E+01	-3.482E+01	0.07	0.24
7.000E+01	-3.500E+01	6.993E+01	-3.476E+01	0.09	0.30
7.500E+01	-3.500E+01	7.476E+01	-3.476E+01	0.29	0.29
1.000E+00	-3.000E+01	1.093E+00	-3.011E+01	0.31	-0.35
5.000E+00	-3.000E+01	5.108E+00	-3.004E+01	0.36	-0.12
1.000E+01	-3.000E+01	1.009E+01	-2.997E+01	0.27	0.08
1.500E+01	-3.000E+01	1.504E+01	-2.994E+01	0.12	0.17
2.000E+01	-3.000E+01	2.000E+01	-2.994E+01	0.01	0.17
2.500E+01	-3.000E+01	2.496E+01	-2.996E+01	0.09	0.10
3.000E+01	-3.000E+01	2.995E+01	-2.999E+01	0.12	0.02
3.500E+01	-3.000E+01	3.496E+01	-3.002E+01	0.09	-0.05
4.000E+01	-3.000E+01	3.998E+01	-3.004E+01	0.03	-0.09
4.500E+01	-3.000E+01	4.502E+01	-3.005E+01	0.03	-0.08
5.000E+01	-3.000E+01	5.005E+01	-3.003E+01	0.08	-0.04
5.500E+01	-3.000E+01	5.506E+01	-2.999E+01	0.09	0.02
6.000E+01	-3.000E+01	6.004E+01	-2.994E+01	0.07	0.09
6.500E+01	-3.000E+01	6.500E+01	-2.990E+01	0.00	0.14
7.000E+01	-3.000E+01	6.992E+01	-2.988E+01	0.11	0.15
7.500E+01	-3.000E+01	7.481E+01	-2.991E+01	0.24	0.11

Table 6.2: Solution of the Inverse Problem
for k_0a=0.10
(Continued)

ε_r		ε_r solution		$\Delta\varepsilon_r$ [%]	
ε'	ε''	ε'	ε''	Re	Im
1.000E+00	-2.500E+01	1.035E+00	-2.507E+01	0.14	-0.26
5.000E+00	-2.500E+01	5.050E+00	-2.503E+01	0.20	-0.14
1.000E+01	-2.500E+01	1.005E+01	-2.500E+01	0.17	0.01
1.500E+01	-2.500E+01	1.503E+01	-2.498E+01	0.09	0.08
2.000E+01	-2.500E+01	2.000E+01	-2.497E+01	0.01	0.09
2.500E+01	-2.500E+01	2.498E+01	-2.498E+01	0.05	0.06
3.000E+01	-2.500E+01	2.998E+01	-2.500E+01	0.06	0.01
3.500E+01	-2.500E+01	3.498E+01	-2.501E+01	0.05	-0.03
4.000E+01	-2.500E+01	3.999E+01	-2.502E+01	0.02	-0.05
4.500E+01	-2.500E+01	4.501E+01	-2.502E+01	0.02	-0.04
5.000E+01	-2.500E+01	5.002E+01	-2.501E+01	0.04	-0.02
5.500E+01	-2.500E+01	5.502E+01	-2.499E+01	0.04	0.02
6.000E+01	-2.500E+01	6.001E+01	-2.497E+01	0.02	0.05
6.500E+01	-2.500E+01	6.498E+01	-2.495E+01	0.03	0.07
7.000E+01	-2.500E+01	6.993E+01	-2.496E+01	0.09	0.06
7.500E+01	-2.500E+01	7.487E+01	-2.500E+01	0.16	0.00
1.000E+00	-2.000E+01	1.010E+00	-2.004E+01	0.05	-0.22
5.000E+00	-2.000E+01	5.020E+00	-2.003E+01	0.10	-0.13
1.000E+01	-2.000E+01	1.002E+01	-2.001E+01	0.10	-0.03
1.500E+01	-2.000E+01	1.501E+01	-1.999E+01	0.06	0.03
2.000E+01	-2.000E+01	2.000E+01	-1.999E+01	0.01	0.05
2.500E+01	-2.000E+01	2.499E+01	-1.999E+01	0.02	0.03
3.000E+01	-2.000E+01	2.999E+01	-2.000E+01	0.03	0.01
3.500E+01	-2.000E+01	3.499E+01	-2.001E+01	0.03	-0.01
4.000E+01	-2.000E+01	4.000E+01	-2.001E+01	0.01	-0.02
4.500E+01	-2.000E+01	4.500E+01	-2.001E+01	0.01	-0.02
5.000E+01	-2.000E+01	5.001E+01	-2.000E+01	0.02	-0.01
5.500E+01	-2.000E+01	5.501E+01	-1.999E+01	0.01	0.01
6.000E+01	-2.000E+01	6.000E+01	-1.999E+01	0.00	0.02
6.500E+01	-2.000E+01	6.498E+01	-1.998E+01	0.03	0.02
7.000E+01	-2.000E+01	6.995E+01	-2.000E+01	0.06	0.00
7.500E+01	-2.000E+01	7.493E+01	-2.003E+01	0.09	-0.04

Table 6.2: Solution of the Inverse Problem
for k_0a=0.10
(Continued)

ε_r		ε_r solution		$\Delta\varepsilon_r$ [%]	
ε'	ε''	ε'	ε''	Re	Im
1.000E+00	-1.500E+01	9.898E-01	-1.503E+01	0.07	-0.20
5.000E+00	-1.500E+01	5.002E+00	-1.502E+01	0.01	-0.11
1.000E+01	-1.500E+01	1.001E+01	-1.501E+01	0.04	-0.04
1.500E+01	-1.500E+01	1.501E+01	-1.500E+01	0.03	0.01
2.000E+01	-1.500E+01	2.000E+01	-1.499E+01	0.01	0.02
2.500E+01	-1.500E+01	2.500E+01	-1.500E+01	0.01	0.02
3.000E+01	-1.500E+01	2.999E+01	-1.500E+01	0.02	0.00
3.500E+01	-1.500E+01	3.499E+01	-1.500E+01	0.01	-0.01
4.000E+01	-1.500E+01	4.000E+01	-1.501E+01	0.01	-0.01
4.500E+01	-1.500E+01	4.500E+01	-1.501E+01	0.00	-0.01
5.000E+01	-1.500E+01	5.000E+01	-1.500E+01	0.01	-0.01
5.500E+01	-1.500E+01	5.500E+01	-1.500E+01	0.00	0.00
6.000E+01	-1.500E+01	6.000E+01	-1.500E+01	0.01	0.01
6.500E+01	-1.500E+01	6.499E+01	-1.500E+01	0.02	0.00
7.000E+01	-1.500E+01	6.998E+01	-1.501E+01	0.03	-0.02
7.500E+01	-1.500E+01	7.497E+01	-1.504E+01	0.04	-0.05
1.000E+00	-1.000E+01	9.785E-01	-1.000E+01	0.21	-0.04
5.000E+00	-1.000E+01	4.994E+00	-1.001E+01	0.05	-0.05
1.000E+01	-1.000E+01	1.000E+01	-1.000E+01	0.01	-0.02
1.500E+01	-1.000E+01	1.500E+01	-1.000E+01	0.01	0.00
2.000E+01	-1.000E+01	2.000E+01	-9.998E+00	0.00	0.01
2.500E+01	-1.000E+01	2.500E+01	-9.998E+00	0.00	0.01
3.000E+01	-1.000E+01	3.000E+01	-1.000E+01	0.01	0.00
3.500E+01	-1.000E+01	3.500E+01	-1.000E+01	0.01	-0.01
4.000E+01	-1.000E+01	4.000E+01	-1.000E+01	0.00	-0.01
4.500E+01	-1.000E+01	4.500E+01	-1.000E+01	0.00	-0.01
5.000E+01	-1.000E+01	5.000E+01	-1.000E+01	0.00	-0.01
5.500E+01	-1.000E+01	5.500E+01	-1.000E+01	0.00	0.00
6.000E+01	-1.000E+01	6.000E+01	-1.000E+01	0.01	0.00
6.500E+01	-1.000E+01	6.499E+01	-1.001E+01	0.01	-0.01
7.000E+01	-1.000E+01	6.999E+01	-1.002E+01	0.01	-0.02
7.500E+01	-1.000E+01	7.500E+01	-1.003E+01	0.00	-0.04

Table 6.2: Solution of the Inverse Problem
for k_0a=0.10
(Continued)

ε_r		ε_r solution		$\Delta\varepsilon_r$ [%]	
ε'	ε''	ε'	ε''	Re	Im
1.000E+00	-5.000E+00	1.002E+00	-4.989E+00	0.05	0.21
5.000E+00	-5.000E+00	4.998E+00	-4.999E+00	0.03	0.01
1.000E+01	-5.000E+00	1.000E+01	-5.001E+00	0.00	-0.01
1.500E+01	-5.000E+00	1.500E+01	-5.000E+00	0.00	0.00
2.000E+01	-5.000E+00	2.000E+01	-4.999E+00	0.00	0.00
2.500E+01	-5.000E+00	2.500E+01	-4.999E+00	0.00	0.00
3.000E+01	-5.000E+00	3.000E+01	-5.000E+00	0.00	0.00
3.500E+01	-5.000E+00	3.500E+01	-5.002E+00	0.00	0.00
4.000E+01	-5.000E+00	4.000E+01	-5.003E+00	0.00	-0.01
4.500E+01	-5.000E+00	4.500E+01	-5.003E+00	0.00	-0.01
5.000E+01	-5.000E+00	5.000E+01	-5.003E+00	0.00	-0.01
5.500E+01	-5.000E+00	5.500E+01	-5.003E+00	0.00	-0.01
6.000E+01	-5.000E+00	6.000E+01	-5.005E+00	0.00	-0.01
6.500E+01	-5.000E+00	6.500E+01	-5.009E+00	0.00	-0.01
7.000E+01	-5.000E+00	7.000E+01	-5.014E+00	0.00	-0.02
7.500E+01	-5.000E+00	7.501E+01	-5.020E+00	0.01	-0.03
1.000E+00	0.000E+00	1.000E+00	1.523E-05	0.00	0.00
5.000E+00	0.000E+00	5.000E+00	1.950E-04	0.00	0.00
1.000E+01	0.000E+00	1.000E+01	-3.131E-04	0.00	0.00
1.500E+01	0.000E+00	1.500E+01	-9.045E-05	0.00	0.00
2.000E+01	0.000E+00	2.000E+01	4.067E-04	0.00	0.00
2.500E+01	0.000E+00	2.500E+01	2.777E-04	0.00	0.00
3.000E+01	0.000E+00	3.000E+01	-5.770E-04	0.00	0.00
3.500E+01	0.000E+00	3.500E+01	-1.670E-03	0.00	0.00
4.000E+01	0.000E+00	4.000E+01	-2.422E-03	0.00	-0.01
4.500E+01	0.000E+00	4.500E+01	-2.571E-03	0.00	-0.01
5.000E+01	0.000E+00	5.000E+01	-2.400E-03	0.00	0.00
5.500E+01	0.000E+00	5.500E+01	-2.634E-03	0.00	0.00
6.000E+01	0.000E+00	6.000E+01	-4.194E-03	0.00	-0.01
6.500E+01	0.000E+00	6.500E+01	-7.653E-03	0.01	-0.01
7.000E+01	0.000E+00	7.001E+01	-1.207E-02	0.01	-0.02
7.500E+01	0.000E+00	7.501E+01	-1.435E-02	0.01	-0.02

Fig. 6.1: Normalized Aperture Conductance
of a Coaxial Line in Contact with Lossless Dielectrics
Computed via the Method of Moments

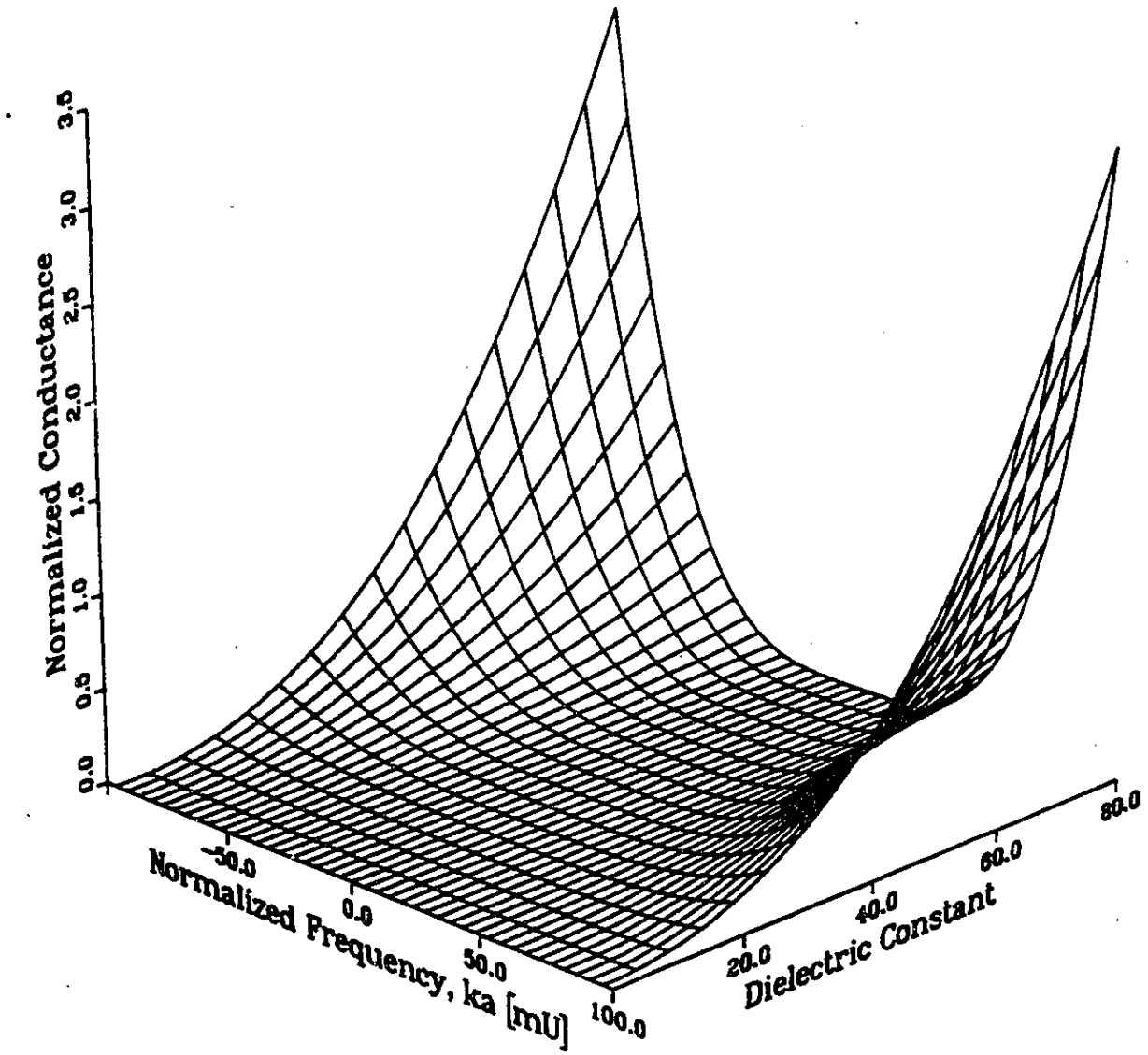

Fig. 6.2: Normalized Aperture Susceptance
of a Coaxial Line in Contact with Lossless Dielectrics
Computed via the Method of Moments

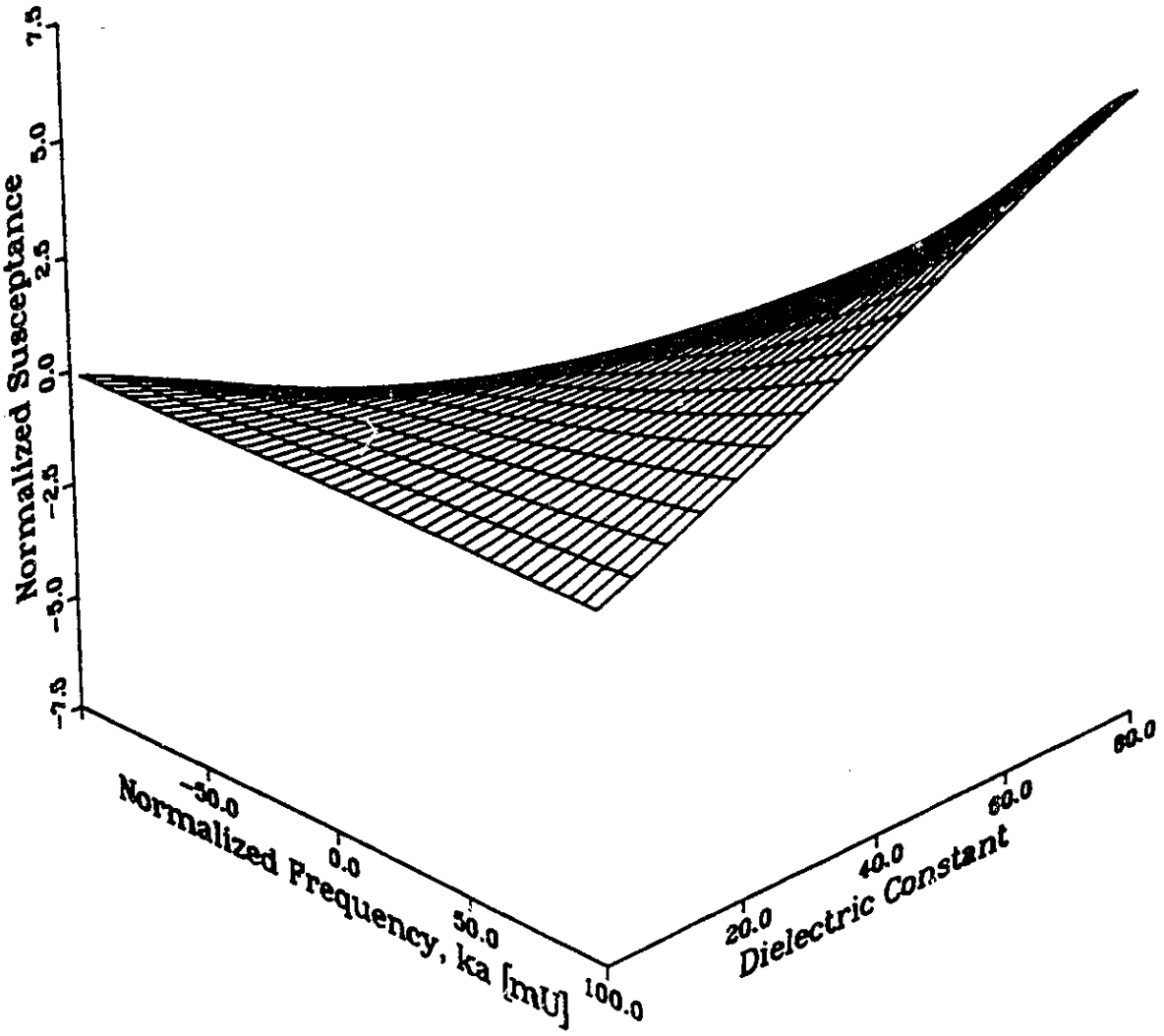

Fig. 6.3: Magnitude of the Normalized Aperture Admittance of a Coaxial Line in Contact with Lossless Dielectrics Computed via the Method of Moments

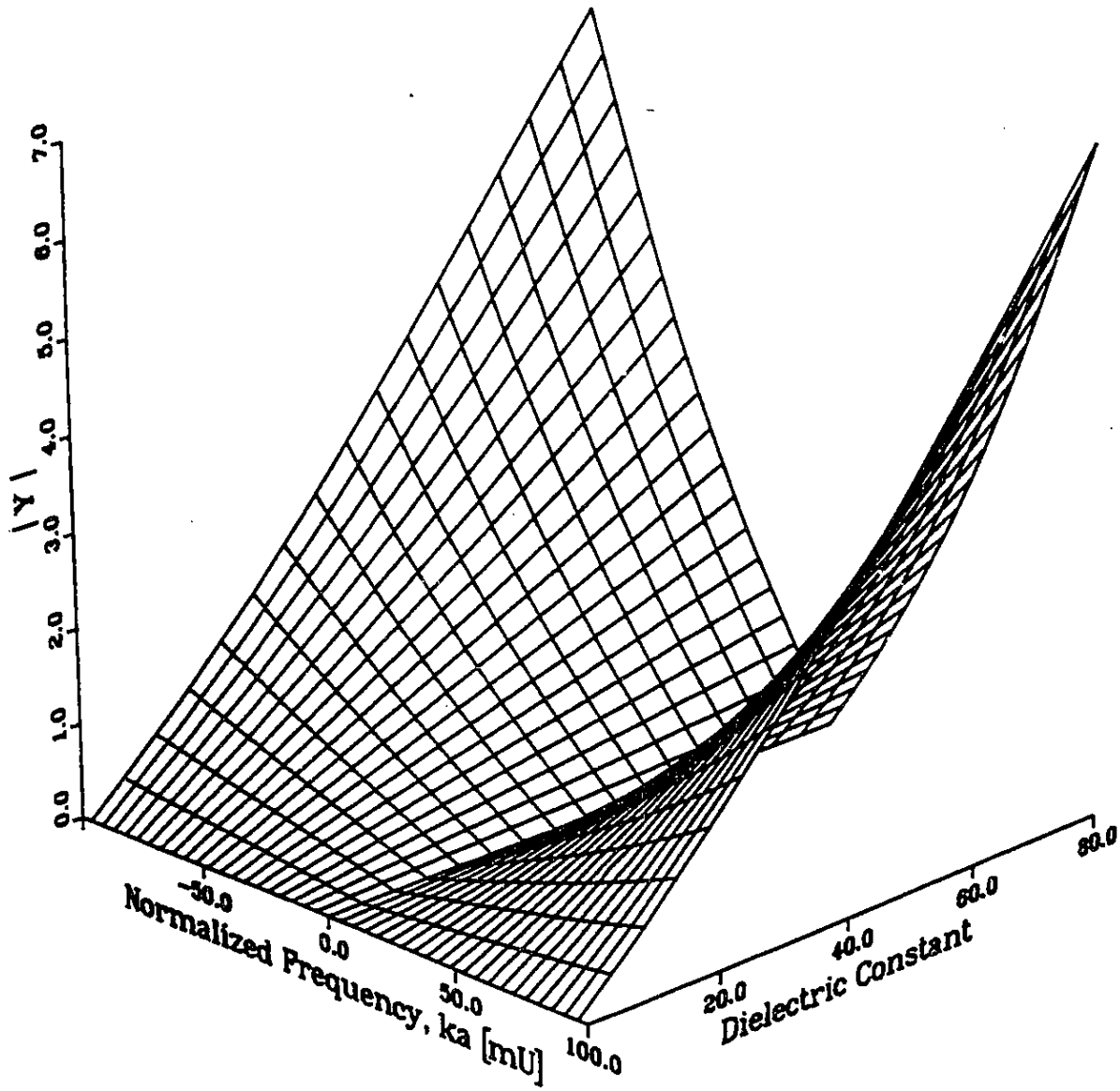

Fig. 6.4: Relative Error in the Magnitude
of the Aperture Admittance
as Computed by the Polynomial Approximation

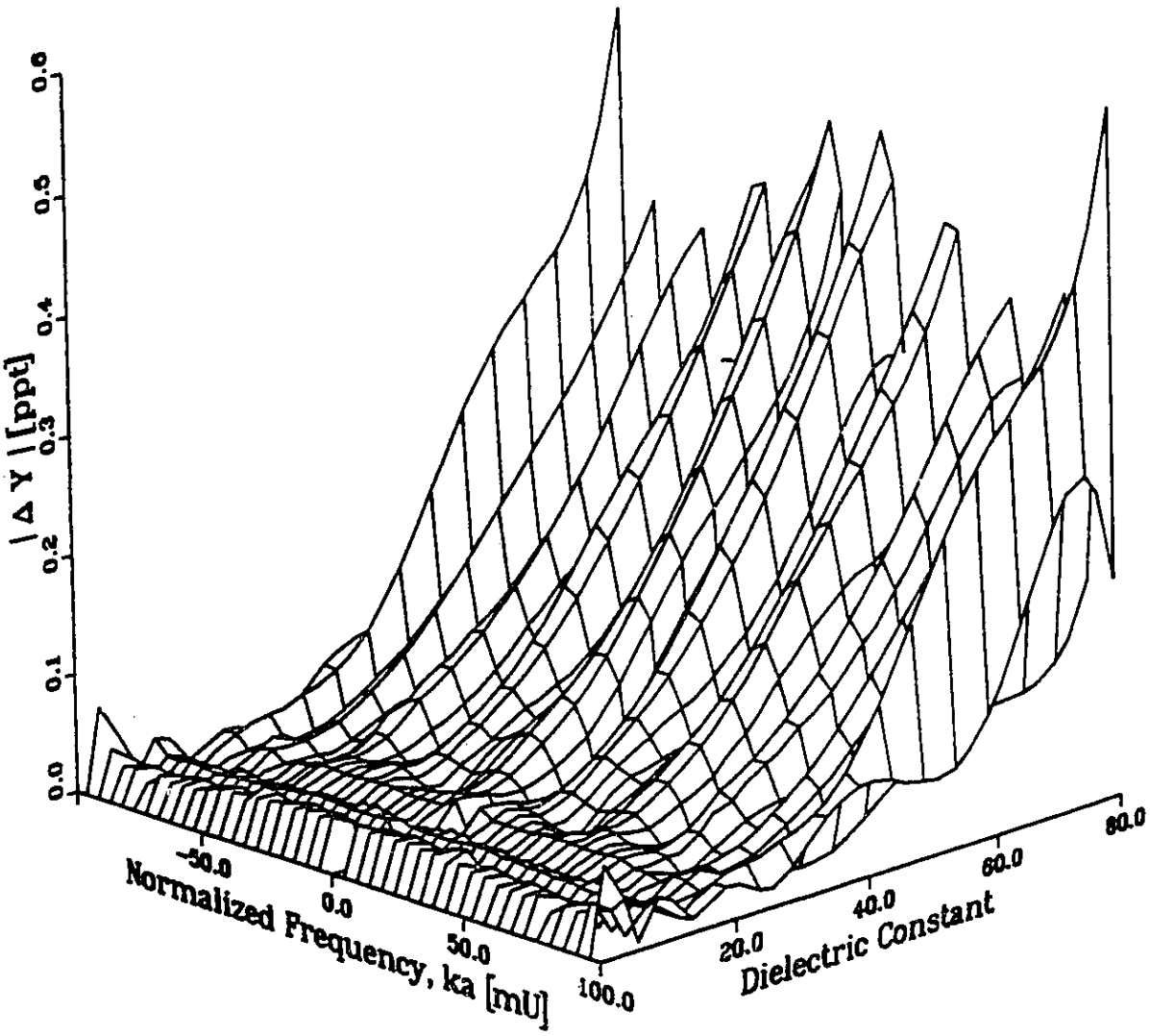

Fig. 6.5: Relative Error in the Computed Aperture Admittance of a Coaxial Line in Contact with Lossy Dielectrics for a Normalized Frequency, Ka=0.01

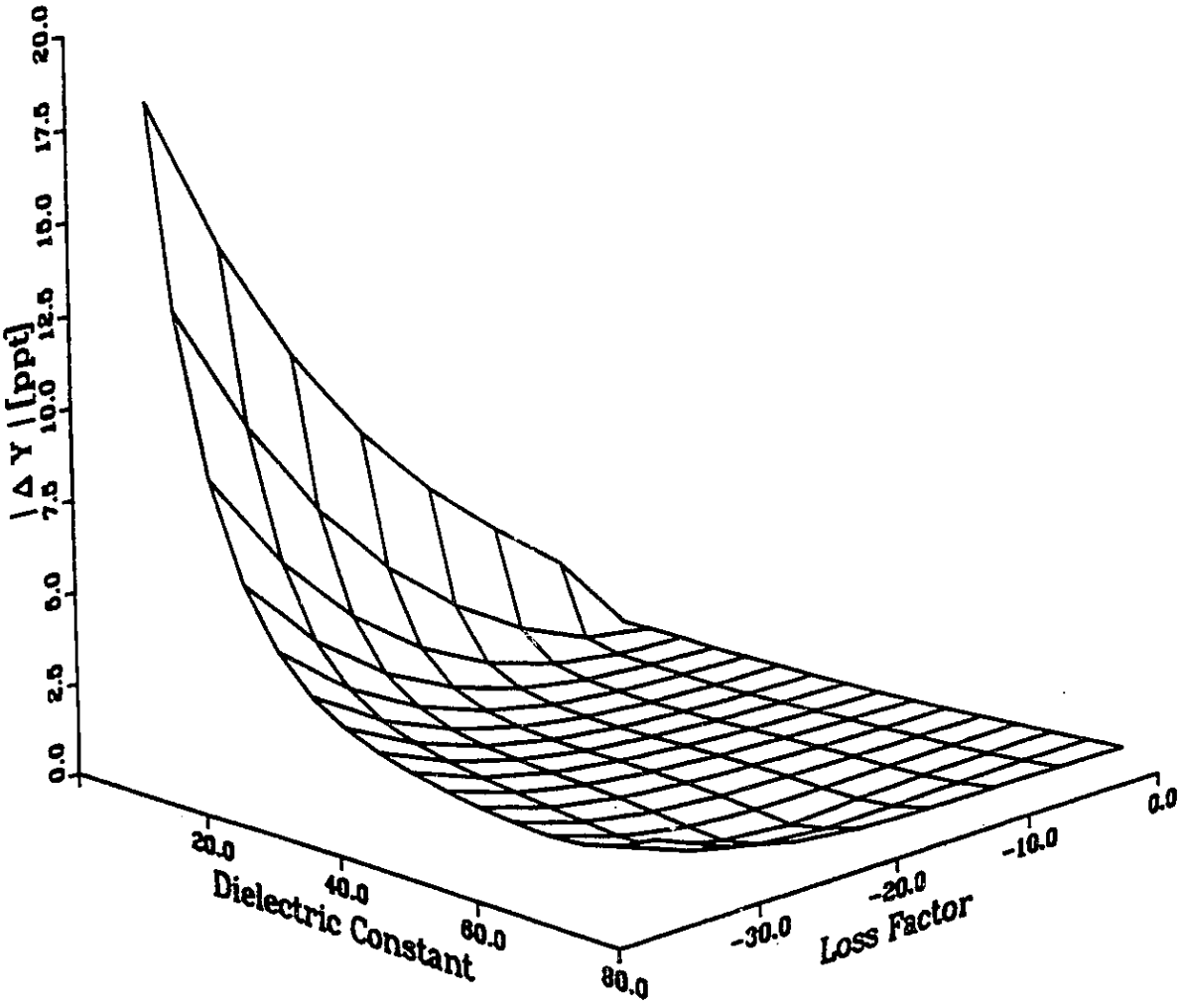

Fig. 6.6: Relative Error in the Computed Aperture Admittance of a Coaxial Line in Contact with Lossy Dielectrics for a Normalized Frequency, Ka=0.05

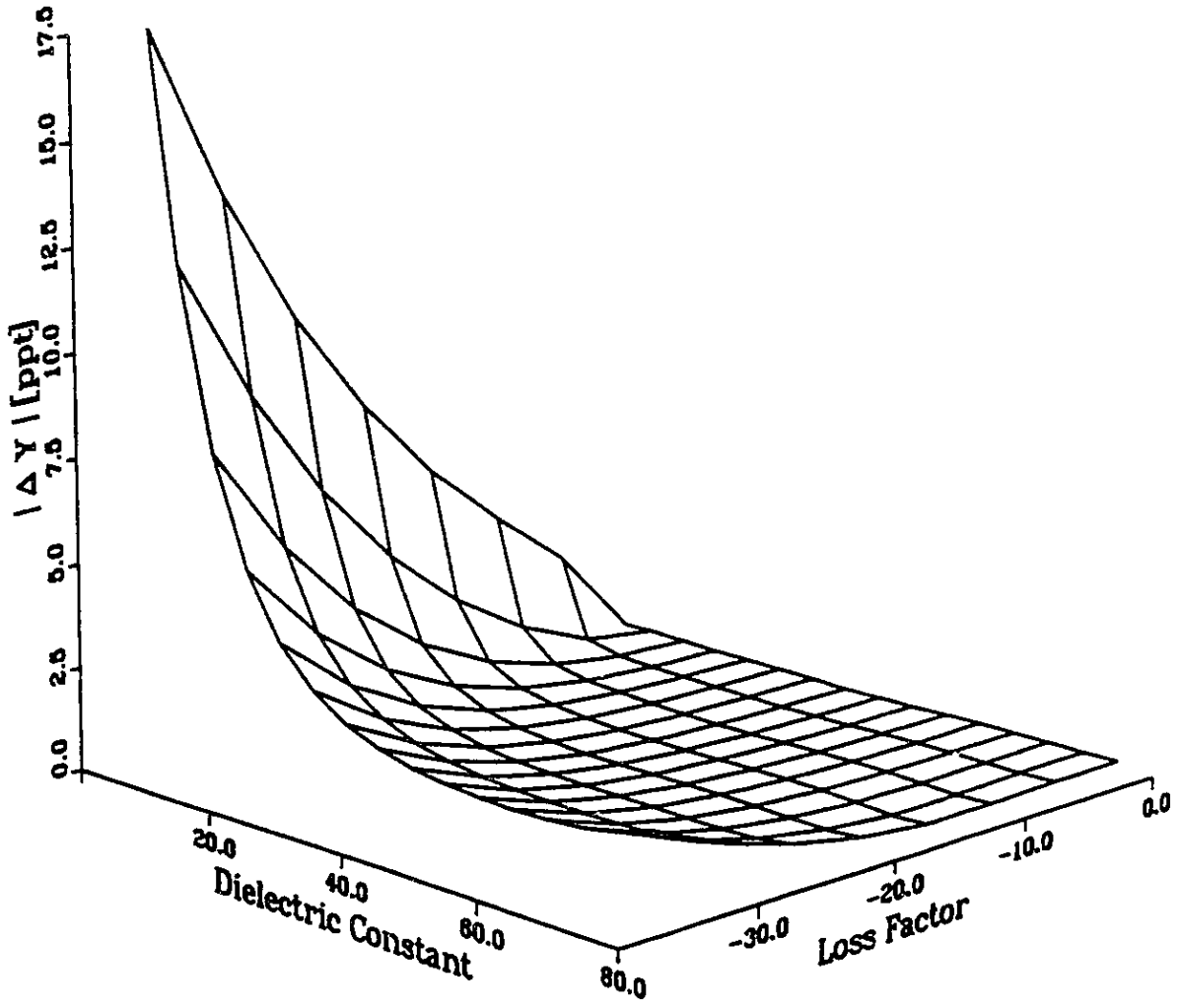

Fig. 6.7: Relative Error in the Computed Aperture Admittance of a Coaxial Line in Contact with Lossy Dielectrics for a Normalized Frequency, Ka=0.10

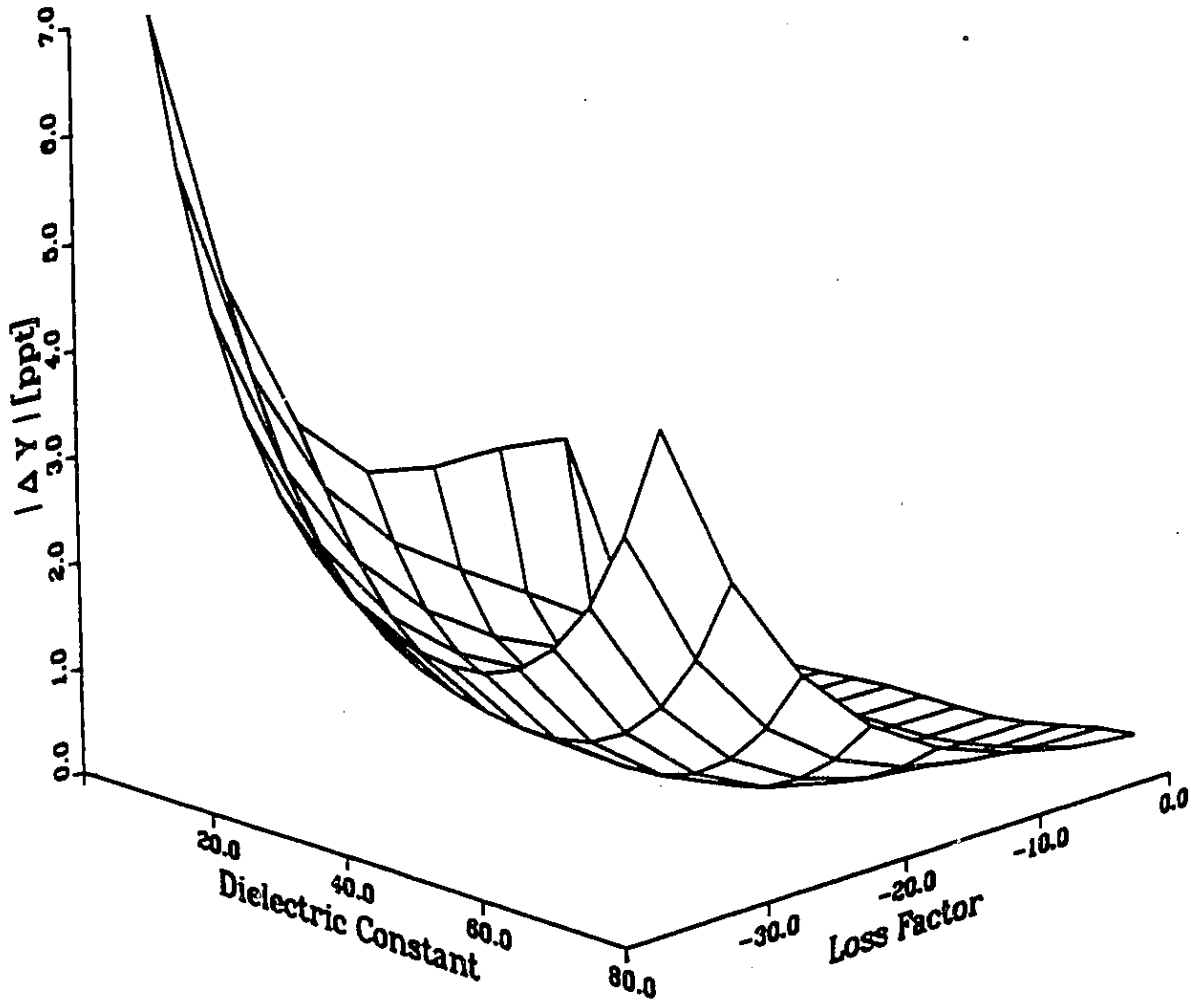

Chapter VII

Discussion and Conclusions

In order to achieve accurate broadband measurements of the permittivity of materials using open-ended waveguide probes, an accurate aperture admittance model of the probe is required. Furthermore, this model must allow solution of the inverse problem of determining the properties of the medium from the measured admittance. Previous attempts at modelling open-ended waveguide probes have failed to meet one or more of these requirements. Techniques based on full-wave numerical solutions of Maxwell's equations yield accurate solutions for the admittance given the properties of the medium, however, are of limited value in solving the inverse problem. Existing "lumped element" methods are based on static, or quasi-static approximations and, hence, are valid only for small apertures. This thesis presents a novel technique for determining simple, accurate, broadband admittance models for open-ended waveguides radiating into homogeneous, lossy dielectrics. The resulting model is a closed form expression and yields solutions for the direct and inverse problems which are as accurate as the full-wave numerical method on which it is based. Furthermore, the expression may be differentiated analytically, permitting a rigorous sensitivity and uncertainty analysis.

The technique, called pole/zero tracking, exploits the physical and mathematical properties of the driving point admittance function of open ended waveguides to derive a rational function explicit in frequency and the permittivity of the external medium. It is demonstrated, that for passive dielectrics, the aperture admittance must be a positive real function of the complex frequency. This guarantees the existence of a rational function approximation for any finite frequency range. The coefficients of this rational function are themselves positive real functions of the permittivity of the

external medium, and hence may be approximated by polynomials. The final expression is a rational function of frequency and permittivity. In some cases, it is noted, the rational function itself may be approximated by a polynomial. The requirement for this further simplification is that there be no poles lying within the circle, centered on the origin of the s-plane, with radius equal to the frequency range of interest.

The coefficients of the rational function, known as the model parameters, depend upon the geometry of the waveguide and of the aperture. Determination of the model parameters for a given structure is accomplished by a non-linear least squares fit to data computed by a full-wave moment method analysis. This proven numerical method includes the effects of radiation, polarization loss, and energy storage in the near-field and evanescent waveguide modes. The resulting accuracy of the method is demonstrated by a comparison with measurements and with the results of other numerical analyses. The curve fit itself is greatly simplified by the analytic properties of the model which reduce a four-dimensional fit to a two dimensional fit.

In order to illustrate and validate the technique, a model was developed for open-ended coaxial lines. The resulting rational function has 68 parameters and is valid for normalized frequencies and permittivities in the range $0.01 \le k_0 a \le 0.19, |\varepsilon_r - 40| \le 40$. In this range, the relative error in the computed admittance, compared to the moment method results, is a few parts-per-thousand. The inverse problem was formulated and seen to yield a unique solution. The relative error in the solution of the inverse problem is also of the order of a few parts-per-thousand.

A polynomial model for the aperture admittance of coaxial lines was also determined. This model is valid over the range $0.005 \le k_0 a \le 0.10$, and $|\varepsilon_r - 40| \le 40$ and contains 88 parameters. The resulting accuracy for both the direct and inverse problems over this range of independent variables is commensurate with the accuracy of the rational approximation. The advantage of a polynomial

approximation is not realized for this structure unless the frequency is severely restricted, however, this exercise is useful if only to demonstrate the feasibility of such a model and to provide some continuity between the rational model and the existing "lumped element" models.

The most important implication of obtaining closed form expressions for the aperture admittance is the insight such expressions yield into the **behavior** of the function. A numerical method can yield a solution for a given input, but cannot yield any information about the functional dependance between the two. This functional dependance is necessary if one wishes to perform a rigorous sensitivity and uncertainty analysis.

At the very least, this information enables one to select the optimum probe. For example, for coaxial lines the sensitivity analysis reveals that an electrically small aperture yields lower uncertainty when measuring materials which have a large permittivity whereas a large aperture yields lower uncertainty when measuring materials which have a small permittivity.

Ultimately, however, this information may enable one to design better probes. For example, with reference to Fig. 5.10 - 5.14. it may be possible to shift the minimum of the relative uncertainty to another region of the ε-plane. This minimum always occurs for a dielectric constant of approximately 2.0, whereas the loss factor corresponding to this minimum varies with normalized frequency. Perhaps it is coincidence that the dielectric constant of the Teflon inside the line is also 2.0, however, if these two are correlated one may simply increase the dielectric constant of the material inside the line and shift this region of low uncertainty correspondingly. This is pure speculation, however, it illustrates the point.

Finally, some recommendations for future work are given. The obvious extension is to analyze other structures. The technique is easily applied to open-ended rectangular waveguides, open-ended circular waveguides, etc. Furthermore, these structures may be modified by introducing irises at

the aperture. Another area of interest is to further simplify the models. This may be accomplished by techniques such a economization of series [64]. This technique uses Tschebycheff polynomials as expansion functions. These functions have interesting properties which enable graceful truncation of series. The basic concept is that fewer terms in the expansion may be used without significantly increasing the error in the approximation. Also of interest is the possibility of determining the location, in the s-plane, of the dominant poles directly from the moment method matrix. A similar technique, known as the singularity expansion method [65] is used in scattering problems.

A great deal of progress has been made in this thesis in the modeling of open-ended waveguides. The dependance of the aperture admittance of these structure upon the properties of the external medium and on frequency is governed by the laws of physics and the theory of functions of a complex variable. The guidelines imposed enable one to specify the functional dependance between these quantities. The marriage of analytical and numerical methods thus allows one to determine models which accurately approximate the complicated interaction of electromagnetic fields and matter.

Appendix A

Calculation of the Generalized Admittance Matrices

The elements of the generalized admittance matrix for the waveguide region are computed according to (3.52), which is repeated here for convenience.

$$Y_{ij}^{I} = \sum_{k=0}^{K}\left(\iint_{Aperture} \vec{M}_j \cdot (\vec{z}\times\vec{e}_k)dS\right) Y_k \left(\iint_{Aperture} \vec{M}_i \cdot (\vec{z}\times\vec{e}_k)dS\right) = \sum_{k=0}^{K} A_{jk}Y_k A_{ik} \qquad (A.1)$$

where $\vec{M}_i$ is the ith magnetic current expansion function and $\vec{e}_k$ is the transverse mode function for the kth waveguide mode. Substituting (4.6)-(4.8) and (4.1)-(4.2) for these quantities one obtains the following expression for the A_{jn} for the dominant mode,

$$A_{j0} = \sqrt{\frac{2\pi}{\ln\frac{e}{a}}}\begin{cases} \displaystyle\int_{a}^{\rho_1}\frac{(\rho_1-\rho)}{\Delta\rho_1}d\rho & j=1 \\ \displaystyle\int_{\rho_{J-2}}^{b}\frac{(\rho-\rho_{J-2})}{\Delta\rho_{J-1}}d\rho & j=J \\ \displaystyle\int_{\rho_{j-2}}^{\rho_{j-1}}\frac{(\rho-\rho_{j-2})}{\Delta\rho_{j-1}}d\rho+\int_{\rho j-1}^{\rho_j}\frac{(\rho_j-\rho)}{\Delta\rho_j}d\rho & j=2,3,\ldots J-1 \end{cases} \qquad (A.2)$$

and one of the following three expressions for the higher order modes:

$$A_{1n} = -\frac{\pi^{1.5}k_n Y_0(k_n b)}{\sqrt{Y_0^2(k_n)-Y_0^2(k_n b)}}\int_{a}^{\rho_1}\frac{(\rho_1-\rho)}{\Delta\rho_1}\{J_0(k_n a)Y_1(k_n\rho)-Y_0(k_n a)J_1(k_n\rho)\}\rho d\rho \qquad (A.3)$$

for subsection 1,

$$A_{Jn} = \frac{\pi^{1.5} k_n Y_0(k_n b)}{\sqrt{Y_0^2(k_n) - Y_0^2(k_n b)}} \int_{\rho_{J-2}}^{b} \frac{(\rho - \rho_{J-2})}{\Delta\rho_{J-1}} \{J_0(k_n a) Y_1(k_n \rho) - Y_0(k_n a) J_1(k_n \rho)\} \rho d\rho \qquad (A.4)$$

for subsection J,

$$A_{jn} = \frac{\pi^{1.5} k_n Y_0(k_n b)}{\sqrt{Y_0^2(k_n) - Y_0^2(k_n b)}} \left(\int_{\rho_{j-2}}^{j-1} \frac{(\rho - \rho_{j-2})}{\Delta\rho_{j-1}} \{J_0(k_n a) Y_1(k_n \rho) - Y_0(k_n a) J_1(k_n \rho)\} \rho d\rho + \right.$$

$$\left. \int_{\rho_{j-1}}^{j} \frac{(\rho_j - \rho)}{\Delta\rho_j} \{J_0(k_n a) Y_1(k_n \rho) - Y_0(k_n a) J_1(k_n \rho)\} \rho d\rho \right) \qquad (A.5)$$

for $j = 2, 3, \ldots, J-1$.

The integrals appearing in (A.2) may be evaluated analytically to yield,

$$A_{j1} = \sqrt{\frac{\pi}{2 \ln \frac{a}{b}}} \begin{cases} \rho_1 - a & j = 1 \\ \rho_{J-1} - \rho_{J-2} & j = J \\ \rho_j - \rho_{j-2} & j = 2, 3, \ldots, J-1 \end{cases} \qquad (A.6)$$

where as the integrals in (A.3)-(A.5) are evaluated numerically. The numerical integration used is a high order Romberg integration [62]. The routine increases the number of samples and the order of the integration rule until convergence is obtained. The Bessel functions are evaluated by an IMSL routine adapted from the NATS FUNPACK [66]. The accuracy of these function are limited only by machine precision, which for double precision is 15 hexadecimal digits.

The elements of the generalized admittance matrix for the half-space region is given by (3.59). For the coaxial line, the ϕ-symmetry of the structure and of the incident mode dictate that the magnetic charge density of (3.58) vanish. Hence, the simplified expression for the half-space matrix elements is,

$$Y_{ij}^{II} = \frac{j\omega\varepsilon}{2\pi} \iint_{Aperture} M_i \left(\iint_{Aperture} M_j \frac{e^{-jk|\vec{r}-\vec{r}'|}}{|\vec{r}-\vec{r}'|} \cos(\phi-\phi')\rho' d\rho' d\phi' \right) \rho d\rho d\phi \qquad (A.7)$$

where ε is the permittivity of the external medium, k is the wavenumber in the external medium, and $|\vec{r}-\vec{r}'|$ is the distance between the source point and the field point. This latter quatity may be expressed in cylindrical coordinates as,

$$R = |\vec{r}-\vec{r}'| = \sqrt{\rho^2 + \rho'^2 - 2\rho\rho'\cos(\phi-\phi') + (z-z')^2} \qquad (A.8)$$

Substitution of the expansion functions (4.6)-(4.8) into (A.7) reduces the limits of integration to the interval for which the expansion functions are non-zero. The integrations over the field coordinates in (A.7) are then approximated by a rectangle rule, with samples taken at the middle of the interval of integration, yielding the following expressions,

$$Y_{ij} \sim j\omega\pi \begin{cases} (\rho_1^2 - a^2) F_j\left(\frac{\rho_1 + a}{2}\right) & i = 1 \\ (b^2 - \rho_{I-2}^2) F_j\left(\frac{b + \rho_{I-2}}{2}\right) & i = I \\ (\rho_{i-1}^2 - \rho_{i-2}^2) F_j\left(\frac{\rho_{i-1} + \rho_{i-2}}{2}\right) + (\rho_i^2 - \rho_{i-1}^2) F_j\left(\frac{\rho_i + \rho_{i-1}}{2}\right) & i = 2, 3, \ldots, I-1 \end{cases} \qquad (A.9)$$

where $I = J$ is the total number of subsections, and $F_j(\rho_c)$ is the electric vector potential evaluated at the center of subinterval j. For this particular field point, (3.34) yields

$$F_j(\rho_c) = \frac{\varepsilon}{2\pi} \int_a^b M_j(\rho') \int_0^\pi \frac{e^{-jkR}}{R} \cos(\phi')\rho' d\rho' d\phi' \qquad (A.10)$$

where

$$R = \sqrt{\rho'^2 + \rho_c^2 - 2\rho'\rho_c\cos(\phi')} \qquad (A.11)$$

The singularity which appears in the integrand of (A.10) may be removed as follows. The ϕ integration may be written as:

$$\int_0^{\pi} \frac{e^{-jkR}}{R}\cos(\phi')d\phi' = \int_0^{\pi} \frac{d\phi'}{R} + \int_0^{\pi} \frac{(e^{-jkR}\cos(\phi')-1)}{R}d\phi' \qquad (A.12)$$

The first integral on the right hand side of (A.12) may be evaluated analytically and yield the complete elliptic integral of the first kind,

$$\int_0^{\pi} \frac{d\phi'}{R} = \frac{2}{(\rho_c+\rho')}\mathrm{K}\left(\frac{4\rho'\rho_c}{(\rho'+\rho_c)^2}\right) \qquad (A.13)$$

This elliptic integral may be evaluated by the polynomial approximation given in [67]. Having removed the singularity, (A.10) may be evaluated numerically. The Romberg integration routine described previously is used for this purpose.

Appendix B

Nomenclature

Symbol		Description
A_{jk}	-	The amplitude of the electric field of mode "k" produced by expansion function $\overrightarrow{M}_j$ in the moment method. $[\frac{volt}{meter}]$
	-	The elements of the design matrix of the least squares problem.
a	-	The radius of the inner conductor of a coaxial transmission line. [*meter*]
a_k	-	Generic model parameters in the discussion on least squares fitting.
B	-	The normalized aperture susceptance. The imaginary part of the normalized aperture admittance.
b	-	The inner radius of the outer conductor of a coaxial transmission line. [*meter*]
c_{np}	-	Parameters of the polynomial approximation to the normalized aperture admittance. $[\frac{second^n}{radian^n}]$
$\hat{c}_{np}$	-	Normalized parameters of the polynomial approximation to the normalized aperture admittance. $[\frac{second^n}{radian^n \cdot meter^n}]$
D	-	The electric flux density. $[\frac{coulomb}{meter}]$
E	-	The electric field intensity. $[\frac{volt}{meter^2}]$

E_{a0} - The total (incident plus reflected) dominant mode electric field in the aperture. $[\frac{volt}{meter}]$

$\vec{E}_t^I$ - Total tangential electric field on the waveguide side of the aperture. $[\frac{volt}{meter}]$

$\vec{E}_t^{II}$ - Total tangential electric field on the half-space side of the aperture. $[\frac{volt}{meter}]$

$\vec{e}_k$ - Transverse mode function for waveguide mode "k". For coaxial lines, the transverse mode function of the TM_{0k} mode.

$\vec{F}_j$ - The electric vector potential due to the magnetic current expansion function $\vec{M}_j$. $[\frac{ampere \cdot second}{meter}]$

G - The normalized aperture conductance. The real part of the normalized aperture admittance.

H_{a0} - The total (incident plus reflected) dominant mode magnetic field in the aperture. $[\frac{ampere}{meter}]$

$\vec{H}_t^I$ - Tangential magnetic field on the waveguide side of the aperture due to the equivalent magnetic current $\vec{M}$. $[\frac{ampere}{meter}]$

$\vec{H}_t^{inc}$ - Tangential magnetic field on the aperture due to the incident magnetic field. $[\frac{ampere}{meter}]$

$\vec{H}_t^{II}$ - Tangential magnetic field on the half-space side of the aperture due to the equivalent magnetic current. $[\frac{ampere}{meter}]$

I_i - The elements of the source vector obtained by applying the method of moments to the aperture problem.

$\Im$ - Operator which extracts the imaginary part of a complex quantity.

j - The imaginary unit. $j^2 = -1$

$J_0(x)$ - Bessel function of the first kind of order 0.

k_0 - The free space wavenumber. $[\frac{radian}{meter}]$

k_k - The cutoff wavenumber of mode "k". For coaxial lines, the cutoff wavenumber of the TM_{0k} mode. $[\frac{radian}{meter}]$

MoM - The Method of Moments.

$\overrightarrow{M}$ - The equivalent magnetic current on the aperture. The unknown in the integral equation solved via the method of moments. $[\frac{volt}{meter}]$

$\overrightarrow{M}_j$ - The moment method expansion functions for the equivalent magnetic current.

m_j - The equivalent magnetic charge density.

p.r. - Abbreviation for positive real, used in connection with positive real functions.

ppt - parts-per-thousand

$\Re$ - Operator which extracts the real part of a complex quantity.

S_A^B - The sensitivity of parameter B to changes in parameter A.

s - The complex frequency variable. $[\frac{radian}{second}]$

V_j - The unknown amplitude of expansion function "j". $[\frac{volt}{meter}]$

Y - The normalized aperture admittance, normalized to the wave admittance of the dominant mode inside the waveguide.

Ymodel - The normalized aperture admittance computed by the new model.

Ymom - The normalized aperture admittance computed by the moment method.

ΔY - Relative error between *Ymodel* and *Ymom*.

Y_0 - The dominant mode wave admittance in a waveguide. [*siemens*]

$Y_0(x)$ - Bessel function of the second kind of order 0.

Y_k - The wave admittance of waveguide mode "k". For coaxial lines, the wave admittance of the TM_{0k} mode. [*siemens*]

Y_{ij}^{I} - The elements of the generalized admittance matrix for the waveguide region. Part of the coefficient matrix of the final system of equations obtained by applying the moment method to the aperture problem.

Y_{ij}^{II} - The elements of the generalized admittance matrix for the half-space region. Part of the coefficient matrix of the final system of equations obtained by applying the moment method to the aperture problem.

α - The distribution parameter in the Cole-Cole dispersion equation.

α_{np} - The numerator parameters of the rational function model for the normalized aperture admittance. $[\frac{second^n}{radian^n}]$

- The elements of the coefficient matrix of the normal equations in the least squares fit.

$\hat{\alpha}_{nm}$ - The normalized numerator parameters of the rational function model for the normalized aperture admittance. $[\frac{second^n}{radian^n \cdot meter^n}]$

β_{mq} - The denominator parameters of the rational function model for the normalized aperture admittance. $[\frac{second^m}{radian^m}]$

$\hat{\beta}_{mq}$ - The normalized denominator parameters of the rational function model for the normalized aperture admittance. $[\frac{second^m}{radian^m \cdot meter^m}]$

Γ or Γ_0 - The dominant mode voltage reflection coefficient.

Γ_k - The amplitude of mode "k" reflected from the aperture.

γ_k - The propagation constant of waveguide mode "k". For coaxial lines, the propagation constant of the TM_{0k} mode.

ε - The permittivity of simple media. $[\frac{farad}{meter}]$

ε' - The relative dielectric constant. The real part of the relative permittivity.

ε'' - The loss factor. The imaginary part of the relative permittivity.

ε_0 - The permittivity of vacuum. $\varepsilon_0 = 8.8542 \times 10$ $[\frac{farad}{meter}]$

ε_r - The relative permittivity of simple media.

ε_s - The static relative permittivity in the Cole-Cole dispersion equation.

ε_∞ - The optical relative permittivity in the Cole-Cole dispersion equation.

ζ - The principle value of the square root of the relative permittivity.

μ - The material permeability. $[\frac{henry}{meter}]$

μ_0 - The permeability of free space. $\mu_0 = 4.0\pi \times 10^{-7}$ $[\frac{henry}{meter}]$

ρ - The radial coordinate in the cylindrical coordinate system. [*meter*]

σ - The real part of the complex frequency. $[\frac{radian}{second}]$

- The standard deviation of data in curve fit.

- The D.C. conductivity of a material. $[\frac{siemens}{meter}]$

τ - The relaxation time in the Cole-Cole dispersion equation. [*second*]

χ^2 - The merit function for least square fitting.

ψ_j - The magnetic scalar potential due to the magnetic current expansion function $\vec{M}_j$. [*ampere*]

ω - The imaginary part of the Complex frequency variable. The angular frequency. $[\frac{radian}{second}]$

* - Operator indicating complex conjugation.

Bibliography

1. Christensen D.A., And Durney C.H., "Hyperthermia Production for Cancer Therapy: A Review of Fundamentals and Methods," J.Microwave Power, Vol. 16, No. 2, pp. 89-105, June 1981.
2. Sterzer F., Paglione R., Nowogrodzki M., Beck E., Mandecki J., Friedenthal E., and Botstein C., "Microwave Apparatus for the Treatment of Cancer," Microwave Journal, Vol. 23, No. 1, pp. 39-44, January 1980.
3. Edrich J., "Centimeter- and Millimeter-Wave Thermography: A Survey of Tumor Detection," J. Microwave Power, Vol. 14, No. 2, pp. 95-104, 1979.
4. Bahl I.J., Thansandote A., Stuchly S.S., "Open-Ended Rectangular Waveguides as Antennas for Medical Diagnostics," J. Microwave Power, Vol. 15, No. 2, pp. 81-86, 1980.
5. Hill N.E., *Dielectric Properties ans Molecular Behavior*, New York: Van Norstrand Reinhold, 1969.
6. Stuchly M.A., Stuchly S.S., Liburdy R.P., And Russeau D.A., "Dielectric Properties of Liposome Vesicles at the Membrane Phase Transition," presented at the Tenth Annual Meeting of the Bioelectromagnetics Society, Stamford, Connecticut, June 1988.
7. Durney C.H., "Electromagnetic Dosimetry for Models of Humans and Animals: A Review of Theoretical and Numerical Techniques," Proc. IEEE, Vol. 68, No. 1, January 1980.
8. Kraszewski A., "Microwave Aquametry - A Review," J. Microwave Power, Vol. 15, No. 4, pp. 209-220, 1980.
9. Von Hippel A.R., *Dielectric Materials and Applications*, New York, MIT Technology Press ans Wiley, 1954.
10. Altschuler H.M., "Dielectric Constant," in *Handbook of Microwave Measurements*, Vol. II, M. Sucher and J. Fox, Eds., Brooklyn, NY: Polytechnic Press, 1963, pp. 495-548.
11. Bussey H.E., "Measurement of RF Properties of Materials - A Survey," Proc. IEEE, Vol. 55, No. 6, pp. 1046-1053, June 1967.
12. Von Hippel A.R., *Dielectric Materials and Applications*, New York, MIT Technology Press ans Wiley, 1954.
13. Hartshorn L., Ward W.H., "The Measurement of the Permittivity and Power Factor of Dielectrics at Frequencies from 10^4 to 10^8 Cycles per Second," J. Inst. Elec. Eng., Vol. 79, pp. 597-609, 1936.
14. Stuchly M.A., Stuchly S.S., "Coaxial Line Reflection Method for Measuring Dielectric Properties of Biological Substances at Radio and Microwave Frequencies - A Review," IEEE Trans. Instrum. Meas., Vol. IM-29, pp. 176-183, 1980.
15. Afsar M.N., Birch J.R., Clark R.N., "The Measurement of the Properties of Materials," G.W. Chantry Ed., Proc. IEEE, Vol. 74, No. 1, pp. 183-199, January 1986.
16. Levine H., Papas C.H., "Theory of the Circular Diffraction Antenna," J. Appl. Phys., Vol. 22, No. 1, January 1951, pp. 29-43.
17. Marcuvitz N., *Waveguide Handbook*, New York: McGraw-Hill, 1951, pp. 213-216.

18. Harrison C.W., Chang D.C., "Theory of the Annular Slot Antenna Based on Duality," IEEE Trans. Electromagnetic Compatibility, Vol. EMC-13, No. 1, February 1971, pp. 8-14.

19. Tsai L.L., "A Numerical Solution for the Near and Far Fields of an Annular Ring of Magnetic Current," IEEE Trans. Antennas Propagat., Vol. AP-20, No. 5, September 1972, pp. 569-576.

20. Chang D.C., "Input Admittance and Complete Near-Field Distribution of an Annular Aperture Antenna Driven by a Coaxial Line," IEEE Trans. Antennas Propagat., Vol. AP-18, No. 5, September 1970, pp. 610-616.

21. Irzinski E.P., "The Input Admittance of a TEM Excited Annular Slot Antenna," IEEE Trans. Antennas Propagat., Vol. AP-23, No. 6, November 1975, pp. 829-834.

22. Mosig J.R., Besson J-C. E., Gex-Fabry M., Gardiol F., "Reflection of an Open-Ended Coaxial Line and Application to Nondestructive Measurement of Materials," IEEE Trans. Instrum. Meas., Vol. IM-30, No. 1, March 1981, pp. 46-51.

23. Nevels R.D., Butler C.M., Yablon W., "The Annular Slot Antenna in a Lossy Biological Medium," IEEE Trans. Microwave Theory Tech., Vol. MTT-33, No. 4, April 1985, pp. 314-319.

24. Jenkins S., Preece A.W., Hodgetts T.E., Symm G.T., Warham A.G.P., Clarke R.N., "Comparison of Three Numerical Treatments for the Open-Ended Coaxial Line Sensor," Electron. Lett., Vol. 26, No. 4, February 1990, pp. 234-236.

25. Hodgetts T.E., "The Open-Ended Coaxial Line: A Rigorous Variational Treatment," Royal Signals and Radar Establishment Memorandum No. 4331, 1989.

26. Grant J.P., Clarke R.N., Symm G.T., Spyrou N.M., "A Critical Study of the Open-Ended Coaxial Line Sensor for Medical and Industrial Dielectric Measurements," IEE Colloquium on Industrial and Medical Applications of Microwaves, IEE Colloquium Digest No. 1986/73, May 1986.

27. Tanabe E., Joines W.T., "A Nondestructive Method for Measuring the Complex Permittivity of Dielectric Materials at Microwave Frequencies Using an Open Transmission Line Resonator," IEEE Trans. Instrum. Meas., Vol. IM-25, No. 3, September 1976, pp. 222-226.

28. Burdette E.C., Cain F.L., Seals J., "In Vivo Probe Measurement Technique for Determining Dielectric Properties at VHF through Microwave Frequencies," IEEE Trans. Microwave Theory Tech., Vol. MTT-28, No. 4, April 1980, pp. 414-427.

29. Deschamps G.A., "Impedance of an antenna in a conducting medium," IRE Trans. Antennas Propagat., September 1962, pp. 648-650.

30. Stuchly M.A., Athey W.T., Samaras G.M., Taylor G.E., "Measurements of Radio Frequency Permittivity of Biological Tissues with an Open-Ended Coaxial Line: Part II - Experimental Results," IEEE Trans. Microwave Theory Tech., Vol. MTT-30, No. 1, January 1982, pp. 87-91.

31. Gajda G., Stuchly S., "Numerical Analysis of Open-Ended Coaxial Lines," IEEE Trans. Microwave Theory Tech., Vol. MTT-31, No. 5, May 1983, pp. 380-384.

32. Kraszewski A., Stuchly S., "Capacitance of Open-Ended Coaxial Lines - Experimental Results," IEEE Trans. Instrum. Meas., Vol. IM-32, No. 4, December 1983, pp. 517-519.

33. Gajda G., Stuchly S., "An Equivalent Circuit of an Open-Ended Coaxial Line," IEEE Trans. Instrum. Meas., Vol. IM-32, No. 4, December 1983, pp. 506-508.

34. Brady M.M., Symons S.A., Stuchly S.S., "Dielectric Behavior of Selected Animal Tissues In Vitro at Frequencies from 2 to 4 GHz," IEEE Trans. Biomed. Eng., Vol. BME-28, No. 3, March 1981, pp. 305-307.

35. Stuchly M.A., Brady M.M., Stuchly S.S., Gajda G., "Equivalent Circuit of an Open-Ended Coaxial Line in a Lossy Dielectric," IEEE Trans. Instrum. Meas., Vol. IM-31, No. 2, June 1982, pp. 116-119.

36. Misra D.K., "A Quasi-Static Analysis of Open-Ended Coaxial Lines," IEEE Trans. Microwave Theory Tech., Vol. MTT-35, No. 10, October 1987, pp. 925-928.

37. Deming Xu, Liping Liu, Zhiyan Jiang, "Measurement of the Dielectric Properties of Biological Substances Using an Improved Open-Ended Coaxial Line Resonator," IEEE Trans. Microwave Theory Tech., Vol. MTT-35, No. 12, December 1987, pp. 1424-1428.

38. Misra D., Chabbra M., Epstein B.R., Mirotznik M., Foster K., "Noninvasive Electrical Characterization of Materials at Microwave Frequencies Using an Open-Ended Coaxial Line: Test of an Improved Calibration Technique," IEEE Trans. Microwave Theory Tech., Vol. MTT-38, No. 1, January 1990, pp. 8-14.

39. Lewin L., *Advanced Theory of Waveguides*, Iliffe, London, 1951.

40. Mautz J.R., Harrington R.F., "Transmission from a Rectangular Waveguide into Half Space through a Rectangular Aperture," Rep. TR-76-5, Dept. of Electrical and Computer Engineering, Syracuse University, New York, 1976.

41. Jamieson A.R., Rozzi T.E., "Rigorous Analysis of Cross-Polarization in Flange-Mounted Rectangular Waveguide Radiators," Electron. Lett., Vol. 13, November 1977, pp. 742-744.

42. MacPhie R.H., Zaghloul A.I., "Radiation from a Rectangular Waveguide with Infinite Flange - Exact Solution by the Correlation Matrix Method," IEEE Trans. Antenna Propagat., Vol. AP-28, No. 4, July 1980, pp. 497-503.

43. Compton R.T., Ph.D. Thesis, Ohio State University, Columbus, 1964.

44. Villeneuve A.T., "Admittance of a Waveguide Radiating into Plasma Environment," IEEE Trans. Antennas Propagat., Vol. AP-13, No. 1, January 1965, pp. 115-121.

45. Galejs J., "Admittance of a Waveguide Radiating into Stratified Plasma," IEEE Trans. Antennas Propagat., Vol. AP-13, No. 1, January 1965, pp. 64-70.

46. Croswell W.F., Taylor W.C., Swift C.T., Cockrell C.R., "Input Admittance of a Rectangular Waveguide-Fed Aperture Under an Inhomogeneous Plasma: Theory and Experiment," IEEE Trans. Antennas Propagat., Vol. AP-16, No. 4, July 1968, pp. 475-487.

47. Audet J., Bolomey J.C., Pichot C., Nguyen D.D., Robillard M., Chive M., Leroy Y., "Electrical Characteristics of Waveguide Apertures for Medical Applications," J. Microwave Power, Vol. 15, No. 3, 1980, pp. 177-186.

48. Encinar J.A., Rebollar J.M., "Convergence of Numerical Solutions of Open-Ended Waveguide by Modal Analysis and Hybrid Modal-Spectral Techniques," IEEE Trans. Microwave Theory Tech., Vol. MTT-34, No. 7, July 1986, pp. 809-814.

49. Decreton M.C., Gardiol F., "Simple Nondestructive Method for the Measurement of Complex Permittivity," IEEE Trans. Instrum. Meas., Vol. IM-23, No. 4, December 1974, pp. 434-438.

50. Sphicopoulos T., Teodoridis V., Gardiol F., "Simple Nondestructive Method for the Measurement of Material Permittivity," J. Microwave Power, 1985.

51. Gex-Fabry M., Mosig J.R., Gardiol F.E., "Reflection and Radiation of an Open-Ended Circular Waveguide: Application to Nondestructive Measurements of Materials," Archiv Fur Elektronik Und Ubertragungstechnik, AEU Band 33, 1979, pp. 473-478.

52. Fray C., Khayata N., Papiernik A., "TM_{01} Admittance and Radiation from a Flanged Open-Ended Waveguide into Layered Absorbing Media," AEU, Band 36, 1982, pp. 107-110.

53. Smith G.S., Nordgard J.D., "Measurement of the Electrical Constitutive Parameters of Materials Using Antennas," IEEE Trans. Antennas Propagat., Vol. AP-33, No. 7, July 1985, pp. 783-792.

54. Guillemin E.A., *Synthesis of Passive Networks, Theory and Methods Appropriate to the Realization and Approximation Problems*, John Wiley & Sons, New York, 1957.

55. Sinclair G., "Theory of Models of Electromagnetic Systems," Proc. IRE, vol. 36, pp. 1364-1370, Nov. 1948.

56. Mautz J.R., Harrington R.F., "Transmission from a Rectangular Waveguide into Half Space through a Rectangular Aperture," Rep. TR-76-5, Dept. of Electrical and Computer Engineering, Syracuse University, New York, 1976.

57. Harrington, R.F., *Time-Harmonic Electromagnetic Fields*, McGraw-Hill, New York, 1961.

58. Harrington, R.F., *Field Computation by Moment Methods*, The Macmillan Co., New York, 1968.

59. Press W.H., Flannery B.P., Teukolsky S.A., Vetterling W.T., *Numerical Recipes: The Art of Scientific Computing*, Cambridge University Press, Cambridge, 1986, Chap. 14.

60. Press W.H., Flannery B.P., Teukolsky S.A., Vetterling W.T., *Numerical Recipes: The Art of Scientific Computing*, Cambridge University Press, Cambridge, 1986, Chap. 11.

61. Garbow B.S., Hillstrom K.E., More J.J., "MINPACK, Double Precision Version," Argonne National Laboratory, March 1980.

62. Press W.H., Flannery B.P., Teukolsky S.A., Vetterling W.T., *Numerical Recipes: The Art of Scientific Computing*, Cambridge University Press, Cambridge, 1986, Chap. 4.

63. *ibid*, Chap. 9.

64. Hildebrand F.B., *Introduction to Numerical Analysis*, McGraw-Hill, New York, Chap. 9, p. 471.

65. Baum C.E., "The Singularity Expansion Method," in *Transient Electromagnetic Fields*, L.B. Felsen, Ed. Berlin:Springer-Verlag, 1976, Chap. 3, pp. 129-179.

66. National Activity to Test Software (NATS) FUNPACK, Argonne National Laboratory, Argonne Code Center, Argonne, Illinois 60439, 1976.

67. Abramowitz M., Stegun I., Handbook of Mathematical Functions, National Bureau of Standards Applied Mathematics Series 55, December 1972, p. 591.